# $\Lambda_c$ polarimetry using the dominant hadronic mode — supplemental material

***0.0.9 (18/01/2023 22:58:41)***

**Mikhail Mikhasenko, Remco de Boer, Miriam Fritsch**

**Jan 18, 2023**

# TABLE OF CONTENTS

DOI 10.48550/arXiv.2301.07010 DOI 10.5281/zenodo.7544989

$\Lambda_c^+$ polarimetry using the dominant hadronic mode The polarimeter vector field for multibody decays of a spin-half baryon is introduced as a generalisation of the baryon asymmetry parameters. Using a recent amplitude analysis of the $\Lambda_c^+ \to pK^-\pi^+$ decay performed at the LHCb experiment, we compute the distribution of the kinematic-dependent polarimeter vector for this process in the space of Mandelstam variables to express the polarised decay rate in a model-agnostic form. The obtained representation can facilitate polarisation measurements of the $\Lambda_c^+$ baryon and eases inclusion of the $\Lambda_c^+ \to pK^-\pi^+$ decay mode in hadronic amplitude analyses.

This website shows all analysis results that led to the publication of LHCb-PAPER-2022-044. More information on this publication can be found on the following pages:

- Publication on arXiv: arXiv:2301.07010
- Record on CDS: cds.cern.ch/record/2838694
- Record for the source code on Zenodo: 10.5281/zenodo.7544989
- Frozen documentation on GitLab Pages: lc2pkpi-polarimetry.docs.cern.ch
- Frozen repository on CERN GitLab: gitlab.cern.ch/polarimetry/Lc2pKpi
- Active repository on GitHub containing discussions: github.com/ComPWA/polarimetry

**Behind SSO login (LHCb members only)**

- LHCb TWiki page: twiki.cern.ch/twiki/bin/viewauth/LHCbPhysics/PolarimetryLc2pKpi
- Charm WG meeting: indico.cern.ch/event/1187317
- RC approval presentation: indico.cern.ch/event/1213570
- Silent approval to submit: indico.cern.ch/event/1242323

**Note:** This document is a PDF rendering of the supplemental material hosted behind SSO-login on lc2pkpi-polarimetry.docs.cern.ch. Go to this webpage for a more extensive and interactive experience.

CHAPTER

ONE

# NOMINAL AMPLITUDE MODEL

## 1.1 Resonances and LS-scheme

Particle definitions for $\Lambda_c^+$ and $p, \pi^+, K^-$ in the sequential order.

| name | LaTeX | $J^P$ | mass (MeV) | width (MeV) |
|---|---|---|---|---|
| Lambda_c+ | $\Lambda_c^+$ | $\frac{1}{2}^+$ | 2,286 | 0 |
| p | $p$ | $\frac{1}{2}^+$ | 938 | 0 |
| pi+ | $\pi^+$ | $0^-$ | 139 | 0 |
| K- | $K^-$ | $0^-$ | 493 | 0 |
| Sigma- | $\Sigma^-$ | $\frac{1}{2}^+$ | 1,189 | 0 |

Particle definitions as defined in `particle-definitions.yaml`:

| name | LaTeX | $J^P$ | mass (MeV) | width (MeV) |
|---|---|---|---|---|
| L(1405) | $\Lambda(1405)$ | $\frac{1}{2}^-$ | 1,405 | 50 |
| L(1520) | $\Lambda(1520)$ | $\frac{3}{2}^-$ | 1,519 | 15 |
| L(1600) | $\Lambda(1600)$ | $\frac{1}{2}^+$ | 1,630 | 250 |
| L(1670) | $\Lambda(1670)$ | $\frac{1}{2}^-$ | 1,670 | 30 |
| L(1690) | $\Lambda(1690)$ | $\frac{3}{2}^-$ | 1,690 | 70 |
| L(1800) | $\Lambda(1800)$ | $\frac{1}{2}^-$ | 1,800 | 300 |
| L(1810) | $\Lambda(1810)$ | $\frac{1}{2}^+$ | 1,810 | 150 |
| L(2000) | $\Lambda(2000)$ | $\frac{1}{2}^-$ | 2,000 | 210 |
| D(1232) | $\Delta(1232)$ | $\frac{3}{2}^+$ | 1,232 | 117 |
| D(1600) | $\Delta(1600)$ | $\frac{3}{2}^+$ | 1,640 | 300 |
| D(1620) | $\Delta(1620)$ | $\frac{1}{2}^-$ | 1,620 | 130 |
| D(1700) | $\Delta(1700)$ | $\frac{3}{2}^-$ | 1,690 | 380 |
| K(700) | $K(700)$ | $0^+$ | 824 | 478 |
| K(892) | $K(892)$ | $1^-$ | 895 | 47 |
| K(1410) | $K(1410)$ | $1^-$ | 1,421 | 236 |
| K(1430) | $K(1430)$ | $0^+$ | 1,375 | 190 |

**See also:**

*Amplitude model with LS-couplings* (page 60)

Most models work take the **minimal $L$-value** in each $LS$-coupling (only model 17 works in the full $LS$-basis. The generated $LS$-couplings look as follows:

| Only minimum $LS$ (12) | All $LS$-couplings (26) |
|---|---|
| $\Lambda_c^+ \xrightarrow[S=3/2]{L=1} \Delta(1232) \xrightarrow[S=1/2]{L=1} p\pi^+K^-$ | $\Lambda_c^+ \xrightarrow[S=3/2]{L=1} \Delta(1232) \xrightarrow[S=1/2]{L=1} p\pi^+K^-$ |
| | $\Lambda_c^+ \xrightarrow[S=3/2]{L=2} \Delta(1232) \xrightarrow[S=1/2]{L=1} p\pi^+K^-$ |
| $\Lambda_c^+ \xrightarrow[S=3/2]{L=1} \Delta(1600) \xrightarrow[S=1/2]{L=1} p\pi^+K^-$ | $\Lambda_c^+ \xrightarrow[S=3/2]{L=1} \Delta(1600) \xrightarrow[S=1/2]{L=1} p\pi^+K^-$ |
| | $\Lambda_c^+ \xrightarrow[S=3/2]{L=2} \Delta(1600) \xrightarrow[S=1/2]{L=1} p\pi^+K^-$ |
| $\Lambda_c^+ \xrightarrow[S=3/2]{L=1} \Delta(1700) \xrightarrow[S=1/2]{L=2} p\pi^+K^-$ | $\Lambda_c^+ \xrightarrow[S=3/2]{L=1} \Delta(1700) \xrightarrow[S=1/2]{L=2} p\pi^+K^-$ |
| | $\Lambda_c^+ \xrightarrow[S=3/2]{L=2} \Delta(1700) \xrightarrow[S=1/2]{L=2} p\pi^+K^-$ |
| $\Lambda_c^+ \xrightarrow[S=1/2]{L=0} K(700) \xrightarrow[S=0]{L=0} \pi^+K^-p$ | $\Lambda_c^+ \xrightarrow[S=1/2]{L=0} K(700) \xrightarrow[S=0]{L=0} \pi^+K^-p$ |
| | $\Lambda_c^+ \xrightarrow[S=1/2]{L=1} K(700) \xrightarrow[S=0]{L=0} \pi^+K^-p$ |
| $\Lambda_c^+ \xrightarrow[S=1/2]{L=0} K(892) \xrightarrow[S=0]{L=1} \pi^+K^-p$ | $\Lambda_c^+ \xrightarrow[S=1/2]{L=0} K(892) \xrightarrow[S=0]{L=1} \pi^+K^-p$ |
| | $\Lambda_c^+ \xrightarrow[S=1/2]{L=1} K(892) \xrightarrow[S=0]{L=1} \pi^+K^-p$ |
| | $\Lambda_c^+ \xrightarrow[S=3/2]{L=1} K(892) \xrightarrow[S=0]{L=1} \pi^+K^-p$ |
| | $\Lambda_c^+ \xrightarrow[S=3/2]{L=2} K(892) \xrightarrow[S=0]{L=1} \pi^+K^-p$ |
| $\Lambda_c^+ \xrightarrow[S=1/2]{L=0} K(1430) \xrightarrow[S=0]{L=0} \pi^+K^-p$ | $\Lambda_c^+ \xrightarrow[S=1/2]{L=0} K(1430) \xrightarrow[S=0]{L=0} \pi^+K^-p$ |
| | $\Lambda_c^+ \xrightarrow[S=1/2]{L=1} K(1430) \xrightarrow[S=0]{L=0} \pi^+K^-p$ |
| $\Lambda_c^+ \xrightarrow[S=1/2]{L=0} \Lambda(1405) \xrightarrow[S=1/2]{L=0} K^-p\pi^+$ | $\Lambda_c^+ \xrightarrow[S=1/2]{L=0} \Lambda(1405) \xrightarrow[S=1/2]{L=0} K^-p\pi^+$ |
| | $\Lambda_c^+ \xrightarrow[S=1/2]{L=1} \Lambda(1405) \xrightarrow[S=1/2]{L=0} K^-p\pi^+$ |
| $\Lambda_c^+ \xrightarrow[S=3/2]{L=1} \Lambda(1520) \xrightarrow[S=1/2]{L=2} K^-p\pi^+$ | $\Lambda_c^+ \xrightarrow[S=3/2]{L=1} \Lambda(1520) \xrightarrow[S=1/2]{L=2} K^-p\pi^+$ |
| | $\Lambda_c^+ \xrightarrow[S=3/2]{L=2} \Lambda(1520) \xrightarrow[S=1/2]{L=2} K^-p\pi^+$ |
| $\Lambda_c^+ \xrightarrow[S=1/2]{L=0} \Lambda(1600) \xrightarrow[S=1/2]{L=1} K^-p\pi^+$ | $\Lambda_c^+ \xrightarrow[S=1/2]{L=0} \Lambda(1600) \xrightarrow[S=1/2]{L=1} K^-p\pi^+$ |
| | $\Lambda_c^+ \xrightarrow[S=1/2]{L=1} \Lambda(1600) \xrightarrow[S=1/2]{L=1} K^-p\pi^+$ |
| $\Lambda_c^+ \xrightarrow[S=1/2]{L=0} \Lambda(1670) \xrightarrow[S=1/2]{L=0} K^-p\pi^+$ | $\Lambda_c^+ \xrightarrow[S=1/2]{L=0} \Lambda(1670) \xrightarrow[S=1/2]{L=0} K^-p\pi^+$ |
| | $\Lambda_c^+ \xrightarrow[S=1/2]{L=1} \Lambda(1670) \xrightarrow[S=1/2]{L=0} K^-p\pi^+$ |
| $\Lambda_c^+ \xrightarrow[S=3/2]{L=1} \Lambda(1690) \xrightarrow[S=1/2]{L=2} K^-p\pi^+$ | $\Lambda_c^+ \xrightarrow[S=3/2]{L=1} \Lambda(1690) \xrightarrow[S=1/2]{L=2} K^-p\pi^+$ |
| | $\Lambda_c^+ \xrightarrow[S=3/2]{L=2} \Lambda(1690) \xrightarrow[S=1/2]{L=2} K^-p\pi^+$ |
| $\Lambda_c^+ \xrightarrow[S=1/2]{L=0} \Lambda(2000) \xrightarrow[S=1/2]{L=0} K^-p\pi^+$ | $\Lambda_c^+ \xrightarrow[S=1/2]{L=0} \Lambda(2000) \xrightarrow[S=1/2]{L=0} K^-p\pi^+$ |
| | $\Lambda_c^+ \xrightarrow[S=1/2]{L=1} \Lambda(2000) \xrightarrow[S=1/2]{L=0} K^-p\pi^+$ |

Or with $J^P$-values:

| Only minimum $LS$ (12) | All $LS$-couplings (26) |
|---|---|
| $\Lambda_c^+\left[\frac{1}{2}^+\right] \xrightarrow[S=3/2]{L=1} \Delta(1232)\left[\frac{3}{2}^+\right] \xrightarrow[S=1/2]{L=1} p\left[\frac{1}{2}^+\right]\pi^+\left[0^-\right]K^-\left[0^-\right]$ | $\Lambda_c^+\left[\frac{1}{2}^+\right] \xrightarrow[S=3/2]{L=1} \Delta(1232)\left[\frac{3}{2}^+\right] \xrightarrow[S=1/2]{L=1} p\left[\frac{1}{2}^+\right]\pi^+\left[0^-\right]K^-\left[0^-\right]$ |
| | $\Lambda_c^+\left[\frac{1}{2}^+\right] \xrightarrow[S=3/2]{L=2} \Delta(1232)\left[\frac{3}{2}^+\right] \xrightarrow[S=1/2]{L=1} p\left[\frac{1}{2}^+\right]\pi^+\left[0^-\right]K^-\left[0^-\right]$ |
| $\Lambda_c^+\left[\frac{1}{2}^+\right] \xrightarrow[S=3/2]{L=1} \Delta(1600)\left[\frac{3}{2}^+\right] \xrightarrow[S=1/2]{L=1} p\left[\frac{1}{2}^+\right]\pi^+\left[0^-\right]K^-\left[0^-\right]$ | $\Lambda_c^+\left[\frac{1}{2}^+\right] \xrightarrow[S=3/2]{L=1} \Delta(1600)\left[\frac{3}{2}^+\right] \xrightarrow[S=1/2]{L=1} p\left[\frac{1}{2}^+\right]\pi^+\left[0^-\right]K^-\left[0^-\right]$ |
| | $\Lambda_c^+\left[\frac{1}{2}^+\right] \xrightarrow[S=3/2]{L=2} \Delta(1600)\left[\frac{3}{2}^+\right] \xrightarrow[S=1/2]{L=1} p\left[\frac{1}{2}^+\right]\pi^+\left[0^-\right]K^-\left[0^-\right]$ |
| $\Lambda_c^+\left[\frac{1}{2}^+\right] \xrightarrow[S=3/2]{L=1} \Delta(1700)\left[\frac{3}{2}^-\right] \xrightarrow[S=1/2]{L=2} p\left[\frac{1}{2}^+\right]\pi^+\left[0^-\right]K^-\left[0^-\right]$ | $\Lambda_c^+\left[\frac{1}{2}^+\right] \xrightarrow[S=3/2]{L=1} \Delta(1700)\left[\frac{3}{2}^-\right] \xrightarrow[S=1/2]{L=2} p\left[\frac{1}{2}^+\right]\pi^+\left[0^-\right]K^-\left[0^-\right]$ |
| | $\Lambda_c^+\left[\frac{1}{2}^+\right] \xrightarrow[S=3/2]{L=2} \Delta(1700)\left[\frac{3}{2}^-\right] \xrightarrow[S=1/2]{L=2} p\left[\frac{1}{2}^+\right]\pi^+\left[0^-\right]K^-\left[0^-\right]$ |
| $\Lambda_c^+\left[\frac{1}{2}^+\right] \xrightarrow[S=1/2]{L=0} K(700)\left[0^+\right] \xrightarrow[S=0]{L=0} \pi^+\left[0^-\right]K^-\left[0^-\right]p\left[\frac{1}{2}^+\right]$ | $\Lambda_c^+\left[\frac{1}{2}^+\right] \xrightarrow[S=1/2]{L=0} K(700)\left[0^+\right] \xrightarrow[S=0]{L=0} \pi^+\left[0^-\right]K^-\left[0^-\right]p\left[\frac{1}{2}^+\right]$ |
| | $\Lambda_c^+\left[\frac{1}{2}^+\right] \xrightarrow[S=1/2]{L=1} K(700)\left[0^+\right] \xrightarrow[S=0]{L=0} \pi^+\left[0^-\right]K^-\left[0^-\right]p\left[\frac{1}{2}^+\right]$ |
| $\Lambda_c^+\left[\frac{1}{2}^+\right] \xrightarrow[S=1/2]{L=0} K(892)\left[1^-\right] \xrightarrow[S=0]{L=1} \pi^+\left[0^-\right]K^-\left[0^-\right]p\left[\frac{1}{2}^+\right]$ | $\Lambda_c^+\left[\frac{1}{2}^+\right] \xrightarrow[S=1/2]{L=0} K(892)\left[1^-\right] \xrightarrow[S=0]{L=1} \pi^+\left[0^-\right]K^-\left[0^-\right]p\left[\frac{1}{2}^+\right]$ |
| | $\Lambda_c^+\left[\frac{1}{2}^+\right] \xrightarrow[S=1/2]{L=1} K(892)\left[1^-\right] \xrightarrow[S=0]{L=1} \pi^+\left[0^-\right]K^-\left[0^-\right]p\left[\frac{1}{2}^+\right]$ |
| | $\Lambda_c^+\left[\frac{1}{2}^+\right] \xrightarrow[S=3/2]{L=1} K(892)\left[1^-\right] \xrightarrow[S=0]{L=1} \pi^+\left[0^-\right]K^-\left[0^-\right]p\left[\frac{1}{2}^+\right]$ |
| | $\Lambda_c^+\left[\frac{1}{2}^+\right] \xrightarrow[S=3/2]{L=2} K(892)\left[1^-\right] \xrightarrow[S=0]{L=1} \pi^+\left[0^-\right]K^-\left[0^-\right]p\left[\frac{1}{2}^+\right]$ |
| $\Lambda_c^+\left[\frac{1}{2}^+\right] \xrightarrow[S=1/2]{L=0} K(1430)\left[0^+\right] \xrightarrow[S=0]{L=0} \pi^+\left[0^-\right]K^-\left[0^-\right]p\left[\frac{1}{2}^+\right]$ | $\Lambda_c^+\left[\frac{1}{2}^+\right] \xrightarrow[S=1/2]{L=0} K(1430)\left[0^+\right] \xrightarrow[S=0]{L=0} \pi^+\left[0^-\right]K^-\left[0^-\right]p\left[\frac{1}{2}^+\right]$ |
| | $\Lambda_c^+\left[\frac{1}{2}^+\right] \xrightarrow[S=1/2]{L=1} K(1430)\left[0^+\right] \xrightarrow[S=0]{L=0} \pi^+\left[0^-\right]K^-\left[0^-\right]p\left[\frac{1}{2}^+\right]$ |
| $\Lambda_c^+\left[\frac{1}{2}^+\right] \xrightarrow[S=1/2]{L=0} \Lambda(1405)\left[\frac{1}{2}^-\right] \xrightarrow[S=1/2]{L=0} K^-\left[0^-\right]p\left[\frac{1}{2}^+\right]\pi^+\left[0^-\right]$ | $\Lambda_c^+\left[\frac{1}{2}^+\right] \xrightarrow[S=1/2]{L=0} \Lambda(1405)\left[\frac{1}{2}^-\right] \xrightarrow[S=1/2]{L=0} K^-\left[0^-\right]p\left[\frac{1}{2}^+\right]\pi^+\left[0^-\right]$ |
| | $\Lambda_c^+\left[\frac{1}{2}^+\right] \xrightarrow[S=1/2]{L=1} \Lambda(1405)\left[\frac{1}{2}^-\right] \xrightarrow[S=1/2]{L=0} K^-\left[0^-\right]p\left[\frac{1}{2}^+\right]\pi^+\left[0^-\right]$ |
| $\Lambda_c^+\left[\frac{1}{2}^+\right] \xrightarrow[S=3/2]{L=1} \Lambda(1520)\left[\frac{3}{2}^-\right] \xrightarrow[S=1/2]{L=2} K^-\left[0^-\right]p\left[\frac{1}{2}^+\right]\pi^+\left[0^-\right]$ | $\Lambda_c^+\left[\frac{1}{2}^+\right] \xrightarrow[S=3/2]{L=1} \Lambda(1520)\left[\frac{3}{2}^-\right] \xrightarrow[S=1/2]{L=2} K^-\left[0^-\right]p\left[\frac{1}{2}^+\right]\pi^+\left[0^-\right]$ |
| | $\Lambda_c^+\left[\frac{1}{2}^+\right] \xrightarrow[S=3/2]{L=2} \Lambda(1520)\left[\frac{3}{2}^-\right] \xrightarrow[S=1/2]{L=2}$ |

## 1.2 Amplitude

### 1.2.1 Spin-alignment amplitude

The full intensity of the amplitude model is obtained by summing the following aligned amplitude over all helicity values $\lambda_i$ in the initial state $0$ and final states $1, 2, 3$:

$$\sum_{\lambda_0'=-1/2}^{1/2} \sum_{\lambda_1'=-1/2}^{1/2} A^{1}_{\lambda_0',\lambda_1'} d^{\frac{1}{2}}_{\lambda_1',\lambda_1}\left(\zeta^{1}_{1(1)}\right) d^{\frac{1}{2}}_{\lambda_0,\lambda_0'}\left(\zeta^{0}_{1(1)}\right) + A^{2}_{\lambda_0',\lambda_1'} d^{\frac{1}{2}}_{\lambda_1',\lambda_1}\left(\zeta^{1}_{2(1)}\right) d^{\frac{1}{2}}_{\lambda_0,\lambda_0'}\left(\zeta^{0}_{2(1)}\right) + A^{3}_{\lambda_0',\lambda_1'} d^{\frac{1}{2}}_{\lambda_1',\lambda_1}\left(\zeta^{1}_{3(1)}\right) d^{\frac{1}{2}}_{\lambda_0,\lambda_0'}\left(\zeta^{0}_{3(1)}\right)$$

Note that we simplified notation here: the amplitude indices for the spinless states are not rendered and their corresponding Wigner-$d$ alignment functions are simply $1$.

The relevant $\zeta^i_{j(k)}$ angles are *defined as* (page 52):

$$\begin{aligned}
\zeta^{0}_{1(1)} &= 0 \\
\zeta^{1}_{1(1)} &= 0 \\
\zeta^{0}_{2(1)} &= -\operatorname{acos}\left(\frac{-2m_0^2(-m_1^2-m_2^2+\sigma_3)+(m_0^2+m_1^2-\sigma_1)(m_0^2+m_2^2-\sigma_2)}{\sqrt{\lambda(m_0^2,m_2^2,\sigma_2)}\sqrt{\lambda(m_0^2,\sigma_1,m_1^2)}}\right) \\
\zeta^{1}_{2(1)} &= \operatorname{acos}\left(\frac{2m_1^2(-m_0^2-m_3^2+\sigma_3)+(m_0^2+m_1^2-\sigma_1)(-m_1^2-m_3^2+\sigma_2)}{\sqrt{\lambda(m_0^2,m_1^2,\sigma_1)}\sqrt{\lambda(\sigma_2,m_1^2,m_3^2)}}\right) \\
\zeta^{0}_{3(1)} &= \operatorname{acos}\left(\frac{-2m_0^2(-m_1^2-m_3^2+\sigma_2)+(m_0^2+m_1^2-\sigma_1)(m_0^2+m_3^2-\sigma_3)}{\sqrt{\lambda(m_0^2,m_1^2,\sigma_1)}\sqrt{\lambda(m_0^2,\sigma_3,m_3^2)}}\right) \\
\zeta^{1}_{3(1)} &= -\operatorname{acos}\left(\frac{2m_1^2(-m_0^2-m_2^2+\sigma_2)+(m_0^2+m_1^2-\sigma_1)(-m_1^2-m_2^2+\sigma_3)}{\sqrt{\lambda(m_0^2,m_1^2,\sigma_1)}\sqrt{\lambda(\sigma_3,m_1^2,m_2^2)}}\right)
\end{aligned}$$

### 1.2.2 Sub-system amplitudes

$$\begin{aligned}
A^{1}_{-\frac{1}{2},-\frac{1}{2}} &= \sum_{\lambda_R=-1}^{1} -\delta_{-\frac{1}{2},\lambda_R+\frac{1}{2}} \mathcal{R}\left(\sigma_1\right) \mathcal{H}^{\text{decay}}_{K(892),0,0} \mathcal{H}^{\text{production}}_{K(892),\lambda_R,-\frac{1}{2}} d^{1}_{\lambda_R,0}\left(\theta_{23}\right) + \sum_{\lambda_R=0} -\delta_{-\frac{1}{2},\lambda_R+\frac{1}{2}} \mathcal{R}_{\text{Bugg}}\left(\sigma_1\right) \mathcal{H}^{\text{decay}}_{K(1430),0,0} \\
A^{2}_{-\frac{1}{2},-\frac{1}{2}} &= \sum_{\lambda_R=-3/2}^{3/2} -\delta_{-\frac{1}{2}\lambda_R} \mathcal{R}\left(\sigma_2\right) \mathcal{H}^{\text{decay}}_{L(1520),0,-\frac{1}{2}} \mathcal{H}^{\text{production}}_{L(1520),\lambda_R,0} d^{\frac{3}{2}}_{\lambda_R,\frac{1}{2}}\left(\theta_{31}\right) + \sum_{\lambda_R=-1/2}^{1/2} -\delta_{-\frac{1}{2}\lambda_R} \mathcal{R}\left(\sigma_2\right) \mathcal{H}^{\text{decay}}_{L(1600),0,-\frac{1}{2}} \mathcal{H} \\
A^{3}_{-\frac{1}{2},-\frac{1}{2}} &= \sum_{\lambda_R=-3/2}^{3/2} \delta_{-\frac{1}{2}\lambda_R} \mathcal{R}\left(\sigma_3\right) \mathcal{H}^{\text{decay}}_{D(1232),-\frac{1}{2},0} \mathcal{H}^{\text{production}}_{D(1232),\lambda_R,0} d^{\frac{3}{2}}_{\lambda_R,-\frac{1}{2}}\left(\theta_{12}\right) + \sum_{\lambda_R=-3/2}^{3/2} \delta_{-\frac{1}{2}\lambda_R} \mathcal{R}\left(\sigma_3\right) \mathcal{H}^{\text{decay}}_{D(1600),-\frac{1}{2},0} \mathcal{H}^{\text{pr}} \\
A^{1}_{-\frac{1}{2},\frac{1}{2}} &= \sum_{\lambda_R=-1}^{1} \delta_{-\frac{1}{2},\lambda_R-\frac{1}{2}} \mathcal{R}\left(\sigma_1\right) \mathcal{H}^{\text{decay}}_{K(892),0,0} \mathcal{H}^{\text{production}}_{K(892),\lambda_R,\frac{1}{2}} d^{1}_{\lambda_R,0}\left(\theta_{23}\right) + \sum_{\lambda_R=0} \delta_{-\frac{1}{2},\lambda_R-\frac{1}{2}} \mathcal{R}_{\text{Bugg}}\left(\sigma_1\right) \mathcal{H}^{\text{decay}}_{K(1430),0,0} \mathcal{H}^{\text{pro}} \\
A^{2}_{-\frac{1}{2},\frac{1}{2}} &= \sum_{\lambda_R=-3/2}^{3/2} \delta_{-\frac{1}{2}\lambda_R} \mathcal{R}\left(\sigma_2\right) \mathcal{H}^{\text{decay}}_{L(1520),0,\frac{1}{2}} \mathcal{H}^{\text{production}}_{L(1520),\lambda_R,0} d^{\frac{3}{2}}_{\lambda_R,-\frac{1}{2}}\left(\theta_{31}\right) + \sum_{\lambda_R=-1/2}^{1/2} \delta_{-\frac{1}{2}\lambda_R} \mathcal{R}\left(\sigma_2\right) \mathcal{H}^{\text{decay}}_{L(1600),0,\frac{1}{2}} \mathcal{H}^{\text{produc}} \\
A^{3}_{-\frac{1}{2},\frac{1}{2}} &= \sum_{\lambda_R=-3/2}^{3/2} \delta_{-\frac{1}{2}\lambda_R} \mathcal{R}\left(\sigma_3\right) \mathcal{H}^{\text{decay}}_{D(1232),\frac{1}{2},0} \mathcal{H}^{\text{production}}_{D(1232),\lambda_R,0} d^{\frac{3}{2}}_{\lambda_R,\frac{1}{2}}\left(\theta_{12}\right) + \sum_{\lambda_R=-3/2}^{3/2} \delta_{-\frac{1}{2}\lambda_R} \mathcal{R}\left(\sigma_3\right) \mathcal{H}^{\text{decay}}_{D(1600),\frac{1}{2},0} \mathcal{H}^{\text{product}} \\
A^{1}_{\frac{1}{2},-\frac{1}{2}} &= \sum_{\lambda_R=-1}^{1} -\delta_{\frac{1}{2},\lambda_R+\frac{1}{2}} \mathcal{R}\left(\sigma_1\right) \mathcal{H}^{\text{decay}}_{K(892),0,0} \mathcal{H}^{\text{production}}_{K(892),\lambda_R,-\frac{1}{2}} d^{1}_{\lambda_R,0}\left(\theta_{23}\right) + \sum_{\lambda_R=0} -\delta_{\frac{1}{2},\lambda_R+\frac{1}{2}} \mathcal{R}_{\text{Bugg}}\left(\sigma_1\right) \mathcal{H}^{\text{decay}}_{K(1430),0,0} \mathcal{H} \\
A^{2}_{\frac{1}{2},-\frac{1}{2}} &= \sum_{\lambda_R=-3/2}^{3/2} -\delta_{\frac{1}{2}\lambda_R} \mathcal{R}\left(\sigma_2\right) \mathcal{H}^{\text{decay}}_{L(1520),0,-\frac{1}{2}} \mathcal{H}^{\text{production}}_{L(1520),\lambda_R,0} d^{\frac{3}{2}}_{\lambda_R,\frac{1}{2}}\left(\theta_{31}\right) + \sum_{\lambda_R=-1/2}^{1/2} -\delta_{\frac{1}{2}\lambda_R} \mathcal{R}\left(\sigma_2\right) \mathcal{H}^{\text{decay}}_{L(1600),0,-\frac{1}{2}} \mathcal{H}^{\text{pro}} \\
A^{3}_{\frac{1}{2},-\frac{1}{2}} &= \sum_{\lambda_R=-3/2}^{3/2} \delta_{\frac{1}{2}\lambda_R} \mathcal{R}\left(\sigma_3\right) \mathcal{H}^{\text{decay}}_{D(1232),-\frac{1}{2},0} \mathcal{H}^{\text{production}}_{D(1232),\lambda_R,0} d^{\frac{3}{2}}_{\lambda_R,-\frac{1}{2}}\left(\theta_{12}\right) + \sum_{\lambda_R=-3/2}^{3/2} \delta_{\frac{1}{2}\lambda_R} \mathcal{R}\left(\sigma_3\right) \mathcal{H}^{\text{decay}}_{D(1600),-\frac{1}{2},0} \mathcal{H}^{\text{produ}} \\
A^{1}_{\frac{1}{2},\frac{1}{2}} &= \sum_{\lambda_R=-1}^{1} \delta_{\frac{1}{2},\lambda_R-\frac{1}{2}} \mathcal{R}\left(\sigma_1\right) \mathcal{H}^{\text{decay}}_{K(892),0,0} \mathcal{H}^{\text{production}}_{K(892),\lambda_R,\frac{1}{2}} d^{1}_{\lambda_R,0}\left(\theta_{23}\right) + \sum_{\lambda_R=0} \delta_{\frac{1}{2},\lambda_R-\frac{1}{2}} \mathcal{R}_{\text{Bugg}}\left(\sigma_1\right) \mathcal{H}^{\text{decay}}_{K(1430),0,0} \mathcal{H}^{\text{product}} \\
A^{2}_{\frac{1}{2},\frac{1}{2}} &= \sum_{\lambda_R=-3/2}^{3/2} \delta_{\frac{1}{2}\lambda_R} \mathcal{R}\left(\sigma_2\right) \mathcal{H}^{\text{decay}}_{L(1520),0,\frac{1}{2}} \mathcal{H}^{\text{production}}_{L(1520),\lambda_R,0} d^{\frac{3}{2}}_{\lambda_R,-\frac{1}{2}}\left(\theta_{31}\right) + \sum_{\lambda_R=-1/2}^{1/2} \delta_{\frac{1}{2}\lambda_R} \mathcal{R}\left(\sigma_2\right) \mathcal{H}^{\text{decay}}_{L(1600),0,\frac{1}{2}} \mathcal{H}^{\text{production}}_{L(1600),} \\
A^{3}_{\frac{1}{2},\frac{1}{2}} &= \sum_{\lambda_R=-3/2}^{3/2} \delta_{\frac{1}{2}\lambda_R} \mathcal{R}\left(\sigma_3\right) \mathcal{H}^{\text{decay}}_{D(1232),\frac{1}{2},0} \mathcal{H}^{\text{production}}_{D(1232),\lambda_R,0} d^{\frac{3}{2}}_{\lambda_R,\frac{1}{2}}\left(\theta_{12}\right) + \sum_{\lambda_R=-3/2}^{3/2} \delta_{\frac{1}{2}\lambda_R} \mathcal{R}\left(\sigma_3\right) \mathcal{H}^{\text{decay}}_{D(1600),\frac{1}{2},0} \mathcal{H}^{\text{production}}_{D(1600),\lambda}
\end{aligned}$$

The $\theta_{ij}$ angles are *defined as* (page 52):

$$
\begin{aligned}
\theta_{23} &= \operatorname{acos}\left(\frac{2\sigma_1\left(-m_1^2-m_2^2+\sigma_3\right)-\left(m_0^2-m_1^2-\sigma_1\right)\left(m_2^2-m_3^2+\sigma_1\right)}{\sqrt{\lambda\left(m_0^2,m_1^2,\sigma_1\right)}\sqrt{\lambda\left(\sigma_1,m_2^2,m_3^2\right)}}\right)\\
\theta_{31} &= \operatorname{acos}\left(\frac{2\sigma_2\left(-m_2^2-m_3^2+\sigma_1\right)-\left(m_0^2-m_2^2-\sigma_2\right)\left(-m_1^2+m_3^2+\sigma_2\right)}{\sqrt{\lambda\left(m_0^2,m_2^2,\sigma_2\right)}\sqrt{\lambda\left(\sigma_2,m_3^2,m_1^2\right)}}\right)\\
\theta_{12} &= \operatorname{acos}\left(\frac{2\sigma_3\left(-m_1^2-m_3^2+\sigma_2\right)-\left(m_0^2-m_3^2-\sigma_3\right)\left(m_1^2-m_2^2+\sigma_3\right)}{\sqrt{\lambda\left(m_0^2,m_3^2,\sigma_3\right)}\sqrt{\lambda\left(\sigma_3,m_1^2,m_2^2\right)}}\right)
\end{aligned}
$$

Definitions for the $\phi_{ij}$ angles can be found under *DPD angles* (page 52).

## 1.3 Parameter definitions

Parameter values are provided in `model-definitions.yaml`, but the **keys** of the helicity couplings have to remapped to the helicity **symbols** that are used in this amplitude model. The function *`parameter_key_to_symbol()`* (page 75) implements this remapping, following the supplementary material of [1]. It is asserted below that:

1. the keys are mapped to symbols that exist in the nominal amplitude model
2. all parameter symbols in the nominal amplitude model have a value assigned to them.

### 1.3.1 Helicity coupling values

### Production couplings

$$
\begin{aligned}
\mathcal{H}^\text{production}_{K(892),-1,-\frac{1}{2}} &= 1.192614 - 1.025814i \\
\mathcal{H}^\text{production}_{L(1405),-\frac{1}{2},0} &= -4.572486 + 3.190144i \\
\mathcal{H}^\text{production}_{L(1520),-\frac{1}{2},0} &= 0.293998 + 0.044324i \\
\mathcal{H}^\text{production}_{L(1600),-\frac{1}{2},0} &= -4.840649 - 3.082786i \\
\mathcal{H}^\text{production}_{L(1670),-\frac{1}{2},0} &= -0.339585 - 0.144678i \\
\mathcal{H}^\text{production}_{L(1690),-\frac{1}{2},0} &= -0.385772 - 0.110235i \\
\mathcal{H}^\text{production}_{L(2000),-\frac{1}{2},0} &= -8.014857 - 7.614006i \\
\mathcal{H}^\text{production}_{D(1232),-\frac{1}{2},0} &= -6.778191 + 3.051805i \\
\mathcal{H}^\text{production}_{D(1600),-\frac{1}{2},0} &= 11.401585 - 3.125511i \\
\mathcal{H}^\text{production}_{D(1700),-\frac{1}{2},0} &= -10.37828 - 1.434872i \\
\mathcal{H}^\text{production}_{K(700),0,\frac{1}{2}} &= 0.068908 + 2.521444i \\
\mathcal{H}^\text{production}_{K(892),0,\frac{1}{2}} &= -0.727145 - 4.155027i \\
\mathcal{H}^\text{production}_{K(1430),0,\frac{1}{2}} &= -6.71516 + 10.479411i \\
\mathcal{H}^\text{production}_{K(700),0,-\frac{1}{2}} &= -2.68563 + 0.03849i \\
\mathcal{H}^\text{production}_{K(892),0,-\frac{1}{2}} &= 1 + 0i \\
\mathcal{H}^\text{production}_{K(1430),0,-\frac{1}{2}} &= 0.219754 + 8.741196i \\
\mathcal{H}^\text{production}_{L(1405),\frac{1}{2},0} &= 10.44608 + 2.787441i \\
\mathcal{H}^\text{production}_{L(1520),\frac{1}{2},0} &= -0.160687 + 1.498833i \\
\mathcal{H}^\text{production}_{L(1600),\frac{1}{2},0} &= 6.971233 - 0.842435i \\
\mathcal{H}^\text{production}_{L(1670),\frac{1}{2},0} &= -0.570978 + 1.011833i \\
\mathcal{H}^\text{production}_{L(1690),\frac{1}{2},0} &= -2.730592 - 0.353613i \\
\mathcal{H}^\text{production}_{L(2000),\frac{1}{2},0} &= -4.336255 - 3.796192i \\
\mathcal{H}^\text{production}_{D(1232),\frac{1}{2},0} &= -12.987193 + 4.528336i \\
\mathcal{H}^\text{production}_{D(1600),\frac{1}{2},0} &= 6.729211 - 1.002383i \\
\mathcal{H}^\text{production}_{D(1700),\frac{1}{2},0} &= -12.874102 - 2.10557i \\
\mathcal{H}^\text{production}_{K(892),1,\frac{1}{2}} &= -3.141446 - 3.29341i
\end{aligned}
$$

### Decay couplings

$$
\begin{aligned}
\mathcal{H}^\mathrm{decay}_{K(892),0,0} &= 1 \\
\mathcal{H}^\mathrm{decay}_{L(1405),0,-\frac{1}{2}} &= 1 \\
\mathcal{H}^\mathrm{decay}_{L(1520),0,-\frac{1}{2}} &= -1 \\
\mathcal{H}^\mathrm{decay}_{L(1600),0,-\frac{1}{2}} &= -1 \\
\mathcal{H}^\mathrm{decay}_{L(1670),0,-\frac{1}{2}} &= 1 \\
\mathcal{H}^\mathrm{decay}_{L(1690),0,-\frac{1}{2}} &= -1 \\
\mathcal{H}^\mathrm{decay}_{L(2000),0,-\frac{1}{2}} &= 1 \\
\mathcal{H}^\mathrm{decay}_{D(1232),-\frac{1}{2},0} &= 1 \\
\mathcal{H}^\mathrm{decay}_{D(1600),-\frac{1}{2},0} &= 1 \\
\mathcal{H}^\mathrm{decay}_{D(1700),-\frac{1}{2},0} &= -1 \\
\mathcal{H}^\mathrm{decay}_{K(700),0,0} &= 1 \\
\mathcal{H}^\mathrm{decay}_{K(1430),0,0} &= 1 \\
\mathcal{H}^\mathrm{decay}_{L(1405),0,\frac{1}{2}} &= 1 \\
\mathcal{H}^\mathrm{decay}_{L(1520),0,\frac{1}{2}} &= 1 \\
\mathcal{H}^\mathrm{decay}_{L(1600),0,\frac{1}{2}} &= 1 \\
\mathcal{H}^\mathrm{decay}_{L(1670),0,\frac{1}{2}} &= 1 \\
\mathcal{H}^\mathrm{decay}_{L(1690),0,\frac{1}{2}} &= 1 \\
\mathcal{H}^\mathrm{decay}_{L(2000),0,\frac{1}{2}} &= 1 \\
\mathcal{H}^\mathrm{decay}_{D(1232),\frac{1}{2},0} &= 1 \\
\mathcal{H}^\mathrm{decay}_{D(1600),\frac{1}{2},0} &= 1 \\
\mathcal{H}^\mathrm{decay}_{D(1700),\frac{1}{2},0} &= 1
\end{aligned}
$$

### 1.3.2 Non-coupling parameters

$$
\begin{aligned}
R_{\mathrm{res}} &= 1.5 \\
R_{\Lambda_c} &= 5 \\
\Gamma_{D(1232)} &= 0.117 \\
\Gamma_{D(1600)} &= 0.3 \\
\Gamma_{D(1700)} &= 0.38 \\
\Gamma_{K(1430)} &= 0.19 \\
\Gamma_{K(700)} &= 0.47800000000000004 \\
\Gamma_{K(892)} &= 0.047299999999999995 \\
\Gamma_{L(1405)\to\Sigma^-\pi^+} &= 0.0505 \\
\Gamma_{L(1405)\to pK^-} &= 0.0505 \\
\Gamma_{L(1520)} &= 0.015195 \\
\Gamma_{L(1600)} &= 0.25 \\
\Gamma_{L(1670)} &= 0.03 \\
\Gamma_{L(1690)} &= 0.07 \\
\Gamma_{L(2000)} &= 0.17926 \\
\gamma_{K(1430)} &= 0.020981 \\
\gamma_{K(700)} &= 0.94106 \\
m_0 &= 2.28646 \\
m_1 &= 0.938272046 \\
m_2 &= 0.13957018 \\
m_3 &= 0.49367700000000003 \\
m_{D(1232)} &= 1.232 \\
m_{D(1600)} &= 1.6400000000000001 \\
m_{D(1700)} &= 1.69 \\
m_{K(1430)} &= 1.375 \\
m_{K(700)} &= 0.8240000000000001 \\
m_{K(892)} &= 0.8955000000000001 \\
m_{K-} &= 0.49367700000000003 \\
m_{L(1405)} &= 1.4051 \\
m_{L(1520)} &= 1.518467 \\
m_{L(1600)} &= 1.6300000000000001 \\
m_{L(1670)} &= 1.67 \\
m_{L(1690)} &= 1.69 \\
m_{L(2000)} &= 1.98819 \\
m_{Lambda_c+} &= 2.28646 \\
m_{Sigma-} &= 1.1893699999999998 \\
m_{pi+} &= 0.13957018 \\
m_p &= 0.938272046
\end{aligned}
$$

CHAPTER

# TWO

# CROSS-CHECK WITH LHCB DATA

## 2.1 Lineshape comparison

We compute a few lineshapes for the following point in phase space and compare it with the values from [1]:

```
{'costhetap': -0.9949949110827053,
 'm2kpi': 0.7980703453578917,
 'm2pk': 3.6486261122281745,
 'phikpi': -0.4,
 'phip': -0.3}
```

The lineshapes are computed for the following decay chains:

$$\Lambda_c^+ \xrightarrow[S=1/2]{L=0} K(892) \xrightarrow[S=0]{L=1} \pi^+ K^- p$$
$$\Lambda_c^+ \xrightarrow[S=1/2]{L=0} \Lambda(1405) \xrightarrow[S=1/2]{L=0} K^- p \pi^+$$
$$\Lambda_c^+ \xrightarrow[S=3/2]{L=1} \Lambda(1690) \xrightarrow[S=1/2]{L=2} K^- p \pi^+$$

```
{'BW_K(892)_p^1_q^0': '(2.1687201455088894+23.58225917009096j)',
 'BW_L(1405)_p^0_q^0': '(-0.5636481410171861+0.13763637759224928j)',
 'BW_L(1690)_p^2_q^1': '(-1.5078327158518026+0.9775036395061584j)'}
```

$$2.16872014550901 + 23.5822591700909i$$
$$-0.563648141017186 + 0.137636377592249i$$
$$-1.5078327158518 + 0.977503639506157i$$

**Tip:** These values are **equal up to 13 decimals**.

## 2.2 Amplitude comparison

The amplitude for each decay chain and each outer state helicity combination are evaluated on the following point in phase space:

$$
\begin{aligned}
\theta_{23} &= 1.821341166520149 \\
\theta_{31} &= 1.8038351483715633 \\
\theta_{12} &= 1.1139045236042229 \\
\zeta^0_{1(1)} &= 0.0 \\
\zeta^1_{1(1)} &= 0.0 \\
\zeta^0_{2(1)} &= -2.0777687076712614 \\
\zeta^1_{2(1)} &= 0.22583331080386268 \\
\zeta^0_{3(1)} &= 2.6540796539955838 \\
\zeta^1_{3(1)} &= -0.5594175047790548 \\
\sigma_1 &= 0.7980703453578917 \\
\sigma_2 &= 3.6486261122281745 \\
\sigma_3 &= 1.9247541217931925
\end{aligned}
$$

### 2.2.1 Default model

**Tip:** Computed amplitudes are equal to LHCb amplitudes up to **13 decimals**.

| | Computed | Expected | Difference |
|---|---|---|---|
| **ArD(1232)1** | $\mathcal{H}^\text{production}_{D(1232),-\frac{1}{2},0}$ | | |
| A++ | -0.488498+0.517710j | -0.488498+0.517710j | 3.08e-14 |
| A+- | 0.894898-0.948412j | 0.894898-0.948412j | 7.14e-15 |
| A-+ | 0.121490-0.128755j | 0.121490-0.128755j | 1.80e-14 |
| A-- | -0.222563+0.235872j | -0.222563+0.235872j | 6.36e-15 |
| **ArD(1232)2** | $\mathcal{H}^\text{production}_{D(1232),\frac{1}{2},0}$ | | |
| A++ | -0.222563+0.235872j | -0.222563+0.235872j | 6.36e-15 |
| A+- | -0.121490+0.128755j | -0.121490+0.128755j | 1.80e-14 |
| A-+ | -0.894898+0.948412j | -0.894898+0.948412j | 7.14e-15 |
| A-- | -0.488498+0.517710j | -0.488498+0.517710j | 3.08e-14 |
| **ArD(1600)1** | $\mathcal{H}^\text{production}_{D(1600),-\frac{1}{2},0}$ | | |
| A++ | 0.289160+0.081910j | 0.289160+0.081910j | 3.07e-14 |
| A+- | -0.529724-0.150054j | -0.529724-0.150054j | 6.87e-15 |
| A-+ | -0.071915-0.020371j | -0.071915-0.020371j | 1.80e-14 |
| A-- | 0.131743+0.037319j | 0.131743+0.037319j | 5.91e-15 |
| **ArD(1600)2** | $\mathcal{H}^\text{production}_{D(1600),\frac{1}{2},0}$ | | |
| A++ | 0.131743+0.037319j | 0.131743+0.037319j | 5.91e-15 |
| A+- | 0.071915+0.020371j | 0.071915+0.020371j | 1.80e-14 |
| A-+ | 0.529724+0.150054j | 0.529724+0.150054j | 6.87e-15 |
| A-- | 0.289160+0.081910j | 0.289160+0.081910j | 3.07e-14 |
| **ArD(1700)1** | $\mathcal{H}^\text{production}_{D(1700),-\frac{1}{2},0}$ | | |
| A++ | -0.018885-0.001757j | -0.018885-0.001757j | 3.20e-13 |
| A+- | 0.315695+0.029366j | 0.315695+0.029366j | 2.00e-14 |
| A-+ | 0.004697+0.000437j | 0.004697+0.000437j | 3.34e-13 |
| A-- | -0.078514-0.007303j | -0.078514-0.007303j | 6.86e-15 |
| **ArD(1700)2** | $\mathcal{H}^\text{production}_{D(1700),\frac{1}{2},0}$ | | |
| A++ | 0.078514+0.007303j | 0.078514+0.007303j | 6.86e-15 |
| A+- | 0.004697+0.000437j | 0.004697+0.000437j | 3.34e-13 |
| A-+ | 0.315695+0.029366j | 0.315695+0.029366j | 2.00e-14 |

continues on next page

Table 2.1 – continued from previous page

| | Computed | Expected | Difference |
|---|---|---|---|
| A-- | 0.018885+0.001757j | 0.018885+0.001757j | 3.20e-13 |
| **ArK(892)1** | $\mathcal{H}^{\text{production}}_{K(892),0,-\frac{1}{2}}$ | | |
| A++ | -0.537695-5.846793j | -0.537695-5.846793j | 4.88e-15 |
| A+- | 0.000000+0.000000j | 0.000000+0.000000j | |
| A-+ | -0.000000+0.000000j | 0.000000+0.000000j | |
| A-- | 0.000000+0.000000j | 0.000000+0.000000j | |
| **ArK(892)2** | $\mathcal{H}^{\text{production}}_{K(892),-1,-\frac{1}{2}}$ | | |
| A++ | -0.000000+0.000000j | 0.000000+0.000000j | |
| A+- | 0.000000+0.000000j | 0.000000+0.000000j | |
| A-+ | 1.485636+16.154534j | 1.485636+16.154534j | 3.42e-15 |
| A-- | 0.000000+0.000000j | 0.000000+0.000000j | |
| **ArK(892)3** | $\mathcal{H}^{\text{production}}_{K(892),1,\frac{1}{2}}$ | | |
| A++ | -0.000000+0.000000j | 0.000000+0.000000j | |
| A+- | -1.485636-16.154534j | -1.485636-16.154534j | 3.32e-15 |
| A-+ | -0.000000+0.000000j | 0.000000+0.000000j | |
| A-- | 0.000000+0.000000j | 0.000000+0.000000j | |
| **ArK(892)4** | $\mathcal{H}^{\text{production}}_{K(892),0,\frac{1}{2}}$ | | |
| A++ | -0.000000+0.000000j | 0.000000+0.000000j | |
| A+- | 0.000000+0.000000j | 0.000000+0.000000j | |
| A-+ | -0.000000+0.000000j | 0.000000+0.000000j | |
| A-- | -0.537695-5.846793j | -0.537695-5.846793j | 4.88e-15 |
| **ArK(1430)1** | $\mathcal{H}^{\text{production}}_{K(1430),0,\frac{1}{2}}$ | | |
| A++ | -0.000000+0.000000j | 0.000000+0.000000j | |
| A+- | 0.000000+0.000000j | 0.000000+0.000000j | |
| A-+ | -0.000000+0.000000j | 0.000000+0.000000j | |
| A-- | 0.909456+0.072819j | 0.909456+0.072819j | 1.37e-16 |
| **ArK(1430)2** | $\mathcal{H}^{\text{production}}_{K(1430),0,-\frac{1}{2}}$ | | |
| A++ | 0.909456+0.072819j | 0.909456+0.072819j | 1.37e-16 |
| A+- | 0.000000+0.000000j | 0.000000+0.000000j | |
| A-+ | -0.000000+0.000000j | 0.000000+0.000000j | |
| A-- | 0.000000+0.000000j | 0.000000+0.000000j | |
| **ArK(700)1** | $\mathcal{H}^{\text{production}}_{K(700),0,\frac{1}{2}}$ | | |
| A++ | -0.000000+0.000000j | 0.000000+0.000000j | |
| A+- | 0.000000+0.000000j | 0.000000+0.000000j | |
| A-+ | -0.000000+0.000000j | 0.000000+0.000000j | |
| A-- | -1.708879+3.380634j | -1.708879+3.380634j | 4.97e-16 |
| **ArK(700)2** | $\mathcal{H}^{\text{production}}_{K(700),0,-\frac{1}{2}}$ | | |
| A++ | -1.708879+3.380634j | -1.708879+3.380634j | 4.97e-16 |
| A+- | 0.000000+0.000000j | 0.000000+0.000000j | |
| A-+ | -0.000000+0.000000j | 0.000000+0.000000j | |
| A-- | 0.000000+0.000000j | 0.000000+0.000000j | |
| **ArL(1405)1** | $\mathcal{H}^{\text{production}}_{L(1405),-\frac{1}{2},0}$ | | |
| A++ | -0.412613+0.100755j | -0.412613+0.100755j | 1.49e-15 |
| A+- | -0.256372+0.062603j | -0.256372+0.062603j | 3.27e-15 |
| A-+ | -0.242818+0.059293j | -0.242818+0.059293j | 1.30e-15 |
| A-- | -0.150872+0.036841j | -0.150872+0.036841j | 3.42e-15 |
| **ArL(1405)2** | $\mathcal{H}^{\text{production}}_{L(1405),\frac{1}{2},0}$ | | |
| A++ | -0.150872+0.036841j | -0.150872+0.036841j | 3.42e-15 |
| A+- | 0.242818-0.059293j | 0.242818-0.059293j | 1.30e-15 |
| A-+ | 0.256372-0.062603j | 0.256372-0.062603j | 3.27e-15 |

continues on next page

Table 2.1 – continued from previous page

| | Computed | Expected | Difference |
|---|---|---|---|
| A-- | -0.412613+0.100755j | -0.412613+0.100755j | 1.49e-15 |
| **ArL(1520)1** | $\mathcal{H}^{\text{production}}_{L(1520),-\frac{1}{2},0}$ | | |
| A++ | 0.257632-0.288056j | 0.257632-0.288056j | 1.56e-14 |
| A+- | 0.731594-0.817988j | 0.731594-0.817988j | 2.29e-14 |
| A-+ | 0.151613-0.169517j | 0.151613-0.169517j | 1.55e-14 |
| A-- | 0.430534-0.481376j | 0.430534-0.481376j | 2.30e-14 |
| **ArL(1520)2** | $\mathcal{H}^{\text{production}}_{L(1520),\frac{1}{2},0}$ | | |
| A++ | -0.430534+0.481376j | -0.430534+0.481376j | 2.29e-14 |
| A+- | 0.151613-0.169517j | 0.151613-0.169517j | 1.55e-14 |
| A-+ | 0.731594-0.817988j | 0.731594-0.817988j | 2.28e-14 |
| A-- | -0.257632+0.288056j | -0.257632+0.288056j | 1.55e-14 |
| **ArL(1600)1** | $\mathcal{H}^{\text{production}}_{L(1600),-\frac{1}{2},0}$ | | |
| A++ | -0.385436+0.424707j | -0.385436+0.424707j | 1.35e-15 |
| A+- | 0.382669-0.421658j | 0.382669-0.421658j | 3.75e-15 |
| A-+ | -0.226825+0.249935j | -0.226825+0.249935j | 1.60e-15 |
| A-- | 0.225196-0.248141j | 0.225196-0.248141j | 3.56e-15 |
| **ArL(1600)2** | $\mathcal{H}^{\text{production}}_{L(1600),\frac{1}{2},0}$ | | |
| A++ | -0.225196+0.248141j | -0.225196+0.248141j | 3.60e-15 |
| A+- | -0.226825+0.249935j | -0.226825+0.249935j | 1.60e-15 |
| A-+ | 0.382669-0.421658j | 0.382669-0.421658j | 3.80e-15 |
| A-- | 0.385436-0.424707j | 0.385436-0.424707j | 1.44e-15 |
| **ArL(1670)1** | $\mathcal{H}^{\text{production}}_{L(1670),-\frac{1}{2},0}$ | | |
| A++ | -0.846639+0.064025j | -0.846639+0.064025j | 1.18e-15 |
| A+- | -0.526049+0.039781j | -0.526049+0.039781j | 3.17e-15 |
| A-+ | -0.498237+0.037678j | -0.498237+0.037678j | 1.11e-15 |
| A-- | -0.309574+0.023411j | -0.309574+0.023411j | 3.59e-15 |
| **ArL(1670)2** | $\mathcal{H}^{\text{production}}_{L(1670),\frac{1}{2},0}$ | | |
| A++ | -0.309574+0.023411j | -0.309574+0.023411j | 3.59e-15 |
| A+- | 0.498237-0.037678j | 0.498237-0.037678j | 1.11e-15 |
| A-+ | 0.526049-0.039781j | 0.526049-0.039781j | 3.17e-15 |
| A-- | -0.846639+0.064025j | -0.846639+0.064025j | 1.18e-15 |
| **ArL(1690)1** | $\mathcal{H}^{\text{production}}_{L(1690),-\frac{1}{2},0}$ | | |
| A++ | 0.232446-0.150691j | 0.232446-0.150691j | 1.66e-14 |
| A+- | 0.660073-0.427915j | 0.660073-0.427915j | 2.37e-14 |
| A-+ | 0.136791-0.088680j | 0.136791-0.088680j | 1.65e-14 |
| A-- | 0.388445-0.251823j | 0.388445-0.251823j | 2.37e-14 |
| **ArL(1690)2** | $\mathcal{H}^{\text{production}}_{L(1690),\frac{1}{2},0}$ | | |
| A++ | -0.388445+0.251823j | -0.388445+0.251823j | 2.36e-14 |
| A+- | 0.136791-0.088680j | 0.136791-0.088680j | 1.65e-14 |
| A-+ | 0.660073-0.427915j | 0.660073-0.427915j | 2.37e-14 |
| A-- | -0.232446+0.150691j | -0.232446+0.150691j | 1.66e-14 |
| **ArL(2000)1** | $\mathcal{H}^{\text{production}}_{L(2000),-\frac{1}{2},0}$ | | |
| A++ | 1.072514+1.195841j | 1.072514+1.195841j | 1.47e-15 |
| A+- | 0.666394+0.743022j | 0.666394+0.743022j | 2.94e-15 |
| A-+ | 0.631162+0.703738j | 0.631162+0.703738j | 1.34e-15 |
| A-- | 0.392165+0.437260j | 0.392165+0.437260j | 3.29e-15 |
| **ArL(2000)2** | $\mathcal{H}^{\text{production}}_{L(2000),\frac{1}{2},0}$ | | |
| A++ | 0.392165+0.437260j | 0.392165+0.437260j | 3.29e-15 |
| A+- | -0.631162-0.703738j | -0.631162-0.703738j | 1.34e-15 |
| A-+ | -0.666394-0.743022j | -0.666394-0.743022j | 2.94e-15 |

continues on next page

Table 2.1 – continued from previous page

| | Computed | Expected | Difference |
|---|---|---|---|
| A-- | 1.072514+1.195841j | 1.072514+1.195841j | 1.47e-15 |

### 2.2.2 LS-model

**Tip:** Computed amplitudes are equal to LHCb amplitudes up to **13 decimals**.

| | Computed | Expected | Difference |
|---|---|---|---|
| **ArD(1232)1** | $\mathcal{H}^{\mathrm{LS,production}}_{D(1232),1,\frac{3}{2}}$ | | |
| A++ | 0.502796-0.532862j | 0.502796-0.532862j | 1.91e-14 |
| A+- | -0.546882+0.579585j | -0.546882+0.579585j | 5.18e-15 |
| A-+ | 0.546882-0.579585j | 0.546882-0.579585j | 5.18e-15 |
| A-- | 0.502796-0.532862j | 0.502796-0.532862j | 1.91e-14 |
| **ArD(1232)2** | $\mathcal{H}^{\mathrm{LS,production}}_{D(1232),2,\frac{3}{2}}$ | | |
| A++ | -0.180489+0.191282j | -0.180489+0.191282j | 5.49e-14 |
| A+- | 0.689818-0.731068j | 0.689818-0.731068j | 2.43e-15 |
| A-+ | 0.689818-0.731068j | 0.689818-0.731068j | 2.32e-15 |
| A-- | 0.180489-0.191282j | 0.180489-0.191282j | 5.49e-14 |
| **ArD(1600)1** | $\mathcal{H}^{\mathrm{LS,production}}_{D(1600),1,\frac{3}{2}}$ | | |
| A++ | -0.297624-0.084307j | -0.297624-0.084307j | 1.79e-14 |
| A+- | 0.323720+0.091699j | 0.323720+0.091699j | 3.99e-15 |
| A-+ | -0.323720-0.091699j | -0.323720-0.091699j | 3.99e-15 |
| A-- | -0.297624-0.084307j | -0.297624-0.084307j | 1.79e-14 |
| **ArD(1600)2** | $\mathcal{H}^{\mathrm{LS,production}}_{D(1600),2,\frac{3}{2}}$ | | |
| A++ | 0.143541+0.040660j | 0.143541+0.040660j | 5.47e-14 |
| A+- | -0.548604-0.155402j | -0.548604-0.155402j | 1.92e-15 |
| A-+ | -0.548604-0.155402j | -0.548604-0.155402j | 1.80e-15 |
| A-- | -0.143541-0.040660j | -0.143541-0.040660j | 5.44e-14 |
| **ArD(1700)1** | $\mathcal{H}^{\mathrm{LS,production}}_{D(1700),1,\frac{3}{2}}$ | | |
| A++ | -0.042164-0.003922j | -0.042164-0.003922j | 1.10e-13 |
| A+- | -0.226551-0.021074j | -0.226551-0.021074j | 1.42e-14 |
| A-+ | -0.226551-0.021074j | -0.226551-0.021074j | 1.42e-14 |
| A-- | 0.042164+0.003922j | 0.042164+0.003922j | 1.11e-13 |
| **ArD(1700)2** | $\mathcal{H}^{\mathrm{LS,production}}_{D(1700),2,\frac{3}{2}}$ | | |
| A++ | -0.105349-0.009800j | -0.105349-0.009800j | 5.87e-14 |
| A+- | 0.336381+0.031290j | 0.336381+0.031290j | 2.29e-14 |
| A-+ | -0.336381-0.031290j | -0.336381-0.031290j | 2.29e-14 |
| A-- | -0.105349-0.009800j | -0.105349-0.009800j | 5.85e-14 |
| **ArK(892)1** | $\mathcal{H}^{\mathrm{LS,production}}_{K(892),0,\frac{1}{2}}$ | | |
| A++ | 0.219513+2.386943j | 0.219513+2.386943j | 4.88e-15 |
| A+- | -0.857733-9.326825j | -0.857733-9.326825j | 3.64e-15 |
| A-+ | -0.857733-9.326825j | -0.857733-9.326825j | 3.64e-15 |
| A-- | -0.219513-2.386943j | -0.219513-2.386943j | 4.88e-15 |
| **ArK(892)2** | $\mathcal{H}^{\mathrm{LS,production}}_{K(892),1,\frac{1}{2}}$ | | |
| A++ | 0.219549+2.387337j | 0.219549+2.387337j | 7.18e-15 |
| A+- | -0.857874-9.328364j | -0.857874-9.328364j | 2.84e-15 |
| A-+ | 0.857874+9.328364j | 0.857874+9.328364j | 2.78e-15 |
| A-- | 0.219549+2.387337j | 0.219549+2.387337j | 7.18e-15 |

continues on next page

Table 2.2 – continued from previous page

| | Computed | Expected | Difference |
|---|---|---|---|
| **ArK(892)3** | $\mathcal{H}^{\mathrm{LS,production}}_{K(892),1,\frac{3}{2}}$ | | |
| A++ | 0.310489+3.376204j | 0.310489+3.376204j | 4.51e-15 |
| A+- | 0.606609+6.596150j | 0.606609+6.596150j | 2.78e-15 |
| A-+ | -0.606609-6.596150j | -0.606609-6.596150j | 2.76e-15 |
| A-- | 0.310489+3.376204j | 0.310489+3.376204j | 4.51e-15 |
| **ArK(892)4** | $\mathcal{H}^{\mathrm{LS,production}}_{K(892),2,\frac{3}{2}}$ | | |
| A++ | 0.310629+3.377724j | 0.310629+3.377724j | 1.38e-14 |
| A+- | 0.606882+6.599119j | 0.606882+6.599119j | 7.79e-15 |
| A-+ | 0.606882+6.599119j | 0.606882+6.599119j | 7.79e-15 |
| A-- | -0.310629-3.377724j | -0.310629-3.377724j | 1.38e-14 |
| **ArK(1430)1** | $\mathcal{H}^{\mathrm{LS,production}}_{K(1430),0,\frac{1}{2}}$ | | |
| A++ | 0.643091+0.051436j | 0.643091+0.051436j | 1.29e-16 |
| A+- | 0.000000+0.000000j | 0.000000+0.000000j | |
| A-+ | -0.000000+0.000000j | 0.000000+0.000000j | |
| A-- | 0.643091+0.051436j | 0.643091+0.051436j | 1.29e-16 |
| **ArK(1430)2** | $\mathcal{H}^{\mathrm{LS,production}}_{K(1430),1,\frac{1}{2}}$ | | |
| A++ | -0.643091-0.051436j | -0.643091-0.051436j | 2.22e-16 |
| A+- | 0.000000+0.000000j | 0.000000+0.000000j | |
| A-+ | -0.000000+0.000000j | 0.000000+0.000000j | |
| A-- | 0.643091+0.051436j | 0.643091+0.051436j | 2.22e-16 |
| **ArK(700)1** | $\mathcal{H}^{\mathrm{LS,production}}_{K(700),0,\frac{1}{2}}$ | | |
| A++ | -1.070937+2.282902j | -1.070937+2.282902j | 3.94e-16 |
| A+- | 0.000000+0.000000j | 0.000000+0.000000j | |
| A-+ | -0.000000+0.000000j | 0.000000+0.000000j | |
| A-- | -1.070937+2.282902j | -1.070937+2.282902j | 3.94e-16 |
| **ArK(700)2** | $\mathcal{H}^{\mathrm{LS,production}}_{K(700),1,\frac{1}{2}}$ | | |
| A++ | 1.070937-2.282902j | 1.070937-2.282902j | 4.40e-16 |
| A+- | 0.000000+0.000000j | 0.000000+0.000000j | |
| A-+ | -0.000000+0.000000j | 0.000000+0.000000j | |
| A-- | -1.070937+2.282902j | -1.070937+2.282902j | 4.40e-16 |
| **ArL(1405)1** | $\mathcal{H}^{\mathrm{LS,production}}_{L(1405),0,\frac{1}{2}}$ | | |
| A++ | -0.398444+0.097295j | -0.398444+0.097295j | 8.23e-16 |
| A+- | -0.009584+0.002340j | -0.009584+0.002340j | 7.99e-14 |
| A-+ | 0.009584-0.002340j | 0.009584-0.002340j | 8.05e-14 |
| A-- | -0.398444+0.097295j | -0.398444+0.097295j | 8.56e-16 |
| **ArL(1405)2** | $\mathcal{H}^{\mathrm{LS,production}}_{L(1405),1,\frac{1}{2}}$ | | |
| A++ | 0.163270-0.039869j | 0.163270-0.039869j | 2.06e-14 |
| A+- | 0.311387-0.076037j | 0.311387-0.076037j | 2.50e-14 |
| A-+ | 0.311387-0.076037j | 0.311387-0.076037j | 2.50e-14 |
| A-- | -0.163270+0.039869j | -0.163270+0.039869j | 2.04e-14 |
| **ArL(1520)1** | $\mathcal{H}^{\mathrm{LS,production}}_{L(1520),1,\frac{3}{2}}$ | | |
| A++ | 0.117387-0.135999j | 0.117387-0.135999j | 3.12e-14 |
| A+- | -0.599627+0.694701j | -0.599627+0.694701j | 1.92e-14 |
| A-+ | -0.599627+0.694701j | -0.599627+0.694701j | 1.92e-14 |
| A-- | -0.117387+0.135999j | -0.117387+0.135999j | 3.12e-14 |
| **ArL(1520)2** | $\mathcal{H}^{\mathrm{LS,production}}_{L(1520),2,\frac{3}{2}}$ | | |
| A++ | 0.330006-0.382330j | 0.330006-0.382330j | 7.45e-14 |
| A+- | 0.278127-0.322225j | 0.278127-0.322225j | 7.90e-14 |
| A-+ | -0.278127+0.322225j | -0.278127+0.322225j | 7.90e-14 |
| A-- | 0.330006-0.382330j | 0.330006-0.382330j | 7.45e-14 |

continues on next page

Table 2.2 – continued from previous page

| | Computed | Expected | Difference |
|---|---|---|---|
| **ArL(1600)1** | $\mathcal{H}^{\mathrm{LS,production}}_{L(1600),0,\frac{1}{2}}$ | | |
| A++ | -0.431782+0.475775j | -0.431782+0.475775j | 1.40e-15 |
| A+- | 0.110199-0.121426j | 0.110199-0.121426j | 9.54e-15 |
| A-+ | 0.110199-0.121426j | 0.110199-0.121426j | 9.90e-15 |
| A-- | 0.431782-0.475775j | 0.431782-0.475775j | 1.40e-15 |
| **ArL(1600)2** | $\mathcal{H}^{\mathrm{LS,production}}_{L(1600),1,\frac{1}{2}}$ | | |
| A++ | 0.102310-0.112734j | 0.102310-0.112734j | 3.05e-14 |
| A+- | -0.389148+0.428797j | -0.389148+0.428797j | 2.21e-14 |
| A-+ | 0.389148-0.428797j | 0.389148-0.428797j | 2.22e-14 |
| A-- | 0.102310-0.112734j | 0.102310-0.112734j | 3.05e-14 |
| **ArL(1670)1** | $\mathcal{H}^{\mathrm{LS,production}}_{L(1670),0,\frac{1}{2}}$ | | |
| A++ | -0.817566+0.061827j | -0.817566+0.061827j | 1.69e-16 |
| A+- | -0.019666+0.001487j | -0.019666+0.001487j | 7.61e-14 |
| A-+ | 0.019666-0.001487j | 0.019666-0.001487j | 7.62e-14 |
| A-- | -0.817566+0.061827j | -0.817566+0.061827j | 1.69e-16 |
| **ArL(1670)2** | $\mathcal{H}^{\mathrm{LS,production}}_{L(1670),1,\frac{1}{2}}$ | | |
| A++ | 0.345271-0.026110j | 0.345271-0.026110j | 1.85e-14 |
| A+- | 0.658498-0.049798j | 0.658498-0.049798j | 2.38e-14 |
| A-+ | 0.658498-0.049798j | 0.658498-0.049798j | 2.39e-14 |
| A-- | -0.345271+0.026110j | -0.345271+0.026110j | 1.87e-14 |
| **ArL(1690)1** | $\mathcal{H}^{\mathrm{LS,production}}_{L(1690),1,\frac{3}{2}}$ | | |
| A++ | 0.110308-0.071511j | 0.110308-0.071511j | 3.03e-14 |
| A+- | -0.563468+0.365287j | -0.563468+0.365287j | 1.82e-14 |
| A-+ | -0.563468+0.365287j | -0.563468+0.365287j | 1.83e-14 |
| A-- | -0.110308+0.071511j | -0.110308+0.071511j | 3.03e-14 |
| **ArL(1690)2** | $\mathcal{H}^{\mathrm{LS,production}}_{L(1690),2,\frac{3}{2}}$ | | |
| A++ | 0.333287-0.216064j | 0.333287-0.216064j | 7.66e-14 |
| A+- | 0.280891-0.182097j | 0.280891-0.182097j | 8.10e-14 |
| A-+ | -0.280891+0.182097j | -0.280891+0.182097j | 8.09e-14 |
| A-- | 0.333287-0.216064j | 0.333287-0.216064j | 7.66e-14 |
| **ArL(2000)1** | $\mathcal{H}^{\mathrm{LS,production}}_{L(2000),0,\frac{1}{2}}$ | | |
| A++ | 1.036314+1.105950j | 1.036314+1.105950j | 1.14e-15 |
| A+- | 0.024928+0.026603j | 0.024928+0.026603j | 7.91e-14 |
| A-+ | -0.024928-0.026603j | -0.024928-0.026603j | 7.92e-14 |
| A-- | 1.036314+1.105950j | 1.036314+1.105950j | 1.14e-15 |
| **ArL(2000)2** | $\mathcal{H}^{\mathrm{LS,production}}_{L(2000),1,\frac{1}{2}}$ | | |
| A++ | -0.529297-0.564863j | -0.529297-0.564863j | 1.86e-14 |
| A+- | -1.009471-1.077303j | -1.009471-1.077303j | 2.35e-14 |
| A-+ | -1.009471-1.077303j | -1.009471-1.077303j | 2.36e-14 |
| A-- | 0.529297+0.564863j | 0.529297+0.564863j | 1.86e-14 |

# INTENSITY DISTRIBUTION

The complete intensity expression contains **43,198 mathematical operations**.

## 3.1 Definition of free parameters

After substituting the parameters that are not production couplings, the total intensity expression contains **9,516 operations**.

## 3.2 Distribution

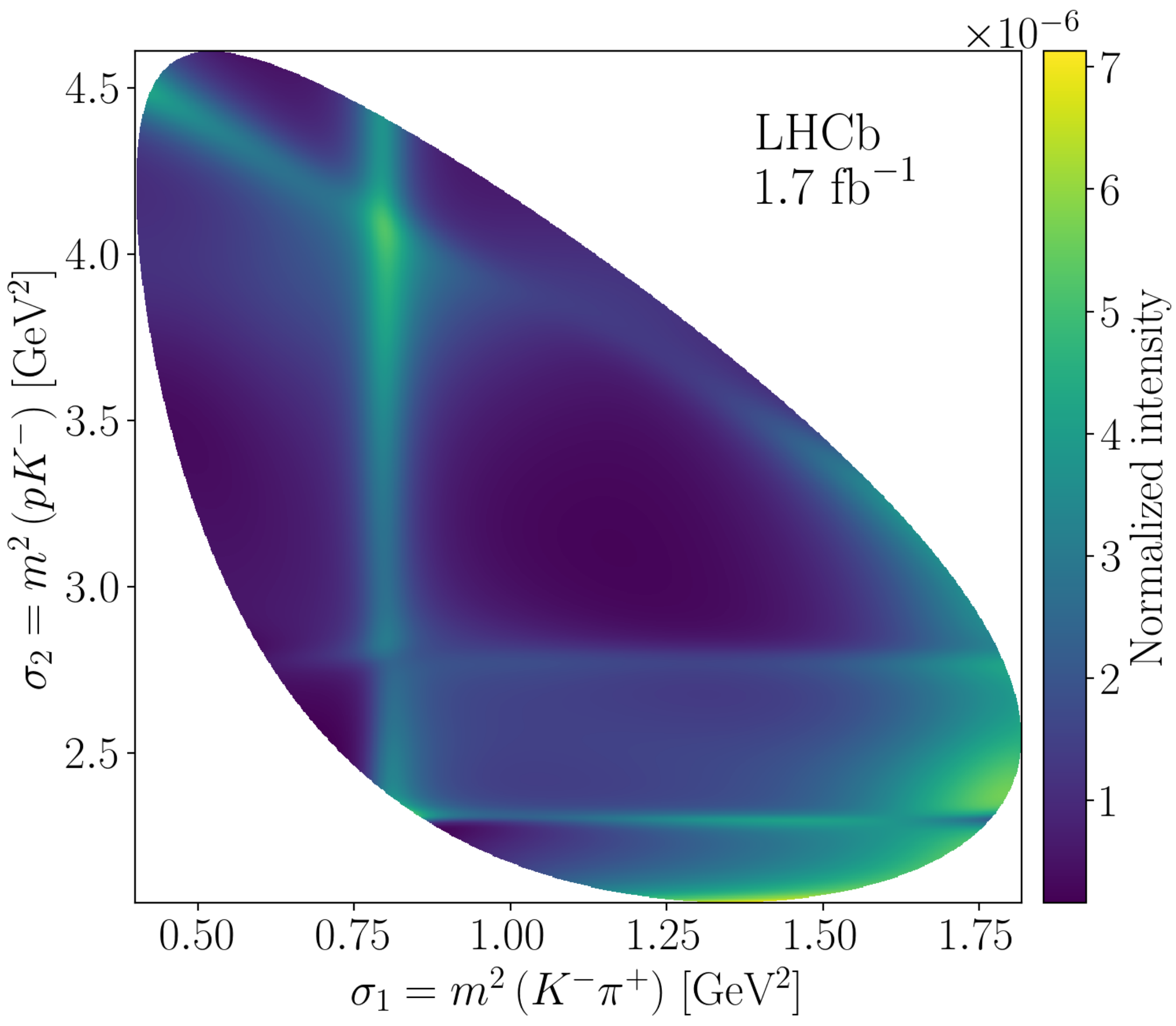

Comparison with Figure 2 from the original LHCb study [1]:

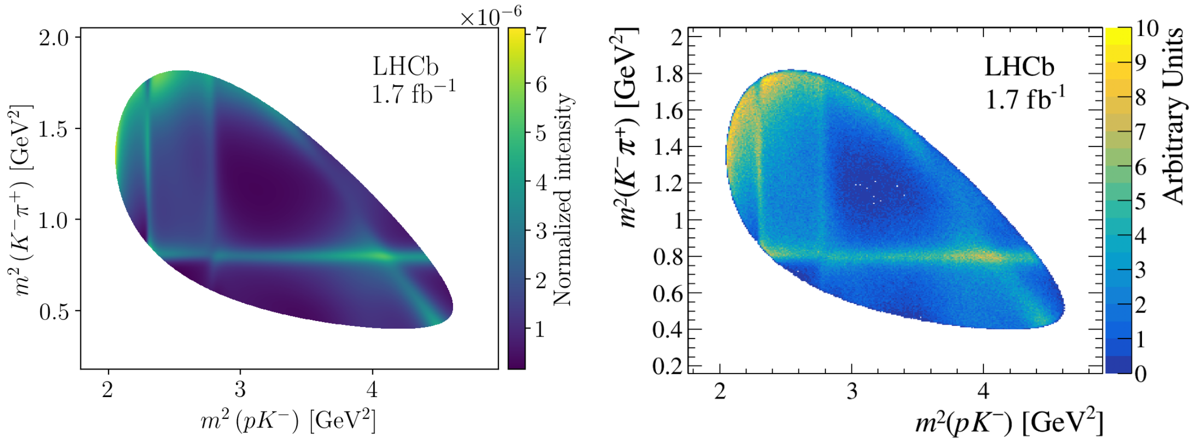


```
<Figure size 1200x500 with 2 Axes>
```

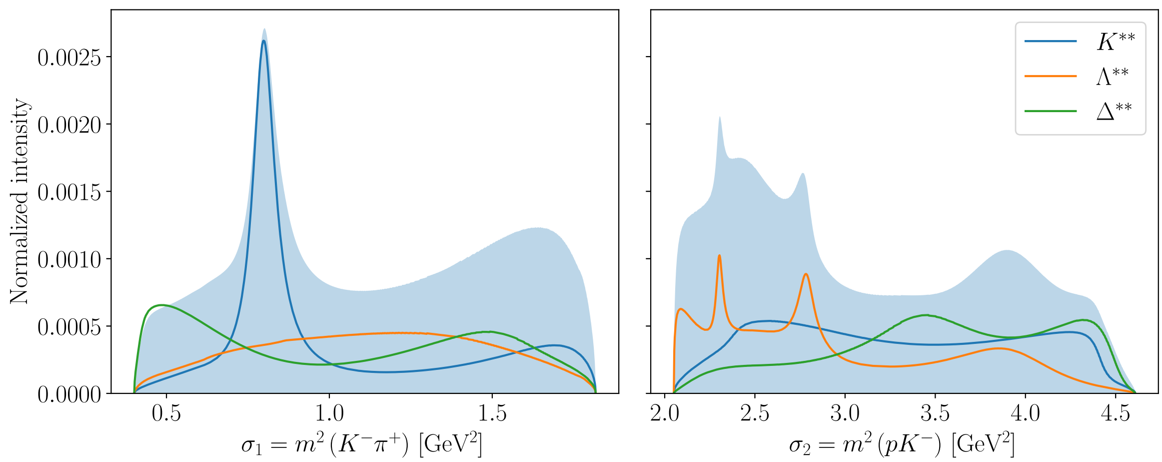


## 3.3 Decay rates

```
Generating intensity-based sample:   0%|          | 0/100000 [00:00<?, ?it/s]
```

```
<Figure size 900x900 with 1 Axes>
```

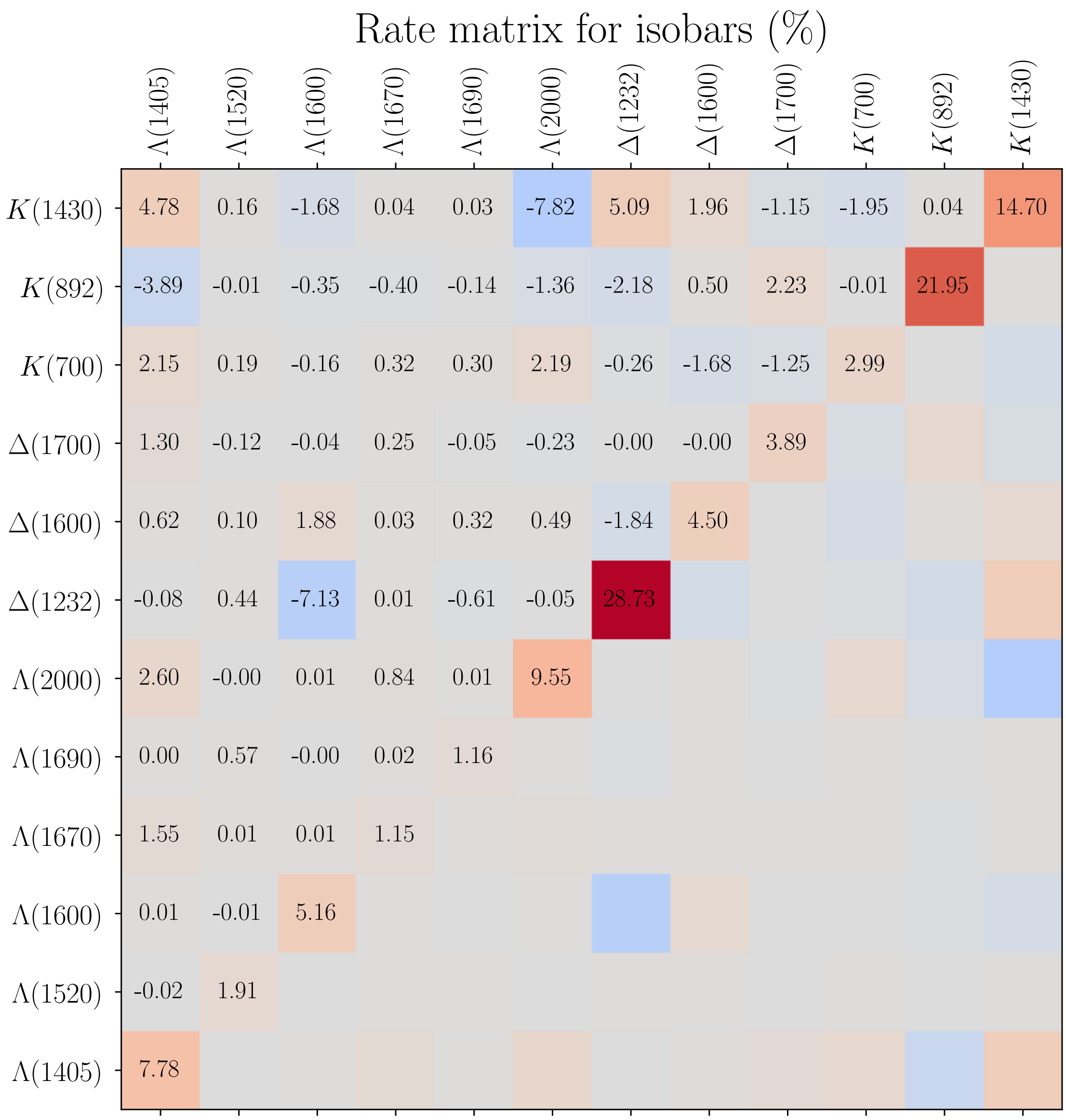


## 3.4 Dominant decays

```
<Figure size 910x700 with 1 Axes>
```

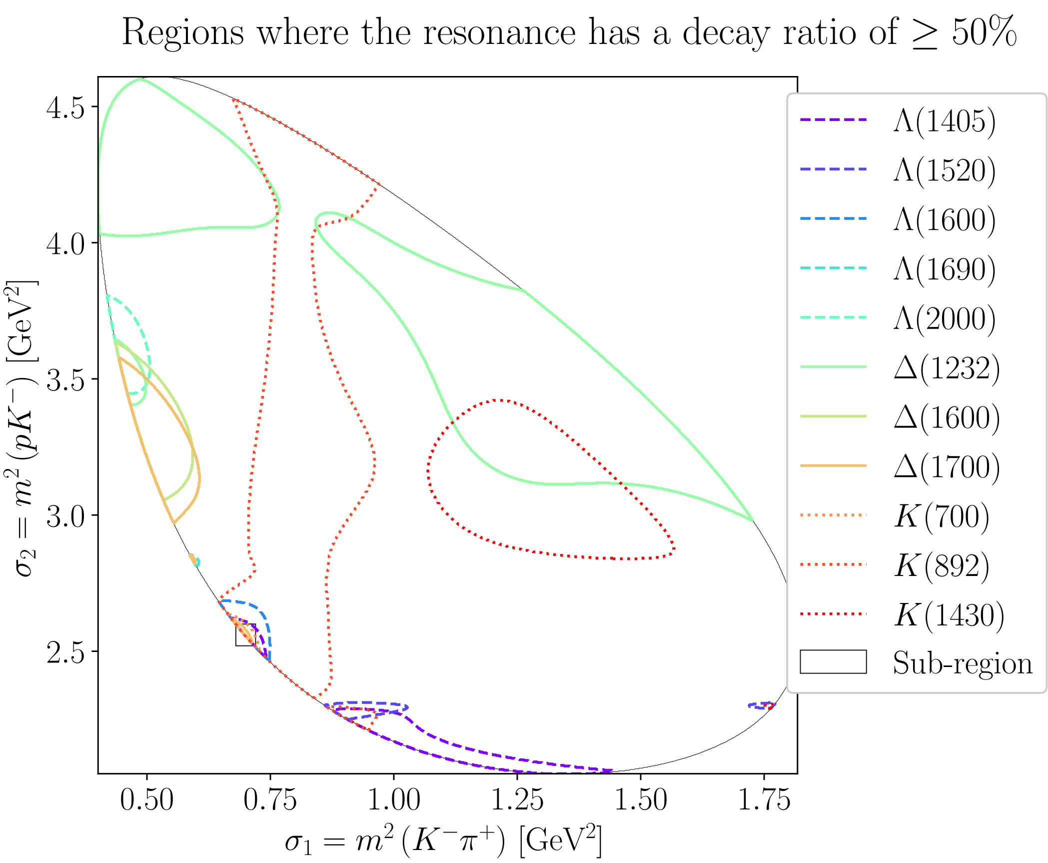


```
<Figure size 900x900 with 1 Axes>
```

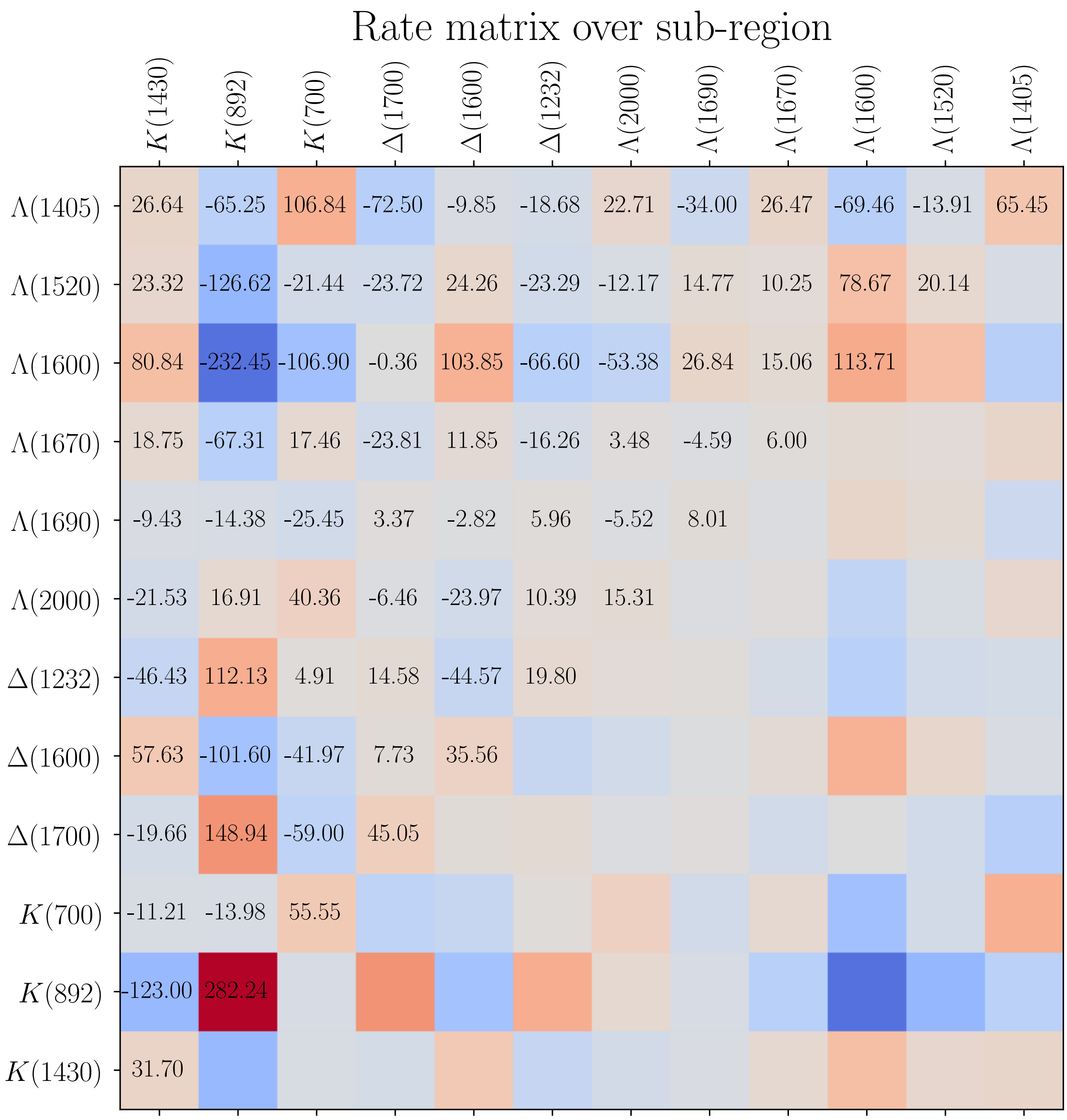
Rate matrix over sub-region
K(1430)
K(892)
K(700)
Δ(1700)
Δ(1600)
Δ(1232)
Λ(2000)
Λ(1690)
Λ(1670)
Λ(1600)
Λ(1520)
Λ(1405)
Λ(1405) 26.64 -65.25 106.84 -72.50 -9.85 -18.68 22.71 -34.00 26.47 -69.46 -13.91 65.45
Λ(1520) 23.32 -126.62 -21.44 -23.72 24.26 -23.29 -12.17 14.77 10.25 78.67 20.14
Λ(1600) 80.84 -232.45 -106.90 -0.36 103.85 -66.60 -53.38 26.84 15.06 113.71
Λ(1670) 18.75 -67.31 17.46 -23.81 11.85 -16.26 3.48 -4.59 6.00
Λ(1690) -9.43 -14.38 -25.45 3.37 -2.82 5.96 -5.52 8.01
Λ(2000) -21.53 16.91 40.36 -6.46 -23.97 10.39 15.31
Δ(1232) -46.43 112.13 4.91 14.58 -44.57 19.80
Δ(1600) 57.63 -101.60 -41.97 7.73 35.56
Δ(1700) -19.66 148.94 -59.00 45.05
K(700) -11.21 -13.98 55.55
K(892) -123.00 282.24
K(1430) 31.70

CHAPTER

FOUR

# POLARIMETER VECTOR FIELD

Final state IDs:

1. $p$
2. $\pi^+$
3. $K^-$

Sub-system definitions:

1. $K^{**} \to \pi^+ K^-$
2. $\Lambda^{**} \to p K^-$
3. $\Delta^{**} \to p \pi^+$

## 4.1 Dominant contributions

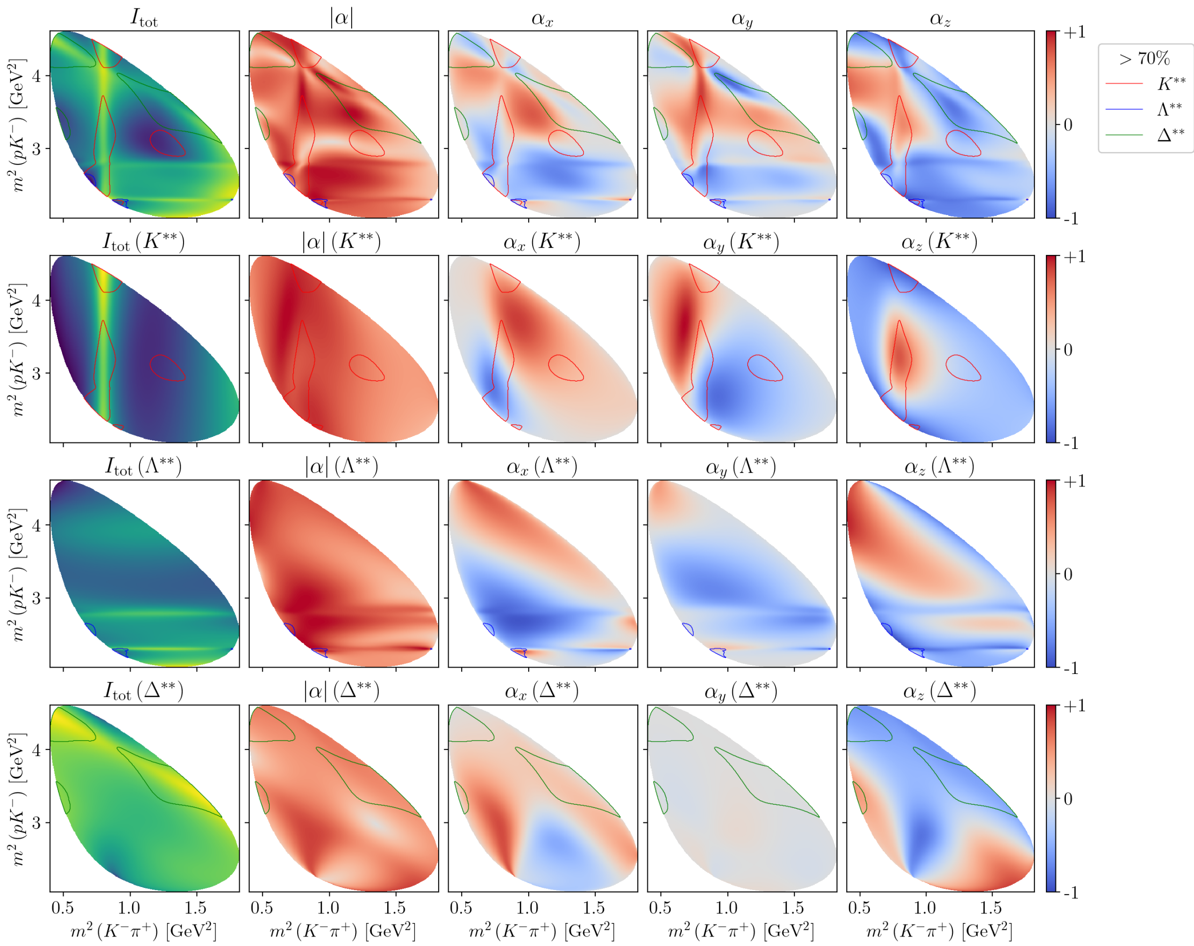


```
CPU times: user 1min 16s, sys: 3.23 s, total: 1min 19s
Wall time: 1min 24s
```

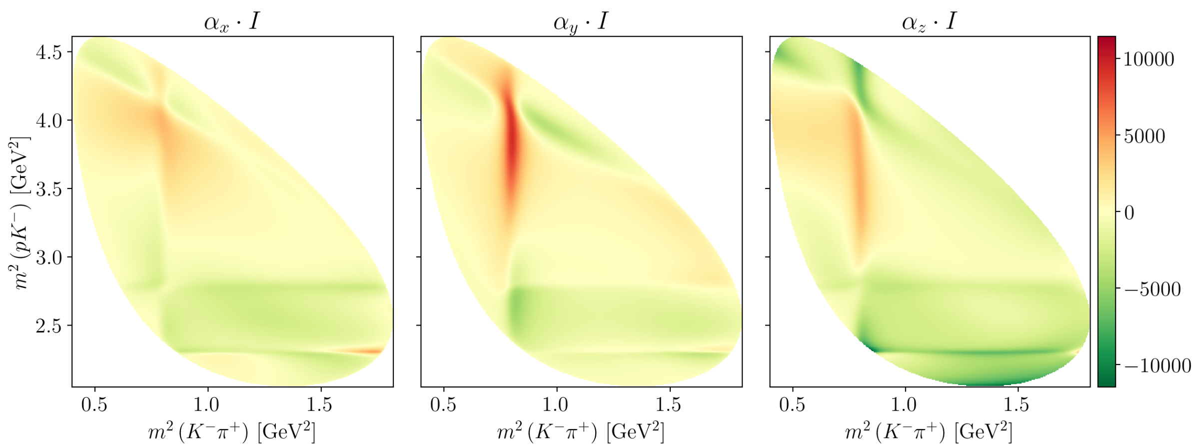

## 4.2 Total polarimetry vector field

```
<IPython.core.display.SVG object>
```

```
<IPython.core.display.SVG object>
```

```
<IPython.core.display.SVG object>
```

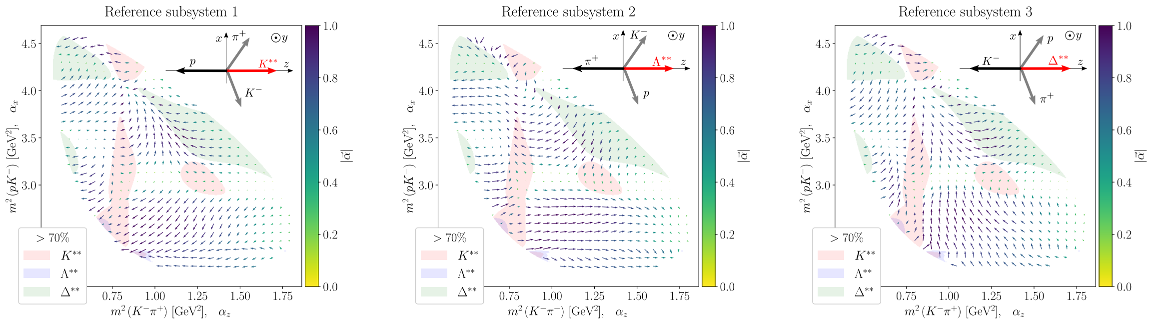


## 4.3 Aligned vector fields per chain

```
<Figure size 1300x500 with 4 Axes>
```

```
<Figure size 1300x900 with 8 Axes>
```

```
<Figure size 1300x500 with 4 Axes>
```

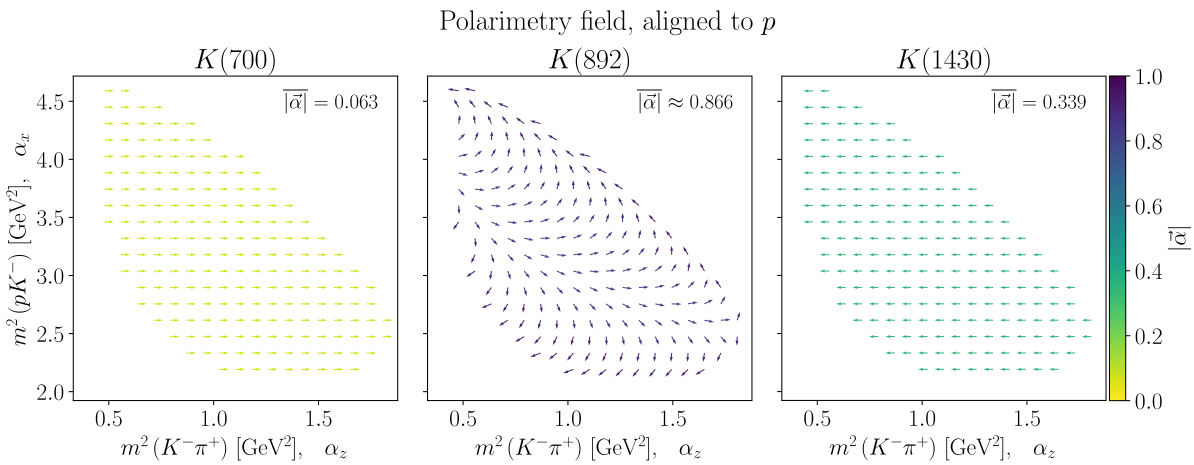

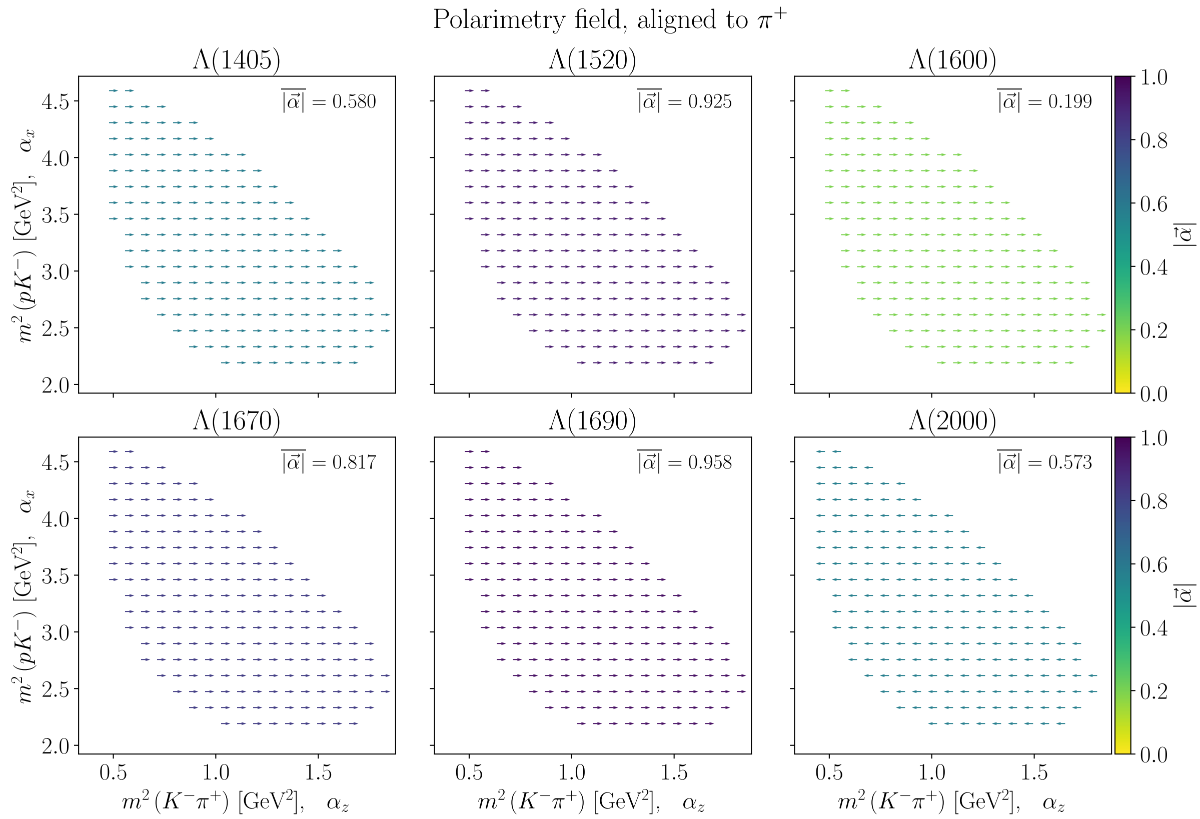


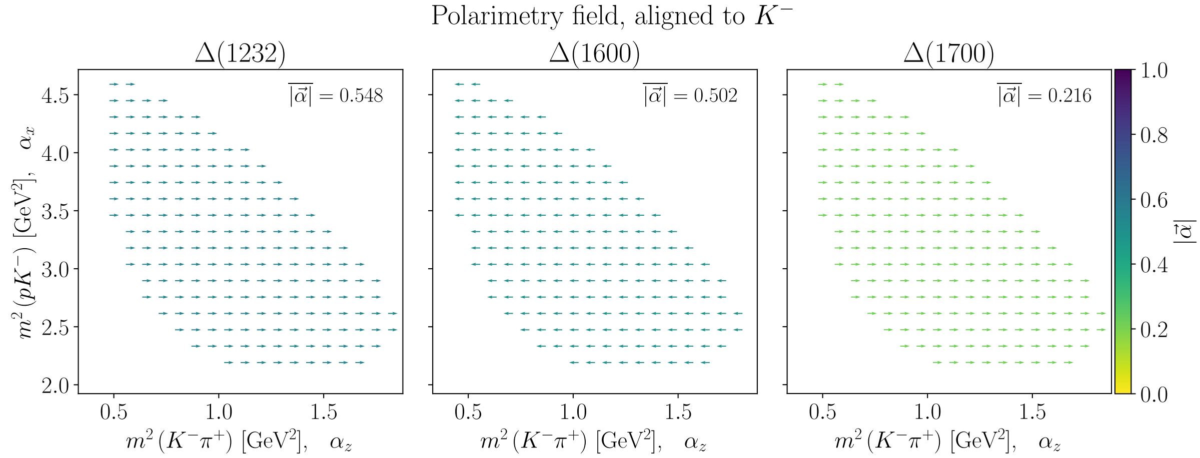


```
<Figure size 1300x450 with 4 Axes>
```

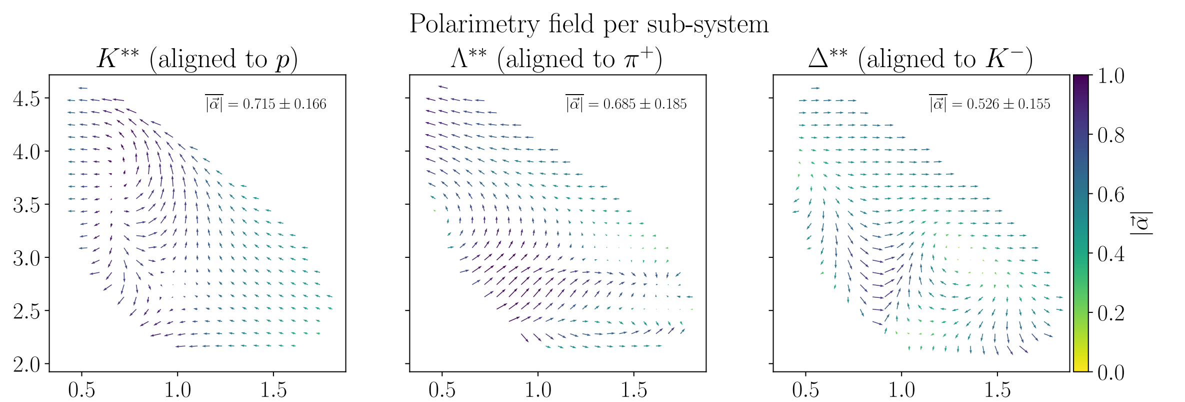

CHAPTER

FIVE

# UNCERTAINTIES

## 5.1 Model loading

Of the 18 models, there are 9 with a unique expression tree.

### Show number of mathematical operations per model

| | | Model description | $n$ ops. |
|---|---|---|---|
| **0** | | Default amplitude model | $43,198$ |
| **1** | $=0$ | Alternative amplitude model with K(892) with free mass and width | $43,198$ |
| **2** | $=0$ | Alternative amplitude model with L(1670) with free mass and width | $43,198$ |
| **3** | $=0$ | Alternative amplitude model with L(1690) with free mass and width | $43,198$ |
| **4** | $=0$ | Alternative amplitude model with D(1232) with free mass and width | $43,198$ |
| **5** | $=0$ | Alternative amplitude model with L(1600), D(1600), D(1700) with free mass and width | $43,198$ |
| **6** | $=0$ | Alternative amplitude model with free L(1405) Flatt'e widths, indicated as G1 (pK channel) and G2 (Sigmapi) | $43,198$ |
| **7** | | Alternative amplitude model with L(1800) contribution added with free mass and width | $44,222$ |
| **8** | | Alternative amplitude model with L(1810) contribution added with free mass and width | $46,782$ |
| **9** | | Alternative amplitude model with D(1620) contribution added with free mass and width | $44,222$ |
| **10** | | Alternative amplitude model in which a Relativistic Breit-Wigner is used for the K(700) contribution | $43,470$ |
| **11** | $=0$ | Alternative amplitude model with K(700) with free mass and width | $43,198$ |
| **12** | | Alternative amplitude model with K(1410) contribution added with mass and width from PDG2020 | $46,780$ |
| **13** | | Alternative amplitude model in which a Relativistic Breit-Wigner is used for the K(1430) contribution | $43,470$ |
| **14** | $=0$ | Alternative amplitude model with K(1430) with free width | $43,198$ |
| **15** | | Alternative amplitude model with an additional overall exponential form factor exp(-alpha q^2) multiplying Bugg lineshapes. The exponential parameter is indicated as ``alpha'' | $43,582$ |
| **16** | $=0$ | Alternative amplitude model with free radial parameter d for the Lc resonance, indicated as dLc | $43,198$ |
| **17** | | Alternative amplitude model obtained using LS couplings | $110,839$ |

## 5.2 Statistical uncertainties

### 5.2.1 Parameter bootstrapping

```
Generating intensity-based sample:   0%|          | 0/100000 [00:00<?, ?it/s]
```

### 5.2.2 Mean and standard deviations

```
(100, 100000)
```

### 5.2.3 Distributions

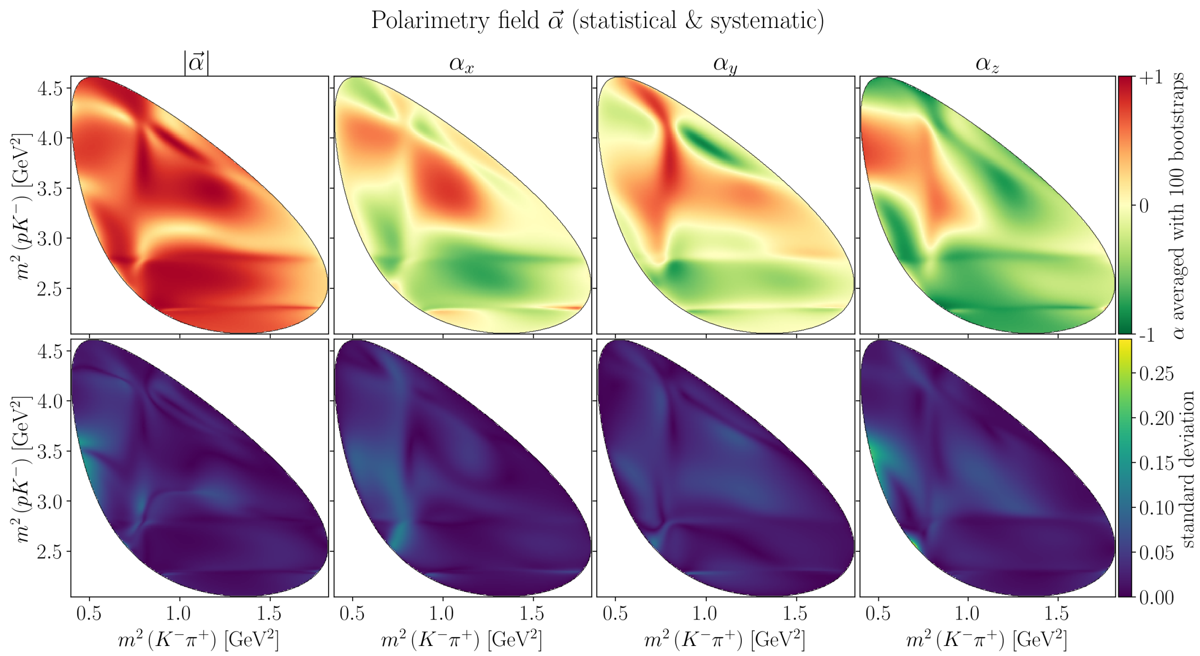


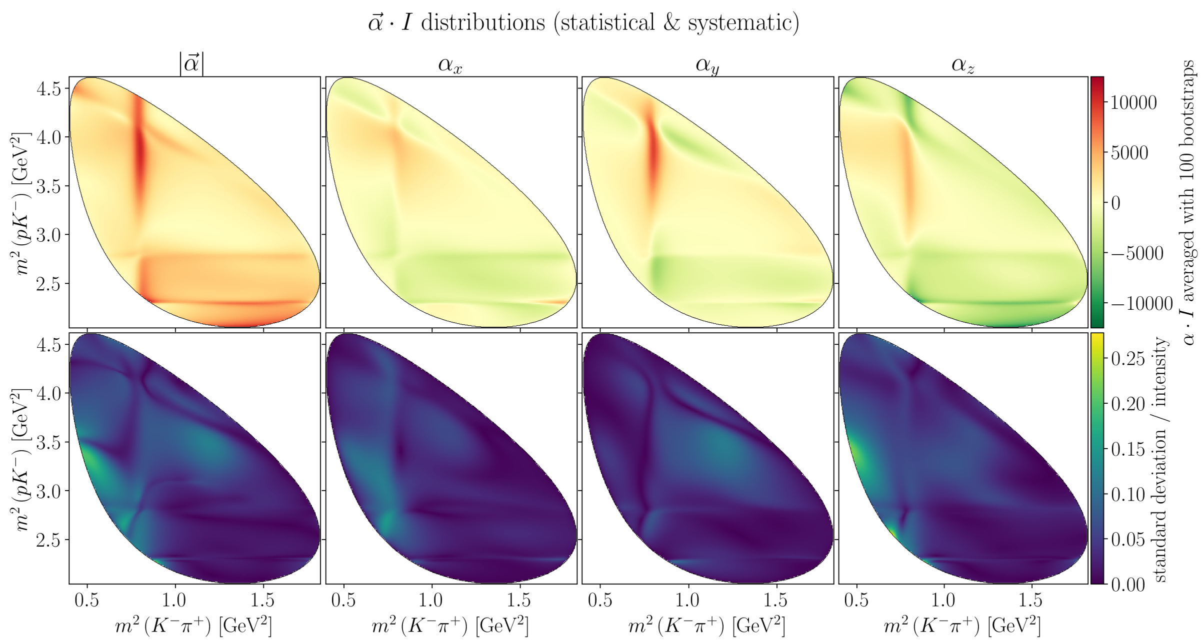

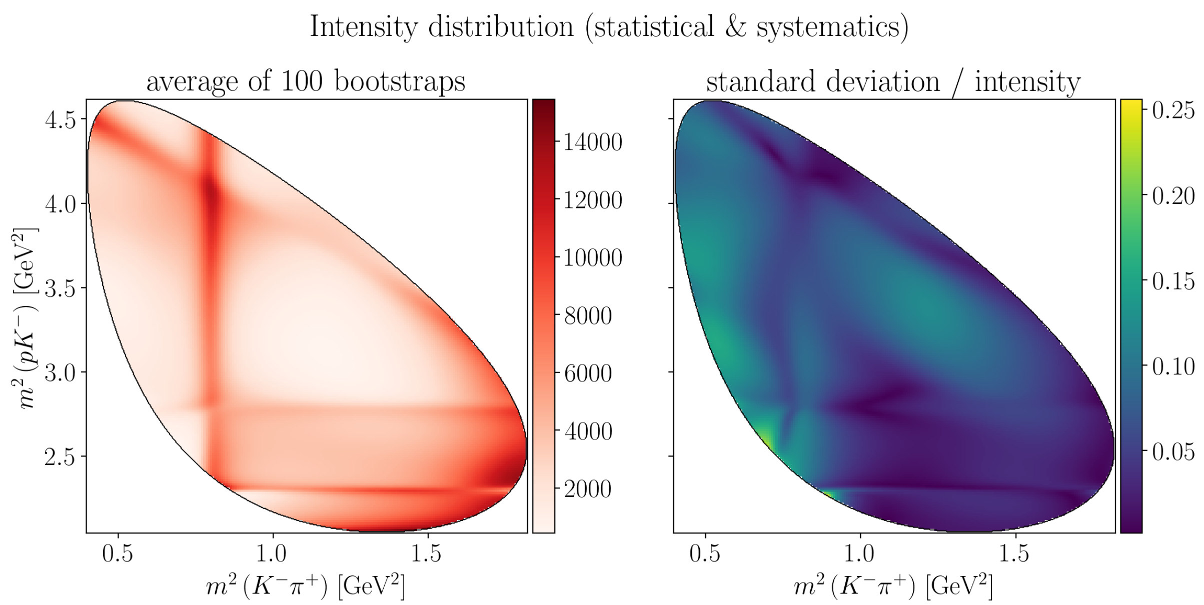


### 5.2.4 Comparison with nominal values

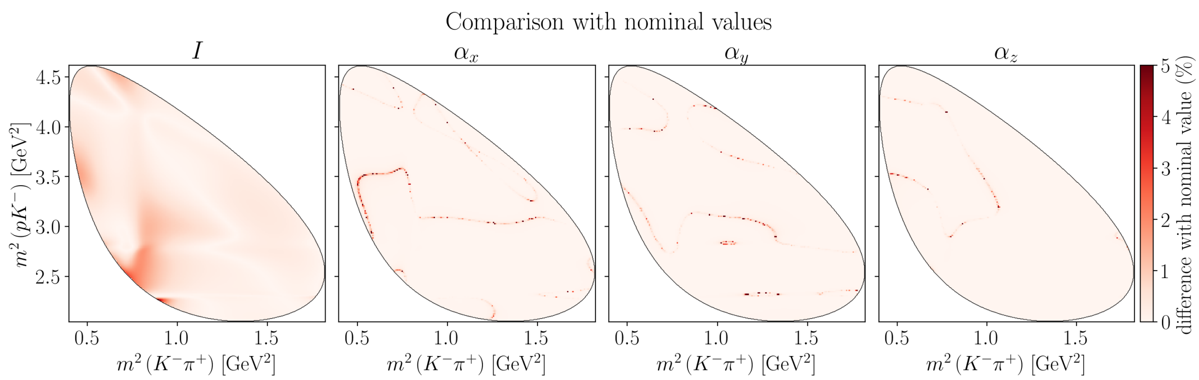


## 5.3 Systematic uncertainties

### 5.3.1 Mean and standard deviations

```
(18, 100000)
```

### 5.3.2 Distributions

```
<Figure size 2000x1600 with 17 Axes>
```

```
<Figure size 2000x1600 with 17 Axes>
```

```
<Figure size 2000x1600 with 17 Axes>
```

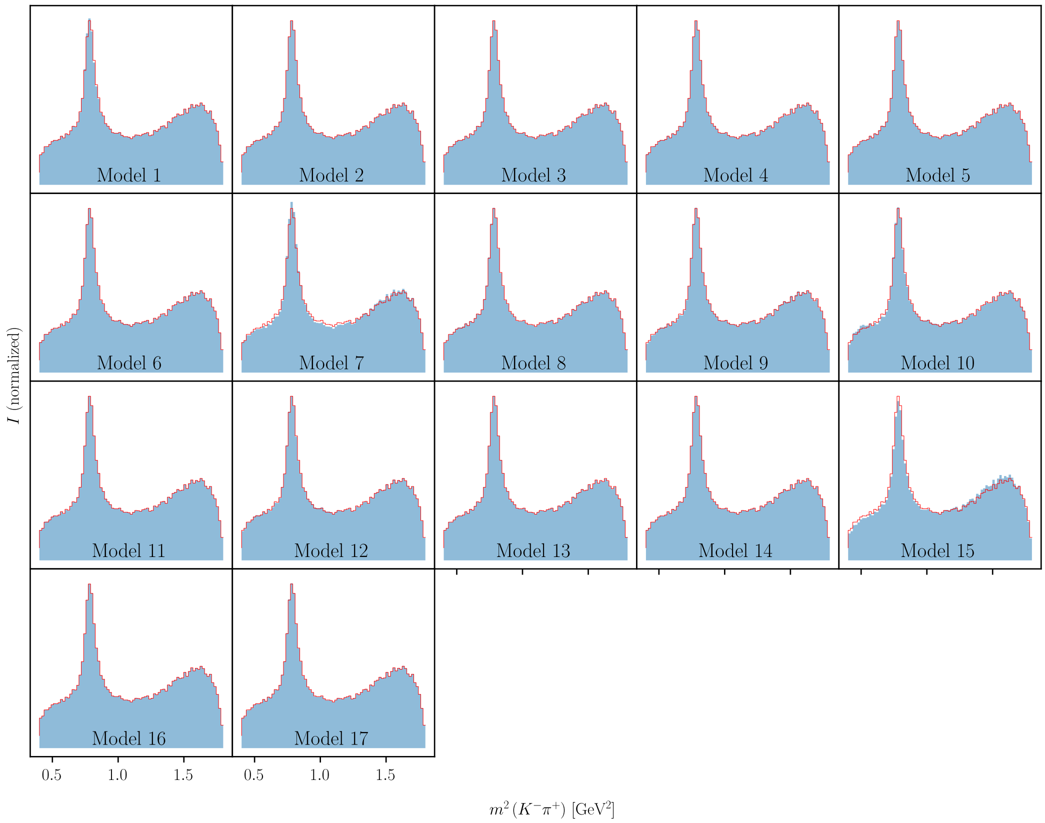

Model 1
Model 2
Model 3
Model 4
Model 5
Model 6
Model 7
Model 8
Model 9
Model 10
Model 11
Model 12
Model 13
Model 14
Model 15
Model 16
Model 17
$I$ (normalized)
0.5
1.0
1.5
$m^2(K^-\pi^+)$ [GeV$^2$]

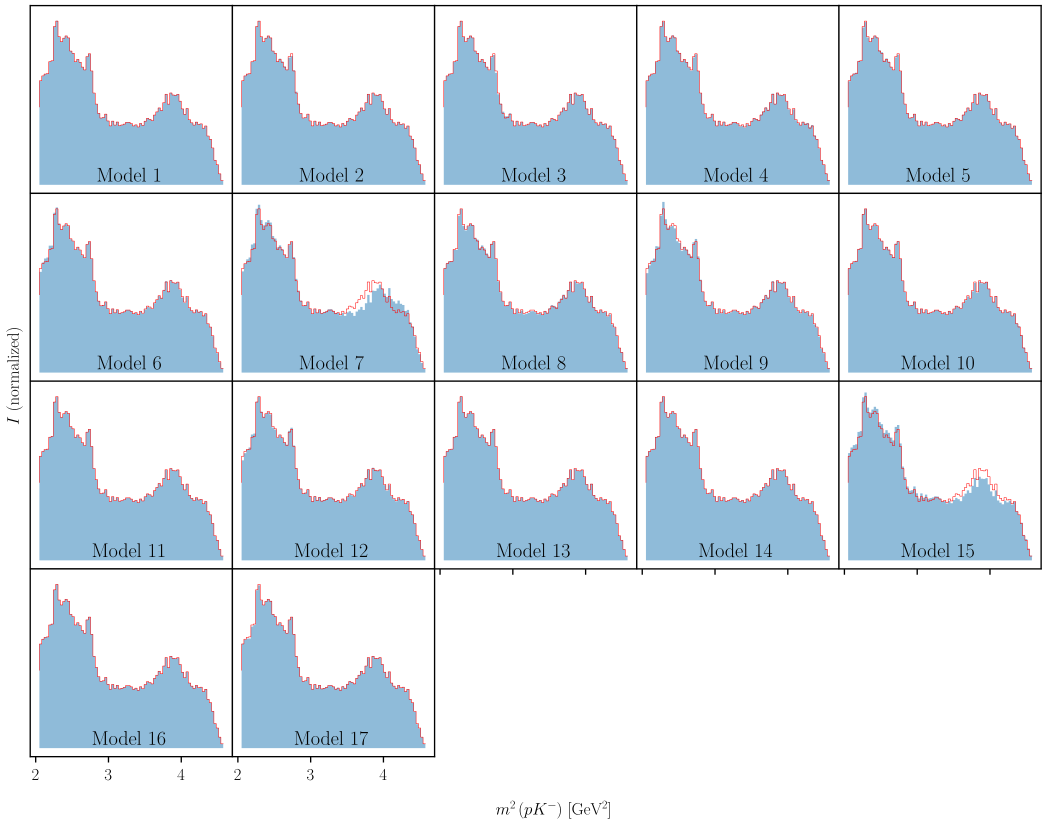
Model 1
Model 2
Model 3
Model 4
Model 5
Model 6
Model 7
Model 8
Model 9
Model 10
Model 11
Model 12
Model 13
Model 14
Model 15
Model 16
Model 17
I (normalized)
2
3
4
$m^2(pK^-)$ [GeV$^2$]

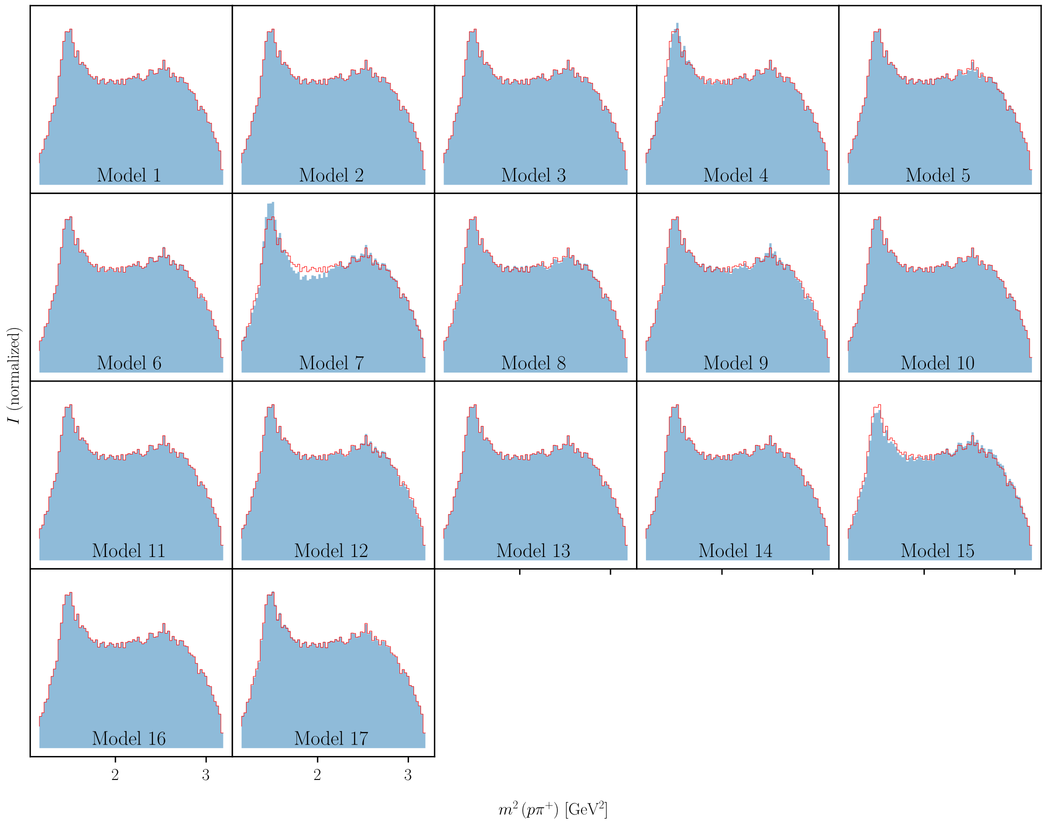
Model 1
Model 2
Model 3
Model 4
Model 5
Model 6
Model 7
Model 8
Model 9
Model 10
Model 11
Model 12
Model 13
Model 14
Model 15
Model 16
Model 17
I (normalized)
m²(pπ⁺) [GeV²]

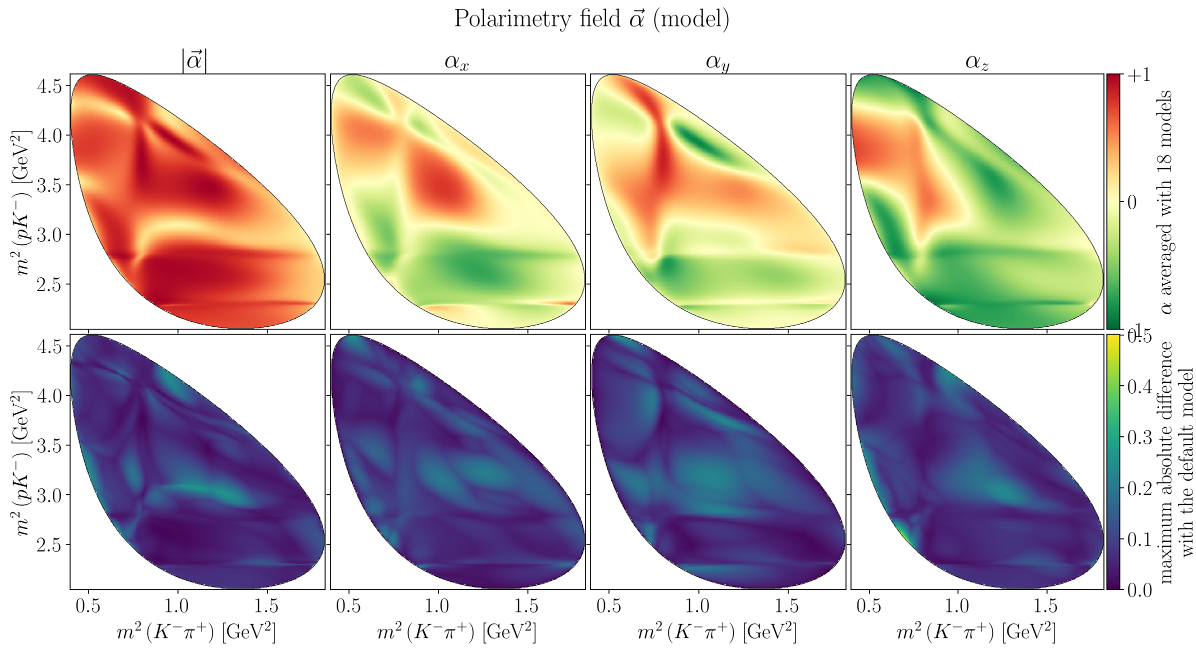
Polarimetry field α⃗ (model)
|α⃗|
αx
αy
αz
m²(pK⁻) [GeV²]
m²(K⁻π⁺) [GeV²]
α averaged with 18 models
maximum absolute difference with the default model

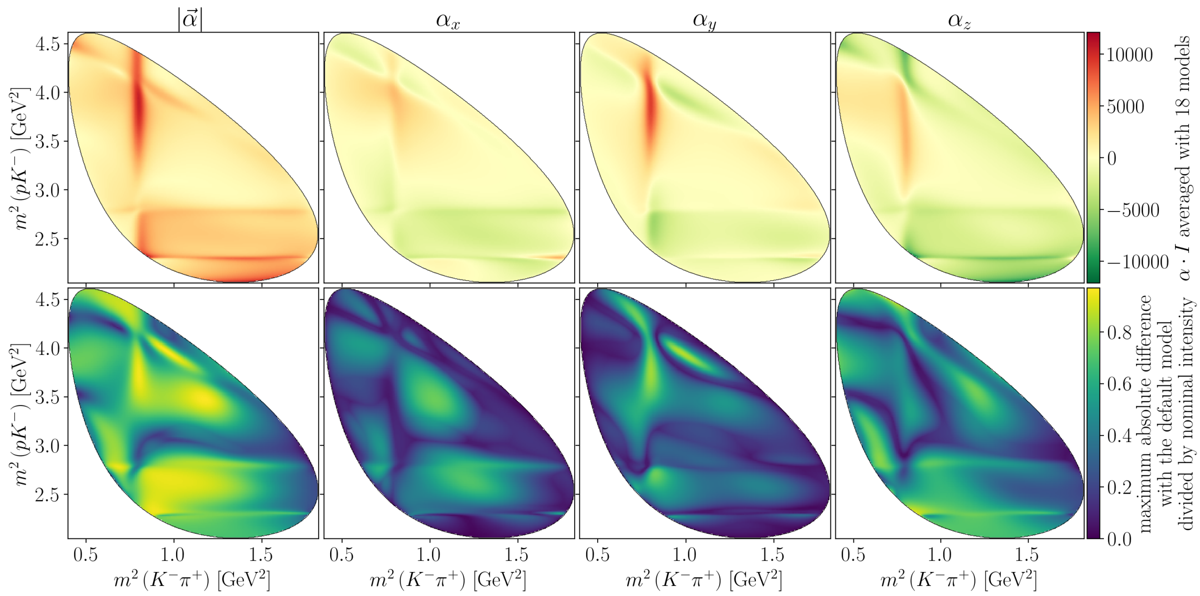


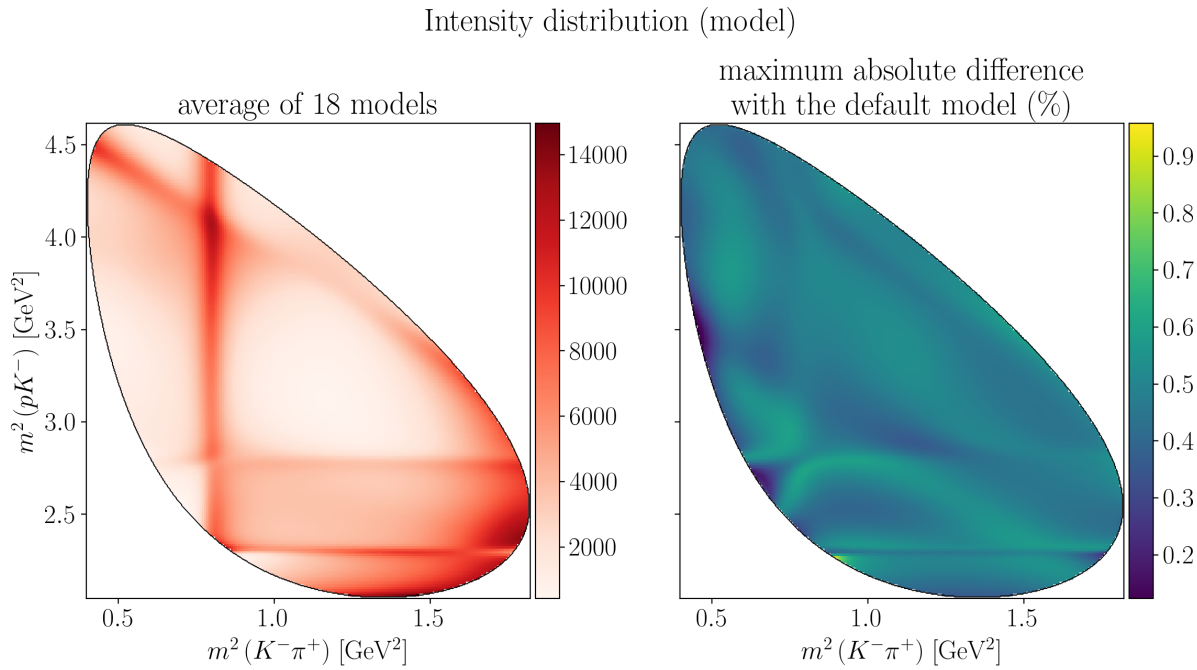


## 5.4 Uncertainty on polarimetry

For each bootstrap or alternative model $i$, we compute the angle between each aligned polarimeter vector $\vec{\alpha}_i$ and the one from the nominal model, $\vec{\alpha}_0$:

$$\cos\theta_i = \frac{\vec{\alpha}_i \cdot \vec{\alpha}_0}{|\alpha_i||\alpha_0|}.$$

The solid angle can then be computed as:

$$\delta\Omega = \int_0^{2\pi}\int_0^{\theta} \mathrm{d}\phi\,\mathrm{d}\cos\theta = 2\pi\left(1-\cos\theta\right).$$

The statistical uncertainty is given by taking the standard deviation on the $\delta\Omega$ distribution and the systematic uncertainty is given by taking finding $\theta_{\mathrm{max}} = \max\theta_i$ and computing $\delta\Omega_{\mathrm{max}}$ from that.

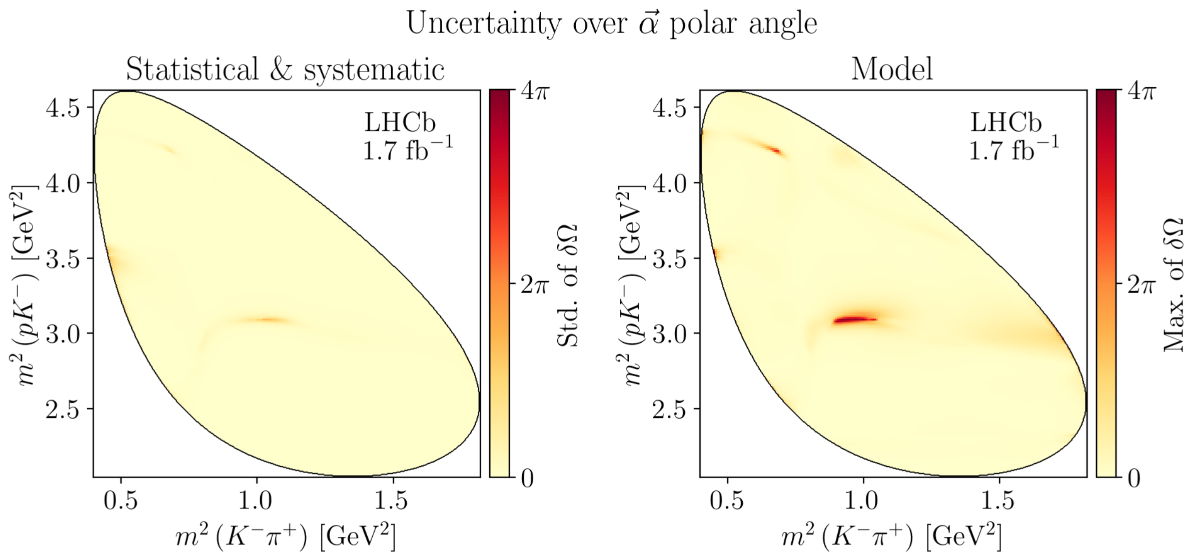
Uncertainty over $\vec{\alpha}$ polar angle
Statistical & systematic
Model
LHCb
1.7 fb$^{-1}$
Std. of $\delta\Omega$
Max. of $\delta\Omega$
0
$2\pi$
$4\pi$
$m^2(pK^-)$ [GeV$^2$]
$m^2(K^-\pi^+)$ [GeV$^2$]

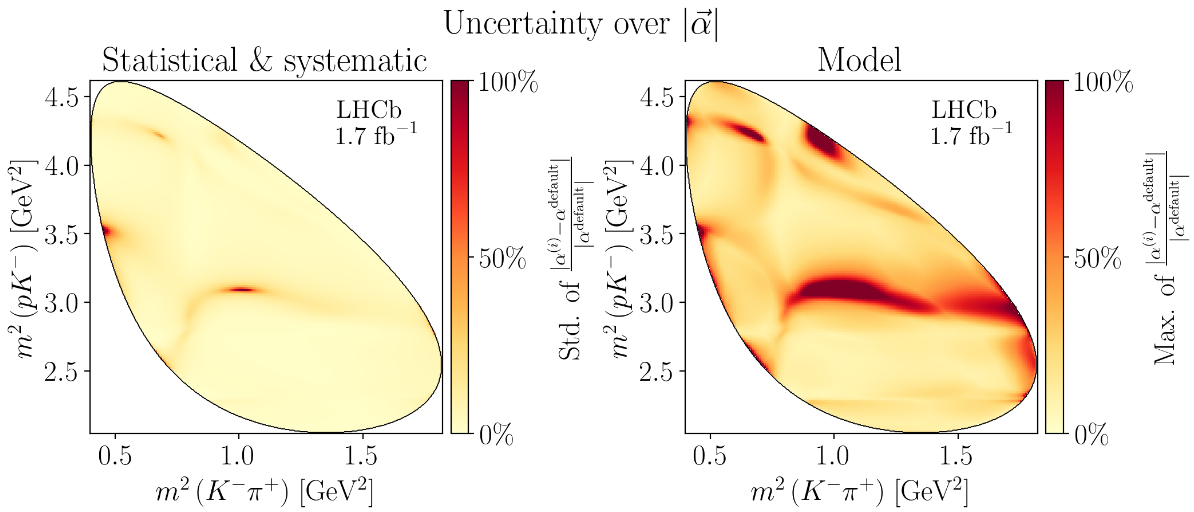
Uncertainty over $|\vec{\alpha}|$
Statistical & systematic
Model
LHCb
1.7 fb$^{-1}$
Std. of $\frac{|\alpha^{(i)}-\alpha^{\text{default}}|}{|\alpha^{\text{default}}|}$
Max. of $\frac{|\alpha^{(i)}-\alpha^{\text{default}}|}{|\alpha^{\text{default}}|}$
0%
50%
100%
$m^2(pK^-)$ [GeV$^2$]
$m^2(K^-\pi^+)$ [GeV$^2$]

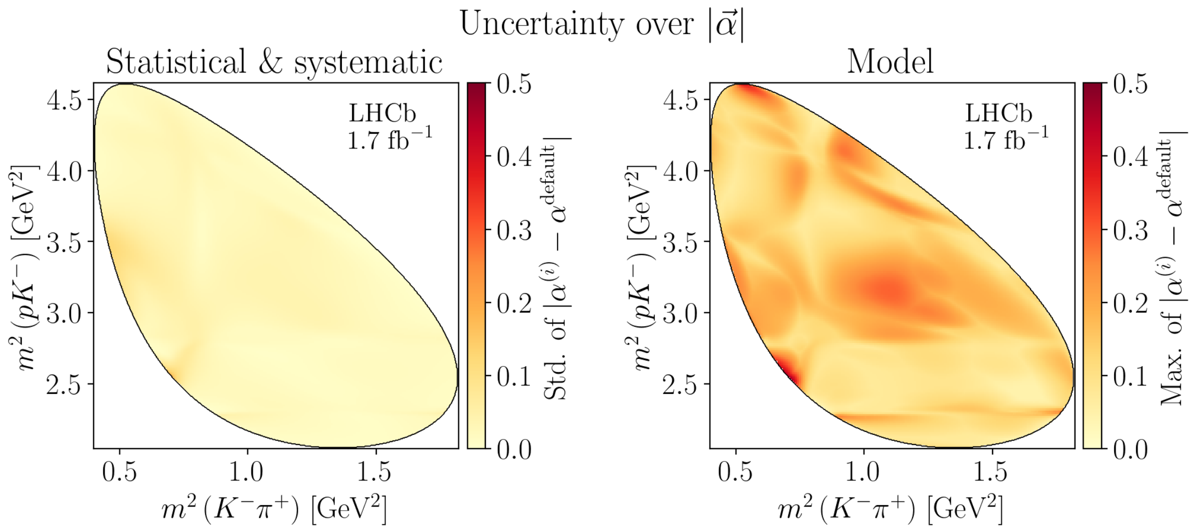
Uncertainty over $|\vec{\alpha}|$
Statistical & systematic
Model
LHCb
1.7 fb$^{-1}$
Std. of $|\alpha^{(i)} - \alpha^{\text{default}}|$
Max. of $|\alpha^{(i)} - \alpha^{\text{default}}|$
$m^2(pK^-)$ [GeV$^2$]
$m^2(K^-\pi^+)$ [GeV$^2$]

## 5.5 Decay rates

| Resonance | Decay rate | LHCb |
|---|---|---|
| $\Lambda(1405)$ | $7.78 \pm 0.43^{+3.01}_{-2.53}$ | $7.7 \pm 0.2 \pm 3.0$ |
| $\Lambda(1520)$ | $1.91 \pm 0.10^{+0.04}_{-0.24}$ | $1.86 \pm 0.09 \pm 0.23$ |
| $\Lambda(1600)$ | $5.16 \pm 0.28^{+0.50}_{-1.93}$ | $5.2 \pm 0.2 \pm 1.9$ |
| $\Lambda(1670)$ | $1.15 \pm 0.04^{+0.06}_{-0.29}$ | $1.18 \pm 0.06 \pm 0.32$ |
| $\Lambda(1690)$ | $1.16 \pm 0.01^{+0.06}_{-0.33}$ | $1.19 \pm 0.09 \pm 0.34$ |
| $\Lambda(2000)$ | $9.55 \pm 0.67^{+0.83}_{-2.26}$ | $9.58 \pm 0.27 \pm 0.93$ |
| $\Delta(1232)$ | $28.73 \pm 1.34^{+1.76}_{-0.79}$ | $28.6 \pm 0.29 \pm 0.76$ |
| $\Delta(1600)$ | $4.50 \pm 0.51^{+0.93}_{-1.40}$ | $4.5 \pm 0.3 \pm 1.5$ |
| $\Delta(1700)$ | $3.89 \pm 0.07^{+0.94}_{-0.48}$ | $3.9 \pm 0.2 \pm 0.94$ |
| $K(700)$ | $2.99 \pm 0.20^{+0.91}_{-0.59}$ | $3.02 \pm 0.16 \pm 0.92$ |
| $K(892)$ | $21.95 \pm 1.24^{+0.59}_{-0.70}$ | $22.14 \pm 0.23 \pm 0.64$ |
| $K(1430)$ | $14.70 \pm 0.80^{+2.78}_{-2.67}$ | $14.7 \pm 0.6 \pm 2.7$ |

| Resonance | 1 | 2 | 3 | 4 | 5 | 6 | 7 | 8 | 9 | 10 | 11 | 12 | 13 |
|---|---|---|---|---|---|---|---|---|---|---|---|---|---|
| $\Lambda(1405)$ | +0.11 | −0.14 | −0.01 | −0.33 | −0.99 | +3.01 | −2.53 | −0.66 | −1.58 | −0.43 | −0.01 | −1.97 | −0.11 |
| $\Lambda(1520)$ | +0.03 | +0.00 | +0.01 | +0.01 | −0.24 | −0.01 | −0.04 | −0.08 | −0.06 | −0.06 | +0.04 | −0.15 | −0.00 |
| $\Lambda(1600)$ | −0.02 | −0.09 | +0.13 | +0.22 | +0.50 | −0.09 | −0.30 | +0.23 | −1.93 | −0.46 | +0.12 | −1.85 | −0.12 |
| $\Lambda(1670)$ | −0.01 | +0.06 | +0.03 | +0.01 | −0.01 | −0.12 | −0.29 | −0.03 | −0.11 | +0.05 | −0.01 | −0.03 | +0.01 |
| $\Lambda(1690)$ | +0.00 | −0.00 | +0.04 | −0.13 | +0.01 | −0.06 | −0.04 | −0.26 | −0.33 | −0.08 | −0.04 | +0.06 | +0.01 |
| $\Lambda(2000)$ | +0.05 | +0.10 | −0.08 | −0.09 | +0.08 | −0.85 | −2.26 | +0.83 | −0.93 | +0.31 | −0.23 | −0.86 | +0.35 |
| $\Delta(1232)$ | −0.27 | +0.02 | +0.31 | +1.76 | −0.44 | −0.14 | +0.49 | −0.63 | −0.77 | +0.53 | −0.31 | +0.65 | +0.10 |
| $\Delta(1600)$ | +0.33 | −0.10 | −0.15 | −0.28 | +0.59 | −0.38 | −1.40 | −0.29 | +0.93 | +0.03 | +0.05 | −0.58 | +0.07 |
| $\Delta(1700)$ | −0.01 | +0.03 | −0.13 | +0.07 | +0.39 | −0.48 | −0.15 | +0.82 | +0.94 | +0.18 | +0.05 | +0.75 | +0.03 |
| $K(700)$ | +0.17 | −0.02 | +0.04 | +0.75 | +0.62 | −0.59 | −0.31 | −0.06 | +0.91 | +0.56 | +0.25 | +0.42 | +0.10 |
| $K(892)$ | −0.53 | −0.02 | −0.12 | −0.46 | −0.58 | +0.55 | +0.59 | −0.06 | +0.18 | +0.28 | −0.16 | +0.25 | −0.01 |
| $K(1430)$ | −0.29 | +0.07 | −0.50 | −0.03 | +0.18 | −0.76 | +2.78 | +2.40 | −2.67 | +1.29 | +0.23 | −2.27 | +0.91 |

- **0**: Default amplitude model
- **1**: Alternative amplitude model with K(892) with free mass and width
- **2**: Alternative amplitude model with L(1670) with free mass and width
- **3**: Alternative amplitude model with L(1690) with free mass and width
- **4**: Alternative amplitude model with D(1232) with free mass and width
- **5**: Alternative amplitude model with L(1600), D(1600), D(1700) with free mass and width
- **6**: Alternative amplitude model with free L(1405) Flatt'e widths, indicated as G1 (pK channel) and G2 (Sigmapi)
- **7**: Alternative amplitude model with L(1800) contribution added with free mass and width
- **8**: Alternative amplitude model with L(1810) contribution added with free mass and width
- **9**: Alternative amplitude model with D(1620) contribution added with free mass and width
- **10**: Alternative amplitude model in which a Relativistic Breit-Wigner is used for the K(700) contribution
- **11**: Alternative amplitude model with K(700) with free mass and width
- **12**: Alternative amplitude model with K(1410) contribution added with mass and width from PDG2020
- **13**: Alternative amplitude model in which a Relativistic Breit-Wigner is used for the K(1430) contribution
- **14**: Alternative amplitude model with K(1430) with free width
- **15**: Alternative amplitude model with an additional overall exponential form factor exp(-alpha q^2) multiplying Bugg lineshapes. The exponential parameter is indicated as ``alpha"
- **16**: Alternative amplitude model with free radial parameter d for the Lc resonance, indicated as dLc
- **17**: Alternative amplitude model obtained using LS couplings

## 5.6 Average polarimetry values

The components of the **averaged polarimeter vector** $\overline{\alpha}$ are defined as:

$$\overline{\alpha}_j = \int I_0(\tau)\, \alpha_j(\tau)\, \mathrm{d}^n\tau \Big/ \int I_0(\tau)\; \mathrm{d}^n\tau$$

The averages of the norm of $\vec{\alpha}$ are computed as follows:

- $|\overline{\alpha}| = \sqrt{\overline{\alpha_x}^2 + \overline{\alpha_y}^2 + \overline{\alpha_z}^2}$, with the statistical uncertainties added in quadrature and the systematic uncertainties by taking the same formula on the extrema values of each $\overline{\alpha_j}$
- $\overline{|\alpha|} = \sqrt{\int I_0(\tau)\, |\vec{\alpha}(\tau)|^2\, \mathrm{d}^n\tau \Big/ \int I_0(\tau)\; \mathrm{d}^n\tau}$

**Cartesian coordinates**:

$$\begin{aligned}
\overline{\alpha_x} &= \left(-62.6 \pm 4.5_{-14.8}^{+8.4}\right) \times 10^{-3} \\
\overline{\alpha_y} &= \left(+8.9 \pm 8.9_{-12.7}^{+9.1}\right) \times 10^{-3} \\
\overline{\alpha_z} &= \left(-278.0 \pm 23.7_{-40.4}^{+12.6}\right) \times 10^{-3} \\
\overline{|\alpha|} &= \left(669.4 \pm 9.3_{-10.4}^{+15.3}\right) \times 10^{-3}
\end{aligned}$$

**Polar coordinates**:

$$\begin{aligned}
\theta(\vec{\alpha}) &= \arccos\left(\alpha_z \big/ |\alpha|\right) \\
\phi(\vec{\alpha}) &= \pi - \mathrm{atan2}\left(\alpha_y, -\alpha_x\right)
\end{aligned}$$

$$\begin{aligned}
|\overline{\alpha}| &= \left(+285.1 \pm 24.0_{-13.8}^{+37.9}\right) \times 10^{-3} \\
\theta(\overline{\alpha}) &= +2.92 \pm 0.01_{-0.04}^{+0.05}\ \mathrm{rad} \\
&= \left(+0.929 \pm 0.002_{-0.011}^{+0.017}\right) \times \pi \\
\phi(\overline{\alpha}) &= +3.00 \pm 0.14_{-0.09}^{+0.21}\ \mathrm{rad} \\
&= \left(+0.955 \pm 0.045_{-0.028}^{+0.067}\right) \times \pi
\end{aligned}$$

Averaged polarimeter values for each model (and the difference with the nominal model):

| **Model** | $\overline{\alpha}_x$ | $\overline{\alpha}_y$ | $\overline{\alpha}_z$ | $\overline{\lvert\alpha\rvert}$ | $\Delta\overline{\alpha}_x$ | $\Delta\overline{\alpha}_y$ | $\Delta\overline{\alpha}_z$ | $\Delta\overline{\lvert\alpha\rvert}$ |
|---|---|---|---|---|---|---|---|---|
| **0** | −62.6 | +8.9 | −278.0 | 669.4 | | | | |
| **1** | −61.6 | +8.5 | −279.4 | 670.7 | +1.0 | −0.4 | −1.4 | +1.3 |
| **2** | −62.9 | +9.1 | −278.4 | 669.8 | −0.3 | +0.2 | −0.5 | +0.4 |
| **3** | −58.4 | +7.4 | −276.2 | 667.7 | +4.2 | −1.5 | +1.8 | −1.6 |
| **4** | −69.3 | +9.5 | −277.2 | 666.9 | −6.6 | +0.6 | +0.8 | −2.5 |
| **5** | −70.7 | +9.6 | −277.4 | 668.7 | −8.0 | +0.8 | +0.6 | −0.6 |
| **6** | −69.7 | +9.1 | −281.7 | 673.0 | −7.1 | +0.2 | −3.8 | +3.7 |
| **7** | −77.4 | +18.0 | −305.4 | 671.4 | −14.8 | +9.1 | −27.5 | +2.1 |
| **8** | −55.8 | +10.9 | −284.6 | 675.5 | +6.8 | +2.0 | −6.7 | +6.1 |
| **9** | −66.9 | +4.4 | −290.4 | 672.8 | −4.3 | −4.5 | −12.4 | +3.5 |
| **10** | −56.4 | +2.4 | −265.4 | 659.0 | +6.2 | −6.5 | +12.6 | −10.4 |
| **11** | −64.7 | +9.3 | −278.6 | 670.4 | −2.1 | +0.4 | −0.6 | +1.0 |
| **12** | −75.1 | +1.8 | −283.4 | 663.5 | −12.5 | −7.1 | −5.4 | −5.8 |
| **13** | −61.8 | +8.1 | −277.3 | 668.8 | +0.9 | −0.8 | +0.7 | −0.6 |
| **14** | −62.2 | +8.7 | −277.6 | 669.2 | +0.5 | −0.2 | +0.4 | −0.2 |
| **15** | −54.2 | −3.8 | −318.4 | 684.6 | +8.4 | −12.7 | −40.4 | +15.3 |
| **16** | −62.1 | +8.2 | −278.1 | 669.5 | +0.5 | −0.7 | −0.1 | +0.2 |
| **17** | −58.1 | +12.1 | −278.6 | 666.5 | +4.5 | +3.2 | −0.6 | −2.9 |

| **Model** | $10^3 \cdot \lvert\overline{\alpha}\rvert$ | $\theta\left(\overline{\alpha}\right)/\pi$ | $\phi\left(\overline{\alpha}\right)/\pi$ | $10^3 \cdot \Delta\lvert\overline{\alpha}\rvert$ | $\Delta\theta\left(\overline{\alpha}\right)/\pi$ | $\Delta\phi\left(\overline{\alpha}\right)/\pi$ |
|---|---|---|---|---|---|---|
| **0** | +285.1 | +0.929 | +0.955 | | | |
| **1** | +286.2 | +0.930 | +0.956 | +1.1 | +0.001 | +0.001 |
| **2** | +285.6 | +0.929 | +0.954 | +0.5 | −0.000 | −0.001 |
| **3** | +282.4 | +0.933 | +0.960 | −2.7 | +0.004 | +0.005 |
| **4** | +285.8 | +0.921 | +0.956 | +0.8 | −0.007 | +0.001 |
| **5** | +286.4 | +0.920 | +0.957 | +1.4 | −0.009 | +0.002 |
| **6** | +290.4 | +0.922 | +0.959 | +5.3 | −0.007 | +0.004 |
| **7** | +315.6 | +0.919 | +0.927 | +30.5 | −0.010 | −0.028 |
| **8** | +290.3 | +0.937 | +0.939 | +5.2 | +0.008 | −0.017 |
| **9** | +298.0 | +0.928 | +0.979 | +12.9 | −0.001 | +0.024 |
| **10** | +271.3 | +0.933 | +0.987 | −13.8 | +0.004 | +0.031 |
| **11** | +286.2 | +0.927 | +0.955 | +1.1 | −0.002 | −0.000 |
| **12** | +293.2 | +0.918 | +0.992 | +8.1 | −0.011 | +0.037 |
| **13** | +284.2 | +0.930 | +0.958 | −0.9 | +0.001 | +0.003 |
| **14** | +284.6 | +0.929 | +0.956 | −0.5 | +0.000 | +0.001 |
| **15** | +323.0 | +0.946 | +1.022 | +37.9 | +0.017 | +0.067 |
| **16** | +285.1 | +0.929 | +0.958 | −0.0 | +0.001 | +0.003 |
| **17** | +284.8 | +0.933 | +0.935 | −0.2 | +0.004 | −0.021 |

**Tip:** These values can be downloaded in serialized JSON format under *Exported distributions* (page 42).

```
<Figure size 1100x500 with 2 Axes>
```

```
<Figure size 1100x500 with 2 Axes>
```

```
<Figure size 900x500 with 2 Axes>
```

```
<Figure size 900x500 with 2 Axes>
```

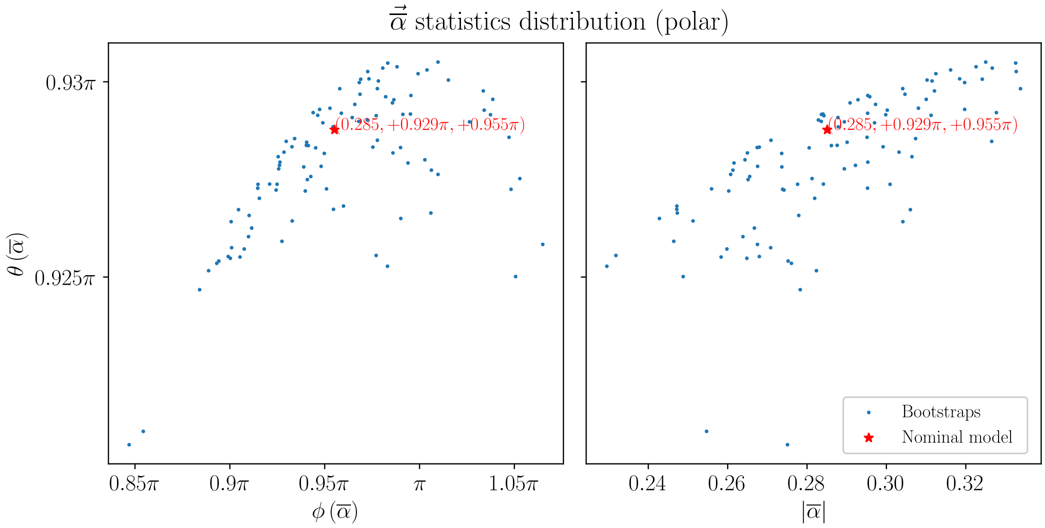

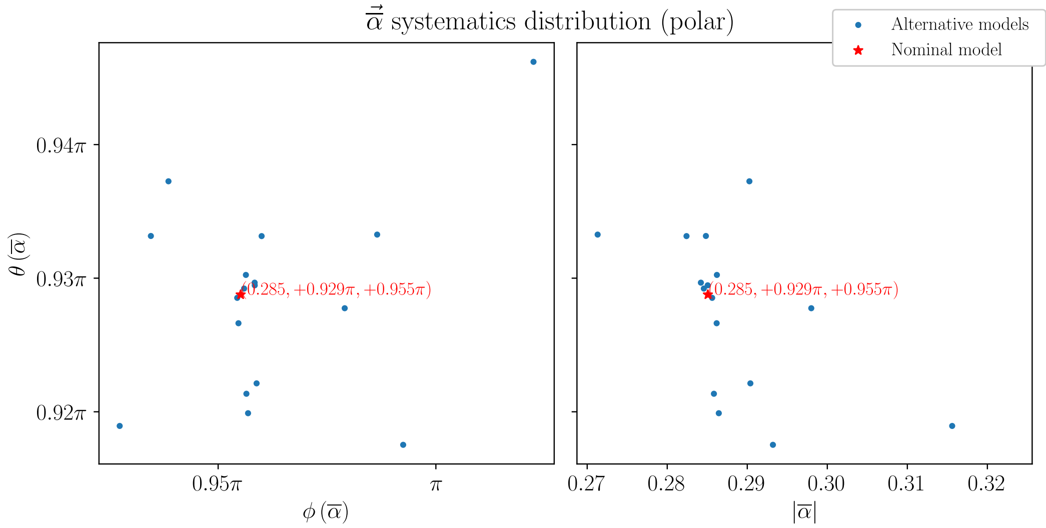


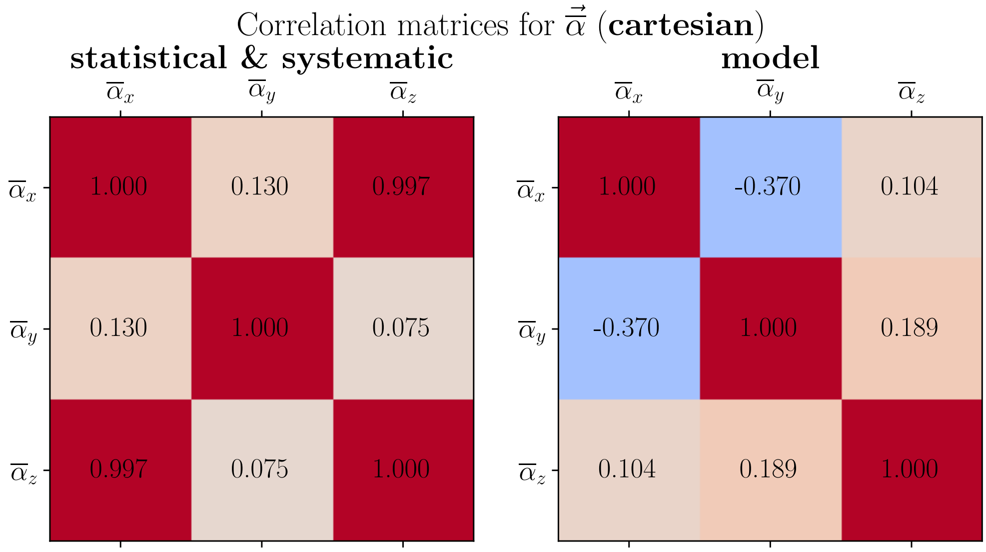


**Tip:** A potential explanation for the $xz$-correlation may be found in Section *XZ-correlations* (page 46).

## 5.7 Exported distributions

The polarimetry fields are computed for each parameter bootstrap (statistics & systematics) and for each model on lc2pkpi-polarimetry.docs.cern.ch/uncertainties.html. All combined fields can be downloaded as single compressed TAR file under lc2pkpi-polarimetry.docs.cern.ch/_static/export/polarimetry-field.json and as a single JSON file under lc2pkpi-polarimetry.docs.cern.ch/_static/export/polarimetry-field.tar.gz.

**Tip:** See *Import and interpolate* (page 59) for how to use these grids in an an analysis and see *Determination of polarization* (page 64) for how to use these fields to determine the polarization from a measured distribution.

CHAPTER

SIX

# AVERAGE POLARIMETER PER RESONANCE

## 6.1 Computations

```
Generating intensity-based sample:   0%|          | 0/100000 [00:00<?, ?it/s]
```

## 6.2 Result and comparison

LHCb values are taken from the original study [1]:

| | this study | LHCb | 1 | 2 | 3 | 4 | 5 | 6 | 7 | 8 | 9 | 10 |
|---|---|---|---|---|---|---|---|---|---|---|---|---|
| $K(700)$ | $+63 \pm 78^{+238}_{-235}$ | $+60 \pm 660 \pm 240$ | $-5$ | $-14$ | $-55$ | $-113$ | $-100$ | $+57$ | $-176$ | $-235$ | $+238$ | $+96$ |
| $K(892)$ | $+29 \pm 15^{+31}_{-17}$ | | $+2$ | $-0$ | $+2$ | $-9$ | $-17$ | $+2$ | $-5$ | $+23$ | $+31$ | $-8$ |
| $K(1430)$ | $-339 \pm 28^{+139}_{-102}$ | $-340 \pm 30 \pm 140$ | $+3$ | $+3$ | $-1$ | $-2$ | $+45$ | $+102$ | $+125$ | $-9$ | $-102$ | $+139$ |
| $\Lambda(1405)$ | $+580 \pm 31^{+278}_{-122}$ | $-580 \pm 50 \pm 280$ | $+14$ | $-7$ | $+3$ | $+31$ | $-3$ | $-30$ | $-122$ | $-22$ | $+124$ | $-64$ |
| $\Lambda(1520)$ | $+925 \pm 8^{+16}_{-84}$ | $-925 \pm 25 \pm 84$ | $+7$ | $+2$ | $+2$ | $+16$ | $-34$ | $+2$ | $+8$ | $+11$ | $+7$ | $-3$ |
| $\Lambda(1600)$ | $+199 \pm 51^{+499}_{-428}$ | $-200 \pm 60 \pm 500$ | $+10$ | $-5$ | $+14$ | $-5$ | $+21$ | $+138$ | $+100$ | $+499$ | $-428$ | $-140$ |
| $\Lambda(1670)$ | $+817 \pm 15^{+73}_{-46}$ | $-817 \pm 42 \pm 73$ | $+9$ | $-10$ | $+12$ | $+70$ | $-41$ | $-5$ | $+73$ | $+30$ | $+47$ | $-46$ |
| $\Lambda(1690)$ | $+958 \pm 8^{+27}_{-35}$ | $-958 \pm 20 \pm 27$ | $-3$ | $+6$ | $-12$ | $-35$ | $-14$ | $+22$ | $+27$ | $-20$ | $+3$ | $-4$ |
| $\Lambda(2000)$ | $-573 \pm 9^{+124}_{-191}$ | $+570 \pm 30 \pm 190$ | $+9$ | $-1$ | $+12$ | $+47$ | $-24$ | $-45$ | $-191$ | $+58$ | $+85$ | $+78$ |
| $\Delta(1232)$ | $+548 \pm 8^{+36}_{-27}$ | $-548 \pm 14 \pm 36$ | $+9$ | $+0$ | $-9$ | $-14$ | $+17$ | $-1$ | $+10$ | $+36$ | $+5$ | $-11$ |
| $\Delta(1600)$ | $-502 \pm 9^{+162}_{-112}$ | $+500 \pm 50 \pm 170$ | $+19$ | $+10$ | $+6$ | $+107$ | $-112$ | $+115$ | $+88$ | $+49$ | $+162$ | $+5$ |
| $\Delta(1700)$ | $+216 \pm 18^{+42}_{-75}$ | $-216 \pm 36 \pm 75$ | $+40$ | $+4$ | $-0$ | $-19$ | $-2$ | $+23$ | $+16$ | $+42$ | $+23$ | $-75$ |

## 6.3 Distribution analysis

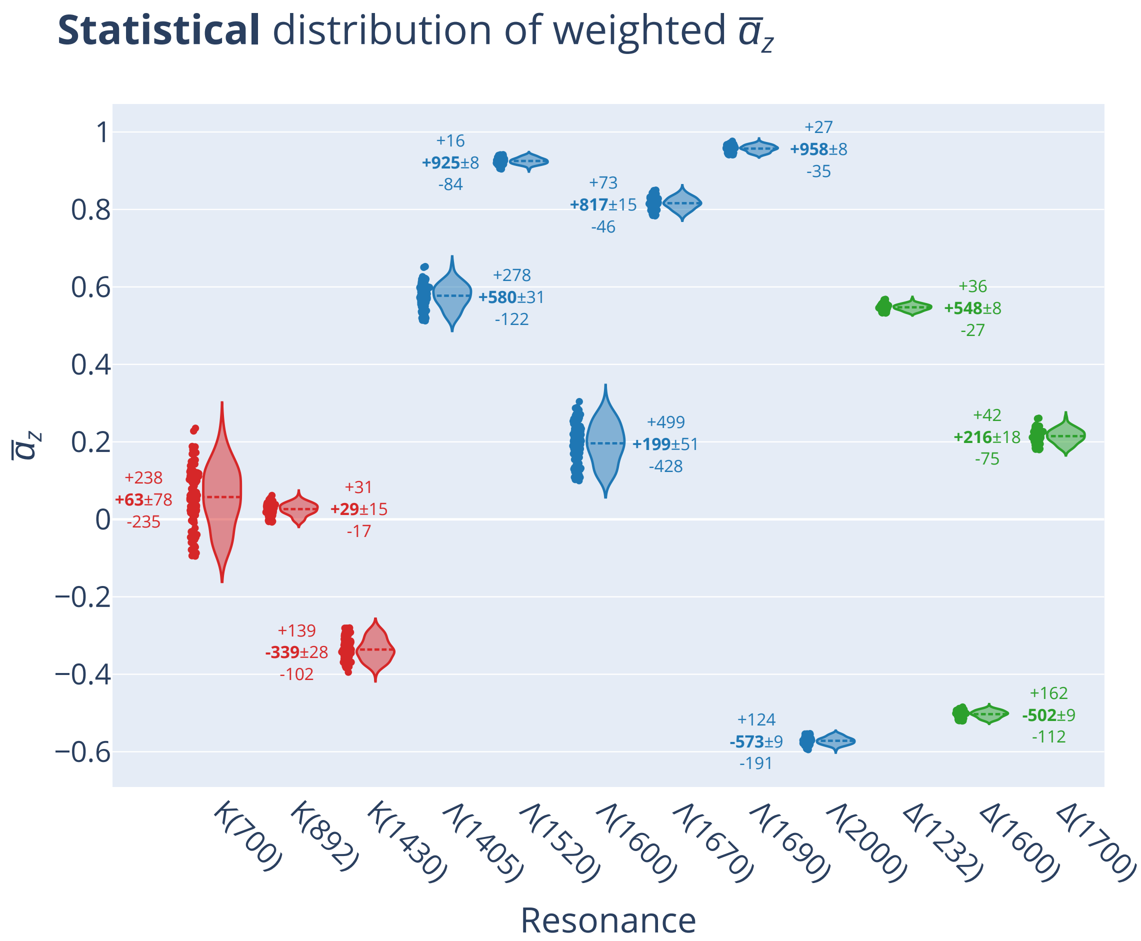


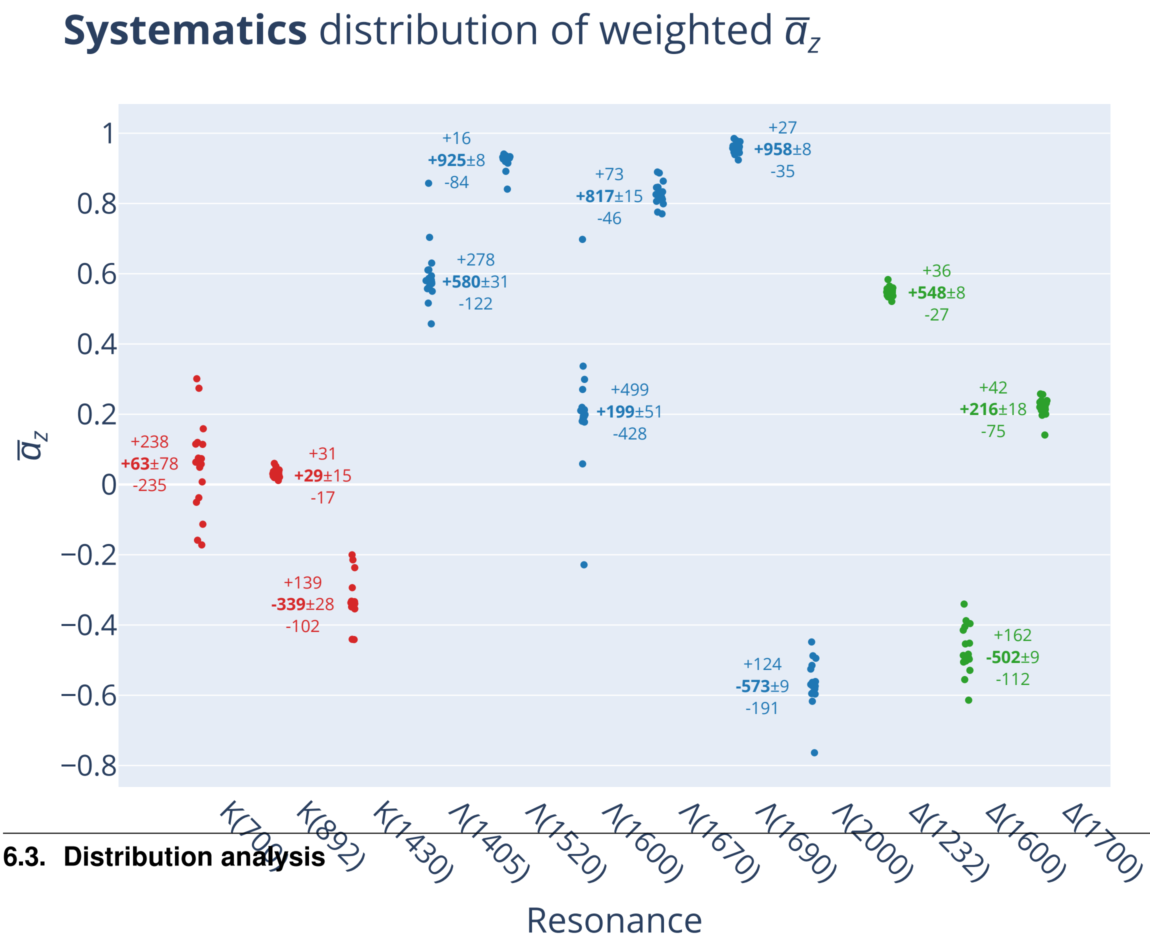

### 6.3.1 XZ-correlations

It follows from the definition of $\vec{\alpha}$ for a single resonance that:

$$\begin{aligned}\alpha_x &= |\vec{\alpha}| \int I_0 \sin\left(\zeta^0\right) \mathrm{d}\tau \Big/ \int I_0 \,\mathrm{d}\tau \\ \alpha_z &= |\vec{\alpha}| \int I_0 \cos\left(\zeta^0\right) \mathrm{d}\tau \Big/ \int I_0 \,\mathrm{d}\tau\end{aligned}$$

This means that the correlation if 100% if $I_0$ does not change in the bootstrap. This may explain the $xz$-correlation observed for $\overline{\alpha}$ over the complete decay as reported in *Average polarimetry values* (page 40).

$$I_{L(2000)} = \frac{155.425\sigma_2^2}{\left|\sigma_2(\sigma_2-3.953)+0.79i\sqrt{0.445\sigma_2^2-\sigma_2+0.18}\right|^2}$$

$$\alpha_{x,L(2000)} = -0.572\sin\left(\zeta^0_{2(1)}\right)$$

$$\alpha_{z,L(2000)} = -0.572\cos\left(\zeta^0_{2(1)}\right)$$

```
<Figure size 1200x800 with 12 Axes>
```

```
<Figure size 1200x800 with 12 Axes>
```

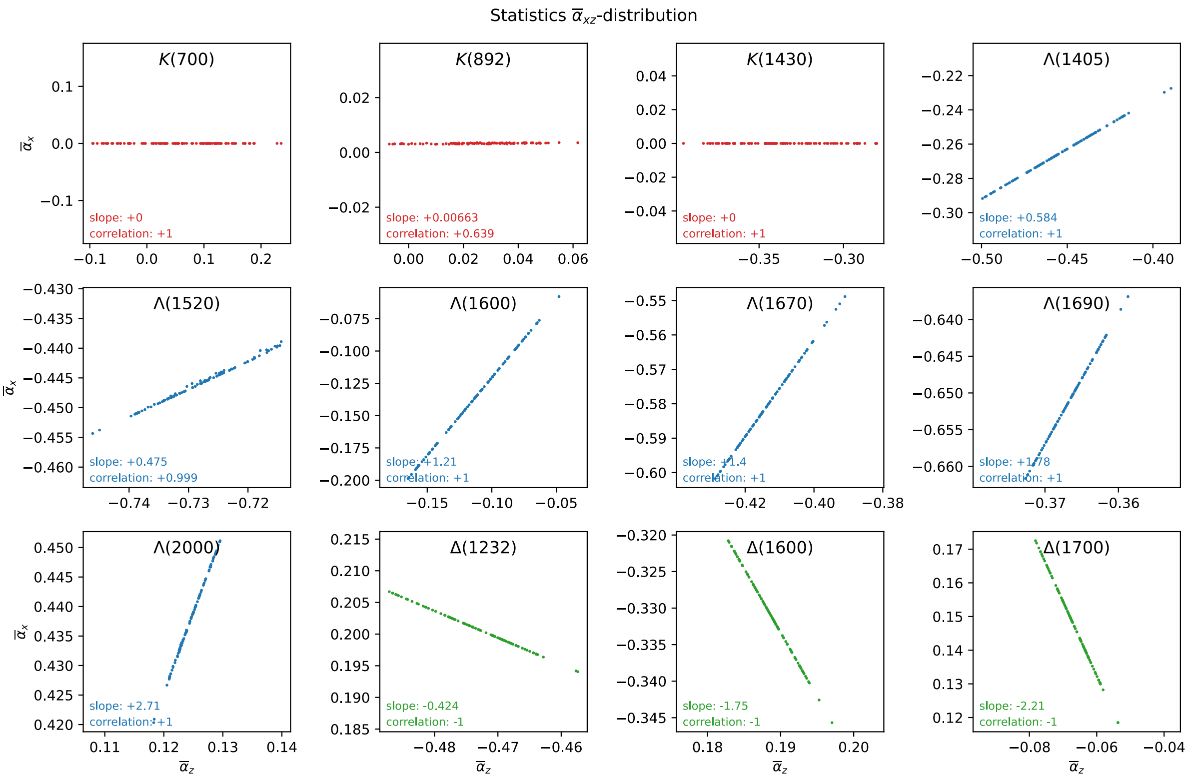

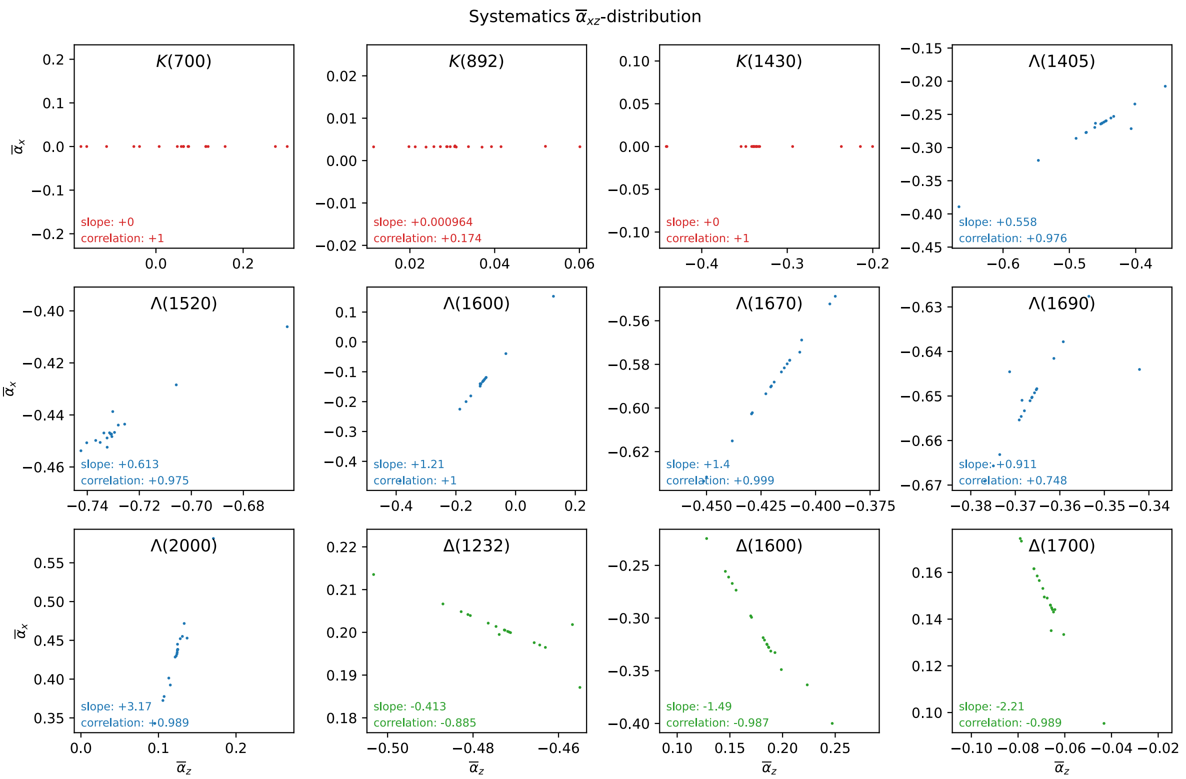


**Tip:** The following plots are interactive and can best be viewed on lc2pkpi-polarimetry.docs.cern.ch.

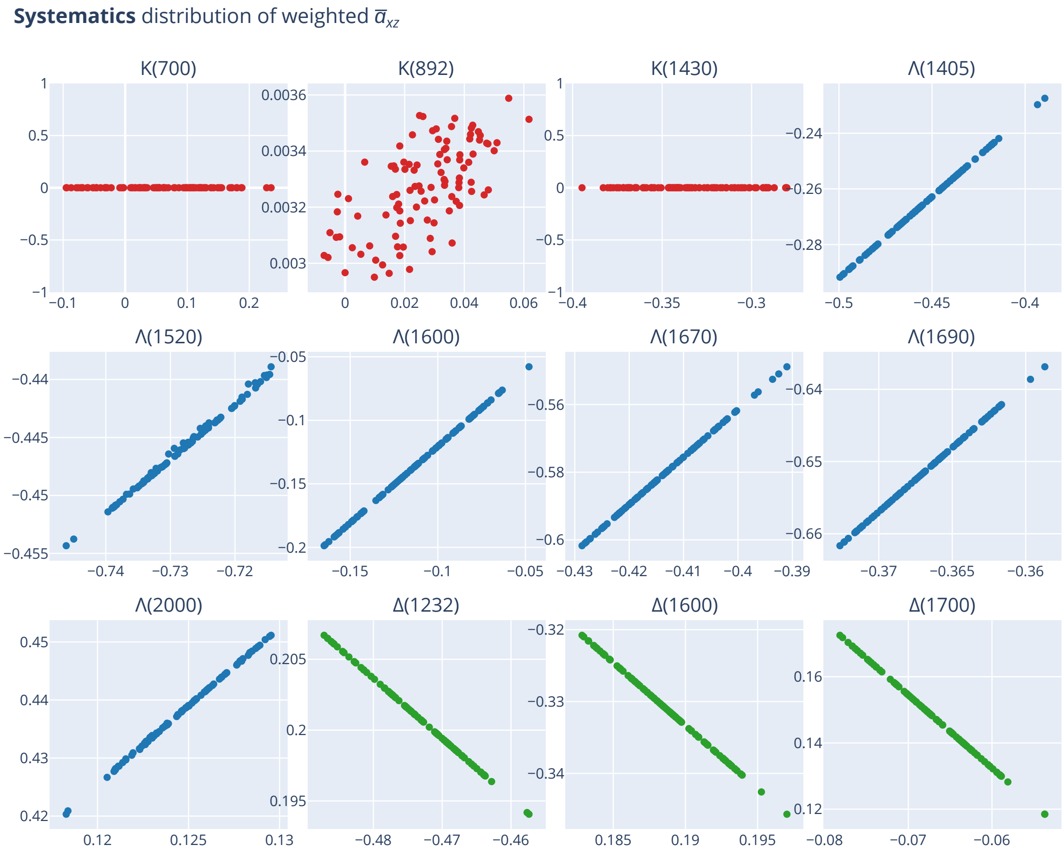
Systematics distribution of weighted $\overline{\alpha}_{xz}$
K(700)
K(892)
K(1430)
Λ(1405)
Λ(1520)
Λ(1600)
Λ(1670)
Λ(1690)
Λ(2000)
Δ(1232)
Δ(1600)
Δ(1700)

**Systematics** distribution of weighted $\overline{\alpha}_{xz}$

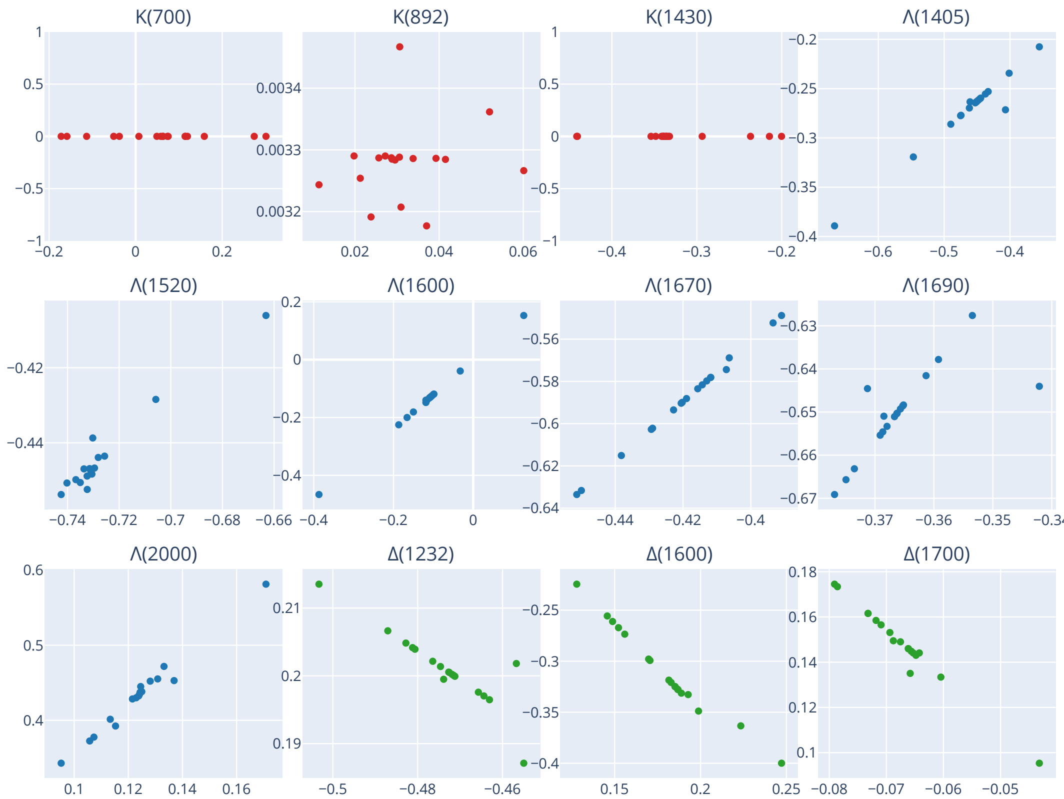

CHAPTER

SEVEN

# APPENDIX

## 7.1 Dynamics lineshapes

$$
\begin{aligned}
F_L\left(z\right) &= \begin{cases} 1 & \text{for } L = 0 \\ \frac{1}{\sqrt{z^2+1}} & \text{for } L = 1 \\ \frac{1}{\sqrt{z^4+3z^2+9}} & \text{for } L = 2 \end{cases} \\
\lambda\left(x, y, z\right) &= x^2 - 2xy - 2xz + y^2 - 2yz + z^2 \\
p_{m_i, m_j}\left(s\right) &= \frac{\sqrt{\lambda\left(s, m_i^2, m_j^2\right)}}{2\sqrt{s}} \\
q_{m_0, m_k}\left(s\right) &= \frac{\sqrt{\lambda\left(s, m_0^2, m_k^2\right)}}{2m_0} \\
\Gamma\left(s\right) &= \Gamma_0 \frac{m}{\sqrt{s}} \frac{F_{l_R}\left(Rp_{m_1,m_2}(s)\right)^2}{F_{l_R}\left(Rp_{m_1,m_2}(m^2)\right)^2} \left(\frac{p_{m_1,m_2}(s)}{p_{m_1,m_2}(m^2)}\right)^{2l_R+1}
\end{aligned}
$$

### 7.1.1 Relativistic Breit-Wigner

$$
\mathcal{R}\left(s\right) = \frac{\frac{F_{l_R}\left(R_{\text{res}} p_{m_1,m_2}(s)\right)}{F_{l_R}\left(R_{\text{res}} p_{m_1,m_2}(m^2)\right)} \frac{F_{l_{\Lambda_c}}\left(R_{\Lambda_c} q_{m_{\text{top}},m_{\text{spectator}}}(s)\right)}{F_{l_{\Lambda_c}}\left(R_{\Lambda_c} q_{m_{\text{top}},m_{\text{spectator}}}(m^2)\right)} \left(\frac{p_{m_1,m_2}(s)}{p_{m_1,m_2}(m^2)}\right)^{l_R} \left(\frac{q_{m_{\text{top}},m_{\text{spectator}}}(s)}{q_{m_{\text{top}},m_{\text{spectator}}}(m^2)}\right)^{l_{\Lambda_c}}}{m^2 - im\Gamma(s) - s}
$$

### 7.1.2 Bugg Breit-Wigner

$$
\begin{aligned}
\mathcal{R}_{\text{Bugg}}\left(m_{K\pi}^2\right) &= \frac{1}{-\frac{i\Gamma_0 m_0 (m_{K\pi}^2 - s_A) e^{-\gamma m_{K\pi}^2}}{m_0^2 - s_A} + m_0^2 - m_{K\pi}^2} \\
s_A &= m_K^2 - \frac{m_\pi^2}{2} \\
p_{m_K, m_\pi}\left(m_{K\pi}^2\right) &= \frac{\sqrt{\lambda(m_{K\pi}^2, m_K^2, m_\pi^2)}}{2\sqrt{m_{K\pi}^2}}
\end{aligned}
$$

One of the models uses a Bugg Breit-Wigner with an exponential factor:

$$
e^{-\alpha q_{m_0,m_1}(s)^2} \mathcal{R}_{\text{Bugg}}\left(m_{K\pi}^2\right)
$$

### 7.1.3 Flatté for S-waves

$$\mathcal{R}_{\text{Flatté}}\left(s\right) = \frac{1}{m^{2} - i m \left(\frac{\Gamma_{1} m p_{m_{11},m_{21}}(s)}{\sqrt{s} p_{m_{12},m_{22}}(m^{2})} + \frac{\Gamma_{2} m p_{m_{12},m_{22}}(s)}{\sqrt{s} p_{m_{12},m_{22}}(m^{2})}\right) - s}$$

## 7.2 DPD angles

Equation (A1) from [2]:

$$\begin{aligned}
\theta_{12} &= \operatorname{acos}\left(\frac{2\sigma_3(-m_1^2-m_3^2+\sigma_2)-(m_0^2-m_3^2-\sigma_3)(m_1^2-m_2^2+\sigma_3)}{\sqrt{\lambda(m_0^2,m_3^2,\sigma_3)}\sqrt{\lambda(\sigma_3,m_1^2,m_2^2)}}\right)\\
\theta_{23} &= \operatorname{acos}\left(\frac{2\sigma_1(-m_1^2-m_2^2+\sigma_3)-(m_0^2-m_1^2-\sigma_1)(m_2^2-m_3^2+\sigma_1)}{\sqrt{\lambda(m_0^2,m_1^2,\sigma_1)}\sqrt{\lambda(\sigma_1,m_2^2,m_3^2)}}\right)\\
\theta_{31} &= \operatorname{acos}\left(\frac{2\sigma_2(-m_2^2-m_3^2+\sigma_1)-(m_0^2-m_2^2-\sigma_2)(-m_1^2+m_3^2+\sigma_2)}{\sqrt{\lambda(m_0^2,m_2^2,\sigma_2)}\sqrt{\lambda(\sigma_2,m_3^2,m_1^2)}}\right)
\end{aligned}$$

Equation (A3):

$$\begin{aligned}
\hat{\theta}_{3(1)} &= \operatorname{acos}\left(\frac{-2m_0^2(-m_1^2-m_3^2+\sigma_2)+(m_0^2+m_1^2-\sigma_1)(m_0^2+m_3^2-\sigma_3)}{\sqrt{\lambda(m_0^2,m_1^2,\sigma_1)}\sqrt{\lambda(m_0^2,\sigma_3,m_3^2)}}\right)\\
\hat{\theta}_{1(2)} &= \operatorname{acos}\left(\frac{-2m_0^2(-m_1^2-m_2^2+\sigma_3)+(m_0^2+m_1^2-\sigma_1)(m_0^2+m_2^2-\sigma_2)}{\sqrt{\lambda(m_0^2,m_2^2,\sigma_2)}\sqrt{\lambda(m_0^2,\sigma_1,m_1^2)}}\right)\\
\hat{\theta}_{2(3)} &= \operatorname{acos}\left(\frac{-2m_0^2(-m_2^2-m_3^2+\sigma_1)+(m_0^2+m_2^2-\sigma_2)(m_0^2+m_3^2-\sigma_3)}{\sqrt{\lambda(m_0^2,m_3^2,\sigma_3)}\sqrt{\lambda(m_0^2,\sigma_2,m_2^2)}}\right)
\end{aligned}$$

Equations (A7):

$$\begin{aligned}
\zeta^1_{1(3)} &= \operatorname{acos}\left(\frac{2m_1^2(-m_0^2-m_2^2+\sigma_2)+(m_0^2+m_1^2-\sigma_1)(-m_1^2-m_2^2+\sigma_3)}{\sqrt{\lambda(m_0^2,m_1^2,\sigma_1)}\sqrt{\lambda(\sigma_3,m_1^2,m_2^2)}}\right)\\
\zeta^1_{2(1)} &= \operatorname{acos}\left(\frac{2m_1^2(-m_0^2-m_3^2+\sigma_3)+(m_0^2+m_1^2-\sigma_1)(-m_1^2-m_3^2+\sigma_2)}{\sqrt{\lambda(m_0^2,m_1^2,\sigma_1)}\sqrt{\lambda(\sigma_2,m_1^2,m_3^2)}}\right)\\
\zeta^2_{2(1)} &= \operatorname{acos}\left(\frac{2m_2^2(-m_0^2-m_3^2+\sigma_3)+(m_0^2+m_2^2-\sigma_2)(-m_2^2-m_3^2+\sigma_1)}{\sqrt{\lambda(m_0^2,m_2^2,\sigma_2)}\sqrt{\lambda(\sigma_1,m_2^2,m_3^2)}}\right)\\
\zeta^2_{3(2)} &= \operatorname{acos}\left(\frac{2m_2^2(-m_0^2-m_1^2+\sigma_1)+(m_0^2+m_2^2-\sigma_2)(-m_1^2-m_2^2+\sigma_3)}{\sqrt{\lambda(m_0^2,m_2^2,\sigma_2)}\sqrt{\lambda(\sigma_3,m_2^2,m_1^2)}}\right)\\
\zeta^3_{3(2)} &= \operatorname{acos}\left(\frac{2m_3^2(-m_0^2-m_1^2+\sigma_1)+(m_0^2+m_3^2-\sigma_3)(-m_1^2-m_3^2+\sigma_2)}{\sqrt{\lambda(m_0^2,m_3^2,\sigma_3)}\sqrt{\lambda(\sigma_2,m_3^2,m_1^2)}}\right)\\
\zeta^3_{1(3)} &= \operatorname{acos}\left(\frac{2m_3^2(-m_0^2-m_2^2+\sigma_2)+(m_0^2+m_3^2-\sigma_3)(-m_2^2-m_3^2+\sigma_1)}{\sqrt{\lambda(m_0^2,m_3^2,\sigma_3)}\sqrt{\lambda(\sigma_1,m_3^2,m_2^2)}}\right)
\end{aligned}$$

Equations (A10):

$$\begin{aligned}
\zeta^1_{2(3)} &= \operatorname{acos}\left(\frac{2m_1^2(m_2^2+m_3^2-\sigma_1)+(-m_1^2-m_2^2+\sigma_3)(-m_1^2-m_3^2+\sigma_2)}{\sqrt{\lambda(\sigma_2,m_3^2,m_1^2)}\sqrt{\lambda(\sigma_3,m_1^2,m_2^2)}}\right)\\
\zeta^2_{3(1)} &= \operatorname{acos}\left(\frac{2m_2^2(m_1^2+m_3^2-\sigma_2)+(-m_1^2-m_2^2+\sigma_3)(-m_2^2-m_3^2+\sigma_1)}{\sqrt{\lambda(\sigma_1,m_2^2,m_3^2)}\sqrt{\lambda(\sigma_3,m_1^2,m_2^2)}}\right)\\
\zeta^3_{1(2)} &= \operatorname{acos}\left(\frac{2m_3^2(m_1^2+m_2^2-\sigma_3)+(-m_1^2-m_3^2+\sigma_2)(-m_2^2-m_3^2+\sigma_1)}{\sqrt{\lambda(\sigma_1,m_2^2,m_3^2)}\sqrt{\lambda(\sigma_2,m_3^2,m_1^2)}}\right)
\end{aligned}$$

## 7.3 Phase space sample

### 7.3.1 Definition

**See also:**

AmpForm's Kinematics page.

$$\begin{cases} 1 & \text{for } \phi\left(\sigma_i,\sigma_j\right) \leq 0 \\ \text{NaN} & \text{otherwise} \end{cases}$$

$$\phi\left(\sigma_i,\sigma_j\right) = \lambda\left(\lambda\left(\sigma_j,m_j^2,m_0^2\right),\lambda\left(\sigma_k,m_k^2,m_0^2\right),\lambda\left(\sigma_i,m_i^2,m_0^2\right)\right)$$

$$\lambda\left(x,y,z\right) = x^2-2xy-2xz+y^2-2yz+z^2$$

$$\sigma_k = m_0^2+m_1^2+m_2^2+m_3^2-\sigma_i-\sigma_j$$

### 7.3.2 Visualization

$$\begin{aligned}
m_0 &= 2.28646\\
m_1 &= 0.938272046\\
m_2 &= 0.13957018\\
m_3 &= 0.49367700000000003
\end{aligned}$$

```
<Figure size 500x500 with 1 Axes>
```

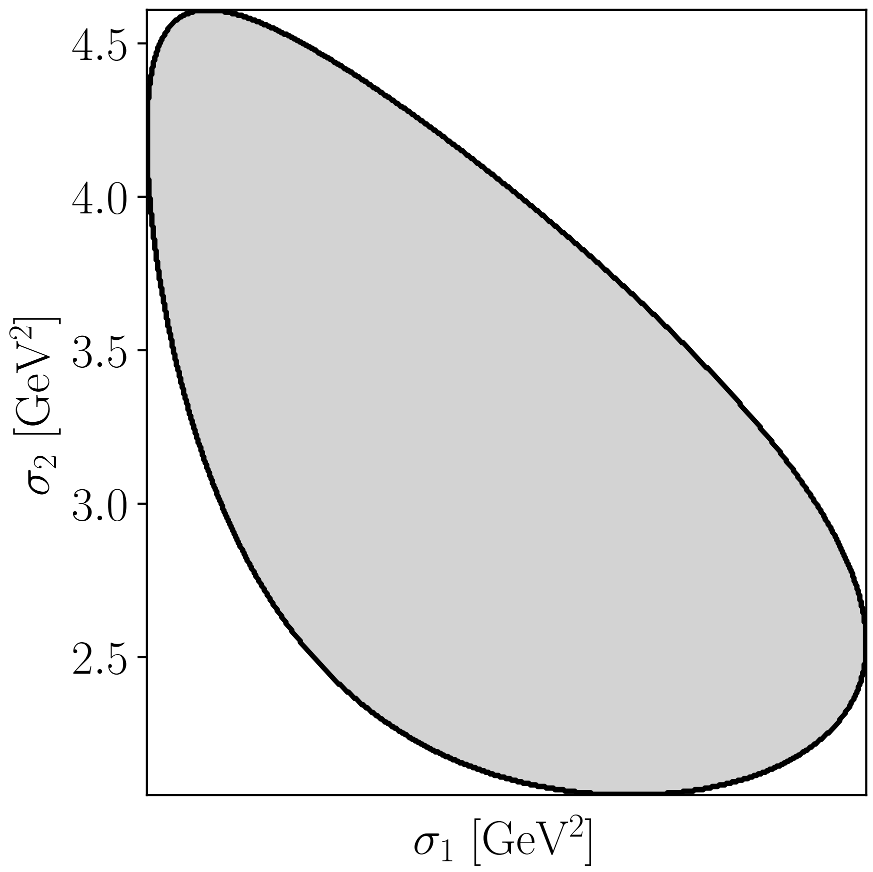


```
Generating intensity-based sample:   0%|          | 0/10000000 [00:00<?, ?it/s]
```

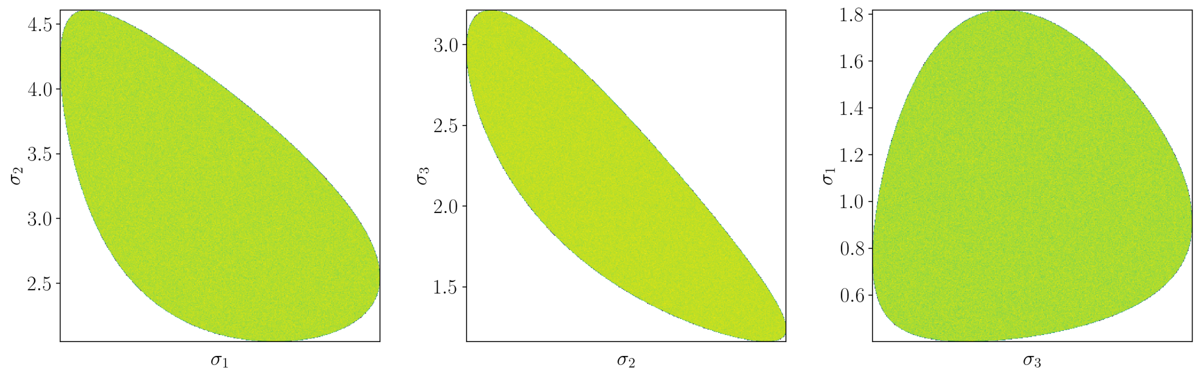


## 7.4 Alignment consistency

$$\sum_{\lambda_0=-1/2}^{1/2}\sum_{\lambda_1=-1/2}^{1/2}\left|\sum_{\lambda_0'=-1/2}^{1/2}\sum_{\lambda_1'=-1/2}^{1/2} A^1_{\lambda_0',\lambda_1',0,0}d^{\frac{1}{2}}_{\lambda_1',\lambda_1}\left(\zeta^1_{1(1)}\right)d^{\frac{1}{2}}_{\lambda_0,\lambda_0'}\left(\zeta^0_{1(1)}\right)+A^2_{\lambda_0',\lambda_1',0,0}d^{\frac{1}{2}}_{\lambda_1',\lambda_1}\left(\zeta^1_{2(1)}\right)d^{\frac{1}{2}}_{\lambda_0,\lambda_0'}\left(\zeta^0_{2(1)}\right)+A^3 \ldots$$
$$\sum_{\lambda_0=-1/2}^{1/2}\sum_{\lambda_1=-1/2}^{1/2}\left|\sum_{\lambda_0'=-1/2}^{1/2}\sum_{\lambda_1'=-1/2}^{1/2} A^1_{\lambda_0',\lambda_1',0,0}d^{\frac{1}{2}}_{\lambda_1',\lambda_1}\left(\zeta^1_{1(2)}\right)d^{\frac{1}{2}}_{\lambda_0,\lambda_0'}\left(\zeta^0_{1(2)}\right)+A^2_{\lambda_0',\lambda_1',0,0}d^{\frac{1}{2}}_{\lambda_1',\lambda_1}\left(\zeta^1_{2(2)}\right)d^{\frac{1}{2}}_{\lambda_0,\lambda_0'}\left(\zeta^0_{2(2)}\right)+A^3 \ldots$$
$$\sum_{\lambda_0=-1/2}^{1/2}\sum_{\lambda_1=-1/2}^{1/2}\left|\sum_{\lambda_0'=-1/2}^{1/2}\sum_{\lambda_1'=-1/2}^{1/2} A^1_{\lambda_0',\lambda_1',0,0}d^{\frac{1}{2}}_{\lambda_1',\lambda_1}\left(\zeta^1_{1(3)}\right)d^{\frac{1}{2}}_{\lambda_0,\lambda_0'}\left(\zeta^0_{1(3)}\right)+A^2_{\lambda_0',\lambda_1',0,0}d^{\frac{1}{2}}_{\lambda_1',\lambda_1}\left(\zeta^1_{2(3)}\right)d^{\frac{1}{2}}_{\lambda_0,\lambda_0'}\left(\zeta^0_{2(3)}\right)+A^3 \ldots$$

See *DPD angles* (page 52) for the definition of each $\zeta^i_{j(k)}$.

Note that a change in reference sub-system requires the production couplings for certain sub-systems to flip sign:

- **Sub-system 2** as reference system: flip signs of $\mathcal{H}^{\text{production}}_{K^{**}}$ and $\mathcal{H}^{\text{production}}_{L^{**}}$
- **Sub-system 3** as reference system: flip signs of $\mathcal{H}^{\text{production}}_{K^{**}}$ and $\mathcal{H}^{\text{production}}_{D^{**}}$

```
{1: Array(3.91663029e+08, dtype=float64),
 2: Array(3.91663029e+08, dtype=float64),
 3: Array(3.91663029e+08, dtype=float64)}
```

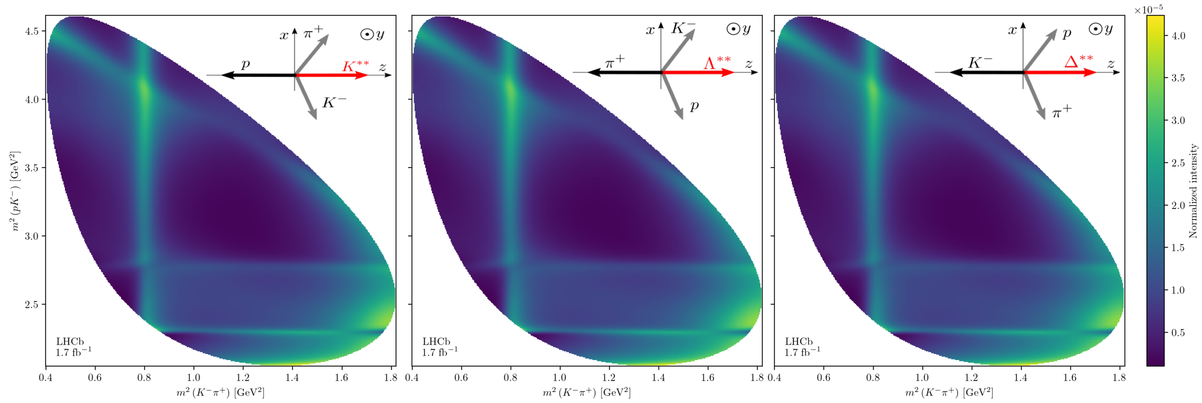

## 7.5 Benchmarking

**Tip:** This notebook benchmarks JAX on a **single CPU core**. Compare with Julia results as reported in ComPWA/polarimetry#27. See also the Extended benchmark #68 discussion.

**Note:** This notebook uses only one run and one loop for `%timeit`, because JAX seems to cache its return values.

```
Physical cores: 8
Total cores: 8
```

```
CPU times: user 25 s, sys: 0 ns, total: 25 s
Wall time: 25.1 s
```

### 7.5.1 `DataTransformer` performance

```
Generating intensity-based sample:   0%|          | 0/100000 [00:00<?, ?it/s]
```

```
524 ms ± 0 ns per loop (mean ± std. dev. of 1 run, 1 loop each)
25.5 ms ± 0 ns per loop (mean ± std. dev. of 1 run, 1 loop each)
25.6 ms ± 0 ns per loop (mean ± std. dev. of 1 run, 1 loop each)
```

```
483 ms ± 0 ns per loop (mean ± std. dev. of 1 run, 1 loop each)
2.73 ms ± 0 ns per loop (mean ± std. dev. of 1 run, 1 loop each)
1.99 ms ± 0 ns per loop (mean ± std. dev. of 1 run, 1 loop each)
```

### 7.5.2 Parametrized function

Compare *All parameters substituted* (page 57).

Total number of mathematical operations:

- $\alpha_x$: 133,630
- $\alpha_y$: 133,634
- $\alpha_z$: 133,630
- $I_{\text{tot}}$: 43,198

```
CPU times: user 23.5 ms, sys: 0 ns, total: 23.5 ms
Wall time: 23.2 ms
```

#### One data point

#### JIT-compilation

```
<TimeitResult : 2.05 s ± 0 ns per loop (mean ± std. dev. of 1 run, 1 loop each)>
```

```
<TimeitResult : 10.8 s ± 0 ns per loop (mean ± std. dev. of 1 run, 1 loop each)>
```

#### Compiled performance

```
<TimeitResult : 1.41 ms ± 0 ns per loop (mean ± std. dev. of 1 run, 1 loop each)>
```

```
<TimeitResult : 2.2 ms ± 0 ns per loop (mean ± std. dev. of 1 run, 1 loop each)>
```

#### 54x54 grid sample

#### Compiled but uncached

```
<TimeitResult : 2.31 s ± 0 ns per loop (mean ± std. dev. of 1 run, 1 loop each)>
```

```
<TimeitResult : 13.3 s ± 0 ns per loop (mean ± std. dev. of 1 run, 1 loop each)>
```

#### Second run with cache

```
<TimeitResult : 3.84 ms ± 0 ns per loop (mean ± std. dev. of 1 run, 1 loop each)>
```

```
<TimeitResult : 19 ms ± 0 ns per loop (mean ± std. dev. of 1 run, 1 loop each)>
```

#### 100.000 event phase space sample

#### Compiled but uncached

```
<TimeitResult : 2.33 s ± 0 ns per loop (mean ± std. dev. of 1 run, 1 loop each)>
```

```
<TimeitResult : 13.1 s ± 0 ns per loop (mean ± std. dev. of 1 run, 1 loop each)>
```

#### Second run with cache

```
<TimeitResult : 63.5 ms ± 0 ns per loop (mean ± std. dev. of 1 run, 1 loop each)>
```

```
<TimeitResult : 235 ms ± 0 ns per loop (mean ± std. dev. of 1 run, 1 loop each)>
```

#### Recompilation after parameter modification

#### Compiled but uncached

```
<TimeitResult : 2.33 s ± 0 ns per loop (mean ± std. dev. of 1 run, 1 loop each)>
```

```
<TimeitResult : 13.3 s ± 0 ns per loop (mean ± std. dev. of 1 run, 1 loop each)>
```

#### Second run with cache

```
<TimeitResult : 53.9 ms ± 0 ns per loop (mean ± std. dev. of 1 run, 1 loop each)>
```

```
<TimeitResult : 286 ms ± 0 ns per loop (mean ± std. dev. of 1 run, 1 loop each)>
```

### 7.5.3 All parameters substituted

Compare *Parametrized function* (page 56).

Number of mathematical operations after substituting all parameters:

- $\alpha_x$: 29,552
- $\alpha_y$: 29,556
- $\alpha_z$: 29,552
- $I_\text{tot}$: 9,624

```
CPU times: user 11.8 ms, sys: 0 ns, total: 11.8 ms
Wall time: 12.2 ms
```

### One data point

#### JIT-compilation

```
<TimeitResult : 1.48 s ± 0 ns per loop (mean ± std. dev. of 1 run, 1 loop each)>
```

```
<TimeitResult : 7.45 s ± 0 ns per loop (mean ± std. dev. of 1 run, 1 loop each)>
```

#### Compiled performance

```
<TimeitResult : 282 µs ± 0 ns per loop (mean ± std. dev. of 1 run, 1 loop each)>
```

```
<TimeitResult : 303 µs ± 0 ns per loop (mean ± std. dev. of 1 run, 1 loop each)>
```

### 54x54 grid sample

#### Compiled but uncached

```
<TimeitResult : 1.62 s ± 0 ns per loop (mean ± std. dev. of 1 run, 1 loop each)>
```

```
<TimeitResult : 8.64 s ± 0 ns per loop (mean ± std. dev. of 1 run, 1 loop each)>
```

#### Second run with cache

```
<TimeitResult : 4.77 ms ± 0 ns per loop (mean ± std. dev. of 1 run, 1 loop each)>
```

```
<TimeitResult : 23.1 ms ± 0 ns per loop (mean ± std. dev. of 1 run, 1 loop each)>
```

### 100.000 event phase space sample

#### Compiled but uncached

```
<TimeitResult : 1.69 s ± 0 ns per loop (mean ± std. dev. of 1 run, 1 loop each)>
```

```
<TimeitResult : 8.9 s ± 0 ns per loop (mean ± std. dev. of 1 run, 1 loop each)>
```

#### Second run with cache

```
<TimeitResult : 46.8 ms ± 0 ns per loop (mean ± std. dev. of 1 run, 1 loop each)>
```

```
<TimeitResult : 301 ms ± 0 ns per loop (mean ± std. dev. of 1 run, 1 loop each)>
```

### 7.5.4 Summary

```
<pandas.io.formats.style.Styler at 0x7f841b7539d0>
```

## 7.6 Serialization

### 7.6.1 File size checks

File sizes for **100x100 grid**:

| File type | Size |
|---|---|
| `export/alpha-x-arrays.json` | **141 kB** |
| `export/alpha-x-pandas.json` | **311 kB** |
| `export/alpha-x-python.json` | **260 kB** |
| `export/alpha-x-pandas-json.zip` | **51 kB** |
| `export/alpha-x-pandas.csv` | **129 kB** |

### 7.6.2 Export polarimetry grids

Decided to use the `alpha-x-arrays.json` format. It can be exported with *`export_polarimetry_field()`* (page 80).

Polarimetry grid can be downloaded here: `export/polarimetry-model-0.json` (540 kB).

### 7.6.3 Import and interpolate

The arrays in the *exported JSON files* (page 42) can be used to create a `RegularGridInterpolator` for the intensity and for each components of $\vec{\alpha}$.

*`import_polarimetry_field()`* (page 80) returns JAX arrays, which are read-only. `RegularGridInterpolator` requires modifiable arrays, so we convert them to NumPy.

Also note that the `values` array needs to be **transposed**!

This is a function that can compute an interpolated value of each of these observables for a random point on the Dalitz plane.

```
array([0.18379986])
```

As opposed to SciPy's deprecated `interp2d`, `RegularGridInterpolator` is already in vectorized form, so there is no need to `vectorize` it.

```
Generating intensity-based sample:   0%|          | 0/100000 [00:00<?, ?it/s]
```

```
array([2165.82154945, 5481.04128781, 6254.96174147, ..., 1369.40657535,
       4456.44114915, 7197.97782088])
```

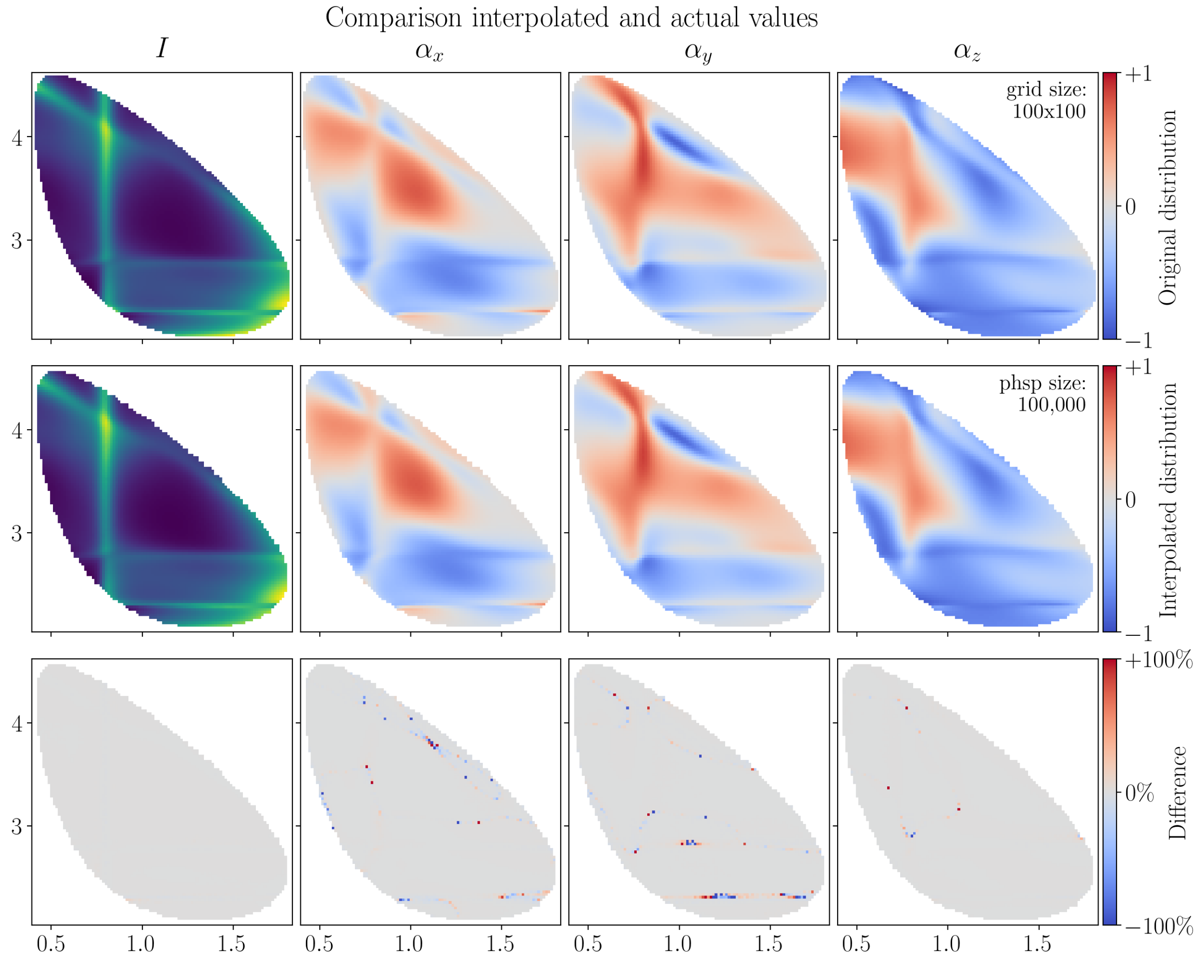


**Note:** The interpolated values over this phase space sample have been visualized by interpolating again over a `meshgrid` with `scipy.interpolate.griddata`.

**Tip:** *Determination of polarization* (page 64) shows how this interpolation method can be used to determine the polarization $\vec{P}$ from a given intensity distribution.

## 7.7 Amplitude model with LS-couplings

### 7.7.1 Model inspection

$$\sum_{\lambda_0'=-1/2}^{1/2} \sum_{\lambda_1'=-1/2}^{1/2} A^1_{\lambda_0',\lambda_1'} d^{\frac{1}{2}}_{\lambda_1',\lambda_1}\left(\zeta^1_{1(1)}\right) d^{\frac{1}{2}}_{\lambda_0,\lambda_0'}\left(\zeta^0_{1(1)}\right) + A^2_{\lambda_0',\lambda_1'} d^{\frac{1}{2}}_{\lambda_1',\lambda_1}\left(\zeta^1_{2(1)}\right) d^{\frac{1}{2}}_{\lambda_0,\lambda_0'}\left(\zeta^0_{2(1)}\right) + A^3_{\lambda_0',\lambda_1'} d^{\frac{1}{2}}_{\lambda_1',\lambda_1}\left(\zeta^1_{3(1)}\right) d^{\frac{1}{2}}_{\lambda_0,\lambda_0'}\left(\zeta^0_{3(1)}\right)$$

$$
\begin{aligned}
A^{1}_{-\frac{1}{2},-\frac{1}{2}} &= \sum_{\lambda_R=-1}^{1} -\frac{\sqrt{10}\delta_{-\frac{1}{2},\lambda_R+\frac{1}{2}}\mathcal{R}(\sigma_1)C^{\frac{3}{2},\lambda_R+\frac{1}{2}}_{1,\lambda_R,\frac{1}{2},\frac{1}{2}}C^{\frac{1}{2},\lambda_R+\frac{1}{2}}_{2,0,\frac{3}{2},\lambda_R+\frac{1}{2}}\mathcal{H}^{\text{LS,production}}_{K(892),2,\frac{3}{2}}\mathcal{H}^{\text{decay}}_{K(892),0,0}d^{1}_{\lambda_R,0}(\theta_{23})}{2} + \sum_{\lambda_R=-1}^{1} -\frac{\sqrt{2}\delta_{-\frac{1}{2},\lambda_R+\frac{1}{2}}\mathcal{R}(\sigma_1)C^{\frac{1}{2},\cdots}_{0,0\cdots}\cdots}{\cdots} \\
A^{2}_{-\frac{1}{2},-\frac{1}{2}} &= \sum_{\lambda_R=-3/2}^{3/2} -\frac{\sqrt{10}\delta_{-\frac{1}{2}\lambda_R}\mathcal{R}(\sigma_2)C^{\frac{3}{2},\lambda_R}_{\frac{3}{2},\lambda_R,0,0}C^{\frac{1}{2},\lambda_R}_{2,0,\frac{3}{2},\lambda_R}\mathcal{H}^{\text{LS,production}}_{L(1520),2,\frac{3}{2}}\mathcal{H}^{\text{decay}}_{L(1520),0,-\frac{1}{2}}d^{\frac{3}{2}}_{\lambda_R,\frac{1}{2}}(\theta_{31})}{2} + \sum_{\lambda_R=-3/2}^{3/2} -\frac{\sqrt{10}\delta_{-\frac{1}{2}\lambda_R}\mathcal{R}(\sigma_2)C^{\frac{3}{2},\cdots}_{\frac{3}{2},\cdots}\cdots}{\cdots} \\
A^{3}_{-\frac{1}{2},-\frac{1}{2}} &= \sum_{\lambda_R=-3/2}^{3/2} \frac{\sqrt{10}\delta_{-\frac{1}{2}\lambda_R}\mathcal{R}(\sigma_3)C^{\frac{3}{2},\lambda_R}_{\frac{3}{2},\lambda_R,0,0}C^{\frac{1}{2},\lambda_R}_{2,0,\frac{3}{2},\lambda_R}\mathcal{H}^{\text{LS,production}}_{D(1232),2,\frac{3}{2}}\mathcal{H}^{\text{decay}}_{D(1232),-\frac{1}{2},0}d^{\frac{3}{2}}_{\lambda_R,-\frac{1}{2}}(\theta_{12})}{2} + \sum_{\lambda_R=-3/2}^{3/2} \frac{\sqrt{10}\delta_{-\frac{1}{2}\lambda_R}\mathcal{R}(\sigma_3)C^{\frac{3}{2},\lambda_R}_{\frac{3}{2},\lambda_R,\cdots}\cdots}{\cdots} \\
A^{1}_{-\frac{1}{2},\frac{1}{2}} &= \sum_{\lambda_R=-1}^{1} \frac{\sqrt{10}\delta_{-\frac{1}{2},\lambda_R-\frac{1}{2}}\mathcal{R}(\sigma_1)C^{\frac{3}{2},\lambda_R-\frac{1}{2}}_{1,\lambda_R,\frac{1}{2},-\frac{1}{2}}C^{\frac{1}{2},\lambda_R-\frac{1}{2}}_{2,0,\frac{3}{2},\lambda_R-\frac{1}{2}}\mathcal{H}^{\text{LS,production}}_{K(892),2,\frac{3}{2}}\mathcal{H}^{\text{decay}}_{K(892),0,0}d^{1}_{\lambda_R,0}(\theta_{23})}{2} + \sum_{\lambda_R=-1}^{1} \frac{\sqrt{2}\delta_{-\frac{1}{2},\lambda_R-\frac{1}{2}}\mathcal{R}(\sigma_1)C^{\frac{1}{2},\lambda_R-\cdots}_{0,0,\frac{1}{2},\cdots}\cdots}{\cdots} \\
A^{2}_{-\frac{1}{2},\frac{1}{2}} &= \sum_{\lambda_R=-3/2}^{3/2} \frac{\sqrt{10}\delta_{-\frac{1}{2}\lambda_R}\mathcal{R}(\sigma_2)C^{\frac{3}{2},\lambda_R}_{\frac{3}{2},\lambda_R,0,0}C^{\frac{1}{2},\lambda_R}_{2,0,\frac{3}{2},\lambda_R}\mathcal{H}^{\text{LS,production}}_{L(1520),2,\frac{3}{2}}\mathcal{H}^{\text{decay}}_{L(1520),0,\frac{1}{2}}d^{\frac{3}{2}}_{\lambda_R,-\frac{1}{2}}(\theta_{31})}{2} + \sum_{\lambda_R=-3/2}^{3/2} \frac{\sqrt{10}\delta_{-\frac{1}{2}\lambda_R}\mathcal{R}(\sigma_2)C^{\frac{3}{2},\lambda_R}_{\frac{3}{2},\lambda_R,0,\cdots}\cdots}{\cdots} \\
A^{3}_{-\frac{1}{2},\frac{1}{2}} &= \sum_{\lambda_R=-3/2}^{3/2} \frac{\sqrt{10}\delta_{-\frac{1}{2}\lambda_R}\mathcal{R}(\sigma_3)C^{\frac{3}{2},\lambda_R}_{\frac{3}{2},\lambda_R,0,0}C^{\frac{1}{2},\lambda_R}_{2,0,\frac{3}{2},\lambda_R}\mathcal{H}^{\text{LS,production}}_{D(1232),2,\frac{3}{2}}\mathcal{H}^{\text{decay}}_{D(1232),\frac{1}{2},0}d^{\frac{3}{2}}_{\lambda_R,\frac{1}{2}}(\theta_{12})}{2} + \sum_{\lambda_R=-3/2}^{3/2} \frac{\sqrt{10}\delta_{-\frac{1}{2}\lambda_R}\mathcal{R}(\sigma_3)C^{\frac{3}{2},\lambda_R}_{\frac{3}{2},\lambda_R,0,0}\cdots}{\cdots} \\
A^{1}_{\frac{1}{2},-\frac{1}{2}} &= \sum_{\lambda_R=-1}^{1} -\frac{\sqrt{10}\delta_{\frac{1}{2},\lambda_R+\frac{1}{2}}\mathcal{R}(\sigma_1)C^{\frac{3}{2},\lambda_R+\frac{1}{2}}_{1,\lambda_R,\frac{1}{2},\frac{1}{2}}C^{\frac{1}{2},\lambda_R+\frac{1}{2}}_{2,0,\frac{3}{2},\lambda_R+\frac{1}{2}}\mathcal{H}^{\text{LS,production}}_{K(892),2,\frac{3}{2}}\mathcal{H}^{\text{decay}}_{K(892),0,0}d^{1}_{\lambda_R,0}(\theta_{23})}{2} + \sum_{\lambda_R=-1}^{1} -\frac{\sqrt{2}\delta_{\frac{1}{2},\lambda_R+\frac{1}{2}}\mathcal{R}(\sigma_1)C^{\frac{1}{2},\lambda_R\cdots}_{0,0,\frac{1}{2}\cdots}\cdots}{\cdots} \\
A^{2}_{\frac{1}{2},-\frac{1}{2}} &= \sum_{\lambda_R=-3/2}^{3/2} -\frac{\sqrt{10}\delta_{\frac{1}{2}\lambda_R}\mathcal{R}(\sigma_2)C^{\frac{3}{2},\lambda_R}_{\frac{3}{2},\lambda_R,0,0}C^{\frac{1}{2},\lambda_R}_{2,0,\frac{3}{2},\lambda_R}\mathcal{H}^{\text{LS,production}}_{L(1520),2,\frac{3}{2}}\mathcal{H}^{\text{decay}}_{L(1520),0,-\frac{1}{2}}d^{\frac{3}{2}}_{\lambda_R,\frac{1}{2}}(\theta_{31})}{2} + \sum_{\lambda_R=-3/2}^{3/2} -\frac{\sqrt{10}\delta_{\frac{1}{2}\lambda_R}\mathcal{R}(\sigma_2)C^{\frac{3}{2},\lambda_R}_{\frac{3}{2},\lambda_R,\cdots}\cdots}{\cdots} \\
A^{3}_{\frac{1}{2},-\frac{1}{2}} &= \sum_{\lambda_R=-3/2}^{3/2} \frac{\sqrt{10}\delta_{\frac{1}{2}\lambda_R}\mathcal{R}(\sigma_3)C^{\frac{3}{2},\lambda_R}_{\frac{3}{2},\lambda_R,0,0}C^{\frac{1}{2},\lambda_R}_{2,0,\frac{3}{2},\lambda_R}\mathcal{H}^{\text{LS,production}}_{D(1232),2,\frac{3}{2}}\mathcal{H}^{\text{decay}}_{D(1232),-\frac{1}{2},0}d^{\frac{3}{2}}_{\lambda_R,-\frac{1}{2}}(\theta_{12})}{2} + \sum_{\lambda_R=-3/2}^{3/2} \frac{\sqrt{10}\delta_{\frac{1}{2}\lambda_R}\mathcal{R}(\sigma_3)C^{\frac{3}{2},\lambda_R}_{\frac{3}{2},\lambda_R,0,0}\cdots}{\cdots} \\
A^{1}_{\frac{1}{2},\frac{1}{2}} &= \sum_{\lambda_R=-1}^{1} \frac{\sqrt{10}\delta_{\frac{1}{2},\lambda_R-\frac{1}{2}}\mathcal{R}(\sigma_1)C^{\frac{3}{2},\lambda_R-\frac{1}{2}}_{1,\lambda_R,\frac{1}{2},-\frac{1}{2}}C^{\frac{1}{2},\lambda_R-\frac{1}{2}}_{2,0,\frac{3}{2},\lambda_R-\frac{1}{2}}\mathcal{H}^{\text{LS,production}}_{K(892),2,\frac{3}{2}}\mathcal{H}^{\text{decay}}_{K(892),0,0}d^{1}_{\lambda_R,0}(\theta_{23})}{2} + \sum_{\lambda_R=-1}^{1} \frac{\sqrt{2}\delta_{\frac{1}{2},\lambda_R-\frac{1}{2}}\mathcal{R}(\sigma_1)C^{\frac{1}{2},\lambda_R-\frac{1}{2}}_{0,0,\frac{1}{2},\lambda_R\cdots}\cdots}{\cdots} \\
A^{2}_{\frac{1}{2},\frac{1}{2}} &= \sum_{\lambda_R=-3/2}^{3/2} \frac{\sqrt{10}\delta_{\frac{1}{2}\lambda_R}\mathcal{R}(\sigma_2)C^{\frac{3}{2},\lambda_R}_{\frac{3}{2},\lambda_R,0,0}C^{\frac{1}{2},\lambda_R}_{2,0,\frac{3}{2},\lambda_R}\mathcal{H}^{\text{LS,production}}_{L(1520),2,\frac{3}{2}}\mathcal{H}^{\text{decay}}_{L(1520),0,\frac{1}{2}}d^{\frac{3}{2}}_{\lambda_R,-\frac{1}{2}}(\theta_{31})}{2} + \sum_{\lambda_R=-3/2}^{3/2} \frac{\sqrt{10}\delta_{\frac{1}{2}\lambda_R}\mathcal{R}(\sigma_2)C^{\frac{3}{2},\lambda_R}_{\frac{3}{2},\lambda_R,0,0}C\cdots}{\cdots} \\
A^{3}_{\frac{1}{2},\frac{1}{2}} &= \sum_{\lambda_R=-3/2}^{3/2} \frac{\sqrt{10}\delta_{\frac{1}{2}\lambda_R}\mathcal{R}(\sigma_3)C^{\frac{3}{2},\lambda_R}_{\frac{3}{2},\lambda_R,0,0}C^{\frac{1}{2},\lambda_R}_{2,0,\frac{3}{2},\lambda_R}\mathcal{H}^{\text{LS,production}}_{D(1232),2,\frac{3}{2}}\mathcal{H}^{\text{decay}}_{D(1232),\frac{1}{2},0}d^{\frac{3}{2}}_{\lambda_R,\frac{1}{2}}(\theta_{12})}{2} + \sum_{\lambda_R=-3/2}^{3/2} \frac{\sqrt{10}\delta_{\frac{1}{2}\lambda_R}\mathcal{R}(\sigma_3)C^{\frac{3}{2},\lambda_R}_{\frac{3}{2},\lambda_R,0,0}C\cdots}{\cdots}
\end{aligned}
$$

| Decay | coupling | | | factor |
|---|---|---|---|---|
| $\Lambda_c^+ \xrightarrow[S=1/2]{L=0} \Lambda(1405) \xrightarrow[S=1/2]{L=0} K^-p\pi^+$ | $\mathcal{H}^{\mathrm{LS,production}}_{L(1405),0,\frac{1}{2}}$ | $=$ | $-1.22-0.0395i$ | $+1$ |
| $\Lambda_c^+ \xrightarrow[S=1/2]{L=1} \Lambda(1405) \xrightarrow[S=1/2]{L=0} K^-p\pi^+$ | $\mathcal{H}^{\mathrm{LS,production}}_{L(1405),1,\frac{1}{2}}$ | $=$ | $1.81-1.63i$ | $-1$ |
| $\Lambda_c^+ \xrightarrow[S=3/2]{L=1} \Lambda(1520) \xrightarrow[S=1/2]{L=2} K^-p\pi^+$ | $\mathcal{H}^{\mathrm{LS,production}}_{L(1520),1,\frac{3}{2}}$ | $=$ | $0.192+0.167i$ | $+1$ |
| $\Lambda_c^+ \xrightarrow[S=3/2]{L=2} \Lambda(1520) \xrightarrow[S=1/2]{L=2} K^-p\pi^+$ | $\mathcal{H}^{\mathrm{LS,production}}_{L(1520),2,\frac{3}{2}}$ | $=$ | $-0.116-0.243i$ | $-1$ |
| $\Lambda_c^+ \xrightarrow[S=1/2]{L=0} \Lambda(1600) \xrightarrow[S=1/2]{L=1} K^-p\pi^+$ | $\mathcal{H}^{\mathrm{LS,production}}_{L(1600),0,\frac{1}{2}}$ | $=$ | $0.134+0.628i$ | $-1$ |
| $\Lambda_c^+ \xrightarrow[S=1/2]{L=1} \Lambda(1600) \xrightarrow[S=1/2]{L=1} K^-p\pi^+$ | $\mathcal{H}^{\mathrm{LS,production}}_{L(1600),1,\frac{1}{2}}$ | $=$ | $1.71-1.13i$ | $+1$ |
| $\Lambda_c^+ \xrightarrow[S=1/2]{L=0} \Lambda(1670) \xrightarrow[S=1/2]{L=0} K^-p\pi^+$ | $\mathcal{H}^{\mathrm{LS,production}}_{L(1670),0,\frac{1}{2}}$ | $=$ | $0.0092-0.201i$ | $+1$ |
| $\Lambda_c^+ \xrightarrow[S=1/2]{L=1} \Lambda(1670) \xrightarrow[S=1/2]{L=0} K^-p\pi^+$ | $\mathcal{H}^{\mathrm{LS,production}}_{L(1670),1,\frac{1}{2}}$ | $=$ | $0.115+0.168i$ | $-1$ |
| $\Lambda_c^+ \xrightarrow[S=3/2]{L=1} \Lambda(1690) \xrightarrow[S=1/2]{L=2} K^-p\pi^+$ | $\mathcal{H}^{\mathrm{LS,production}}_{L(1690),1,\frac{3}{2}}$ | $=$ | $-0.379+0.331i$ | $+1$ |
| $\Lambda_c^+ \xrightarrow[S=3/2]{L=2} \Lambda(1690) \xrightarrow[S=1/2]{L=2} K^-p\pi^+$ | $\mathcal{H}^{\mathrm{LS,production}}_{L(1690),2,\frac{3}{2}}$ | $=$ | $0.286-0.248i$ | $-1$ |
| $\Lambda_c^+ \xrightarrow[S=1/2]{L=0} \Lambda(2000) \xrightarrow[S=1/2]{L=0} K^-p\pi^+$ | $\mathcal{H}^{\mathrm{LS,production}}_{L(2000),0,\frac{1}{2}}$ | $=$ | $2.81+0.0715i$ | $+1$ |
| $\Lambda_c^+ \xrightarrow[S=1/2]{L=1} \Lambda(2000) \xrightarrow[S=1/2]{L=0} K^-p\pi^+$ | $\mathcal{H}^{\mathrm{LS,production}}_{L(2000),1,\frac{1}{2}}$ | $=$ | $0.891+0.0874i$ | $-1$ |
| $\Lambda_c^+ \xrightarrow[S=3/2]{L=1} \Delta(1232) \xrightarrow[S=1/2]{L=1} p\pi^+K^-$ | $\mathcal{H}^{\mathrm{LS,production}}_{D(1232),1,\frac{3}{2}}$ | $=$ | $-1.5+3.16i$ | $+1$ |
| $\Lambda_c^+ \xrightarrow[S=3/2]{L=2} \Delta(1232) \xrightarrow[S=1/2]{L=1} p\pi^+K^-$ | $\mathcal{H}^{\mathrm{LS,production}}_{D(1232),2,\frac{3}{2}}$ | $=$ | $0.587-0.839i$ | $-1$ |
| $\Lambda_c^+ \xrightarrow[S=3/2]{L=1} \Delta(1600) \xrightarrow[S=1/2]{L=1} p\pi^+K^-$ | $\mathcal{H}^{\mathrm{LS,production}}_{D(1600),1,\frac{3}{2}}$ | $=$ | $1.6-2.46i$ | $+1$ |
| $\Lambda_c^+ \xrightarrow[S=3/2]{L=2} \Delta(1600) \xrightarrow[S=1/2]{L=1} p\pi^+K^-$ | $\mathcal{H}^{\mathrm{LS,production}}_{D(1600),2,\frac{3}{2}}$ | $=$ | $0.432-0.689i$ | $-1$ |
| $\Lambda_c^+ \xrightarrow[S=3/2]{L=1} \Delta(1700) \xrightarrow[S=1/2]{L=2} p\pi^+K^-$ | $\mathcal{H}^{\mathrm{LS,production}}_{D(1700),1,\frac{3}{2}}$ | $=$ | $-3.16+2.29i$ | $-1$ |
| $\Lambda_c^+ \xrightarrow[S=3/2]{L=2} \Delta(1700) \xrightarrow[S=1/2]{L=2} p\pi^+K^-$ | $\mathcal{H}^{\mathrm{LS,production}}_{D(1700),2,\frac{3}{2}}$ | $=$ | $0.179-0.299i$ | $+1$ |
| $\Lambda_c^+ \xrightarrow[S=1/2]{L=0} K(700) \xrightarrow[S=0]{L=0} \pi^+K^-p$ | $\mathcal{H}^{\mathrm{LS,production}}_{K(700),0,\frac{1}{2}}$ | $=$ | $-0.000167-0.685i$ | $+1$ |
| $\Lambda_c^+ \xrightarrow[S=1/2]{L=1} K(700) \xrightarrow[S=0]{L=0} \pi^+K^-p$ | $\mathcal{H}^{\mathrm{LS,production}}_{K(700),1,\frac{1}{2}}$ | $=$ | $-0.631+0.0404i$ | $+1$ |
| $\Lambda_c^+ \xrightarrow[S=1/2]{L=0} K(892) \xrightarrow[S=0]{L=1} \pi^+K^-p$ | $\mathcal{H}^{\mathrm{LS,production}}_{K(892),0,\frac{1}{2}}$ | $=$ | $1.0$ | $+1$ |
| $\Lambda_c^+ \xrightarrow[S=1/2]{L=1} K(892) \xrightarrow[S=0]{L=1} \pi^+K^-p$ | $\mathcal{H}^{\mathrm{LS,production}}_{K(892),1,\frac{1}{2}}$ | $=$ | $-0.342+0.064i$ | $-1$ |
| $\Lambda_c^+ \xrightarrow[S=3/2]{L=1} K(892) \xrightarrow[S=0]{L=1} \pi^+K^-p$ | $\mathcal{H}^{\mathrm{LS,production}}_{K(892),1,\frac{3}{2}}$ | $=$ | $-0.755-0.592i$ | $+1$ |
| $\Lambda_c^+ \xrightarrow[S=3/2]{L=2} K(892) \xrightarrow[S=0]{L=1} \pi^+K^-p$ | $\mathcal{H}^{\mathrm{LS,production}}_{K(892),2,\frac{3}{2}}$ | $=$ | $-0.0938-0.38i$ | $-1$ |
| $\Lambda_c^+ \xrightarrow[S=1/2]{L=0} K(1430) \xrightarrow[S=0]{L=0} \pi^+K^-p$ | $\mathcal{H}^{\mathrm{LS,production}}_{K(1430),0,\frac{1}{2}}$ | $=$ | $-1.35-3.15i$ | $+1$ |
| $\Lambda_c^+ \xrightarrow[S=1/2]{L=1} K(1430) \xrightarrow[S=0]{L=0} \pi^+K^-p$ | $\mathcal{H}^{\mathrm{LS,production}}_{K(1430),1,\frac{1}{2}}$ | $=$ | $0.598-0.956i$ | $+1$ |

It is asserted that these amplitude expressions to not evaluate to 0 once the Clebsch-Gordan coefficients are evaluated.

**See also:**

See *Resonances and LS-scheme* (page 3) for the allowed $LS$-values.

### 7.7.2 Distribution

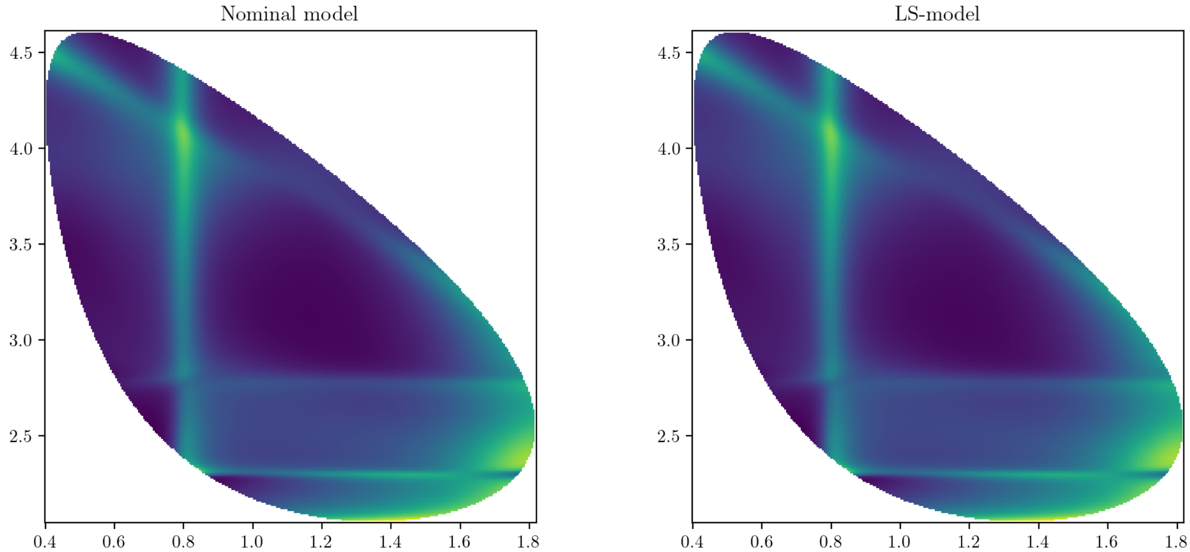


### 7.7.3 Decay rates

| Resonance | Nominal | LS-model | Difference |
|---|---|---|---|
| $\Lambda(1405)$ | 7.78 | 7.02 | −0.75 |
| $\Lambda(1520)$ | 1.91 | 1.95 | +0.03 |
| $\Lambda(1600)$ | 5.16 | 5.21 | +0.05 |
| $\Lambda(1670)$ | 1.15 | 1.18 | +0.02 |
| $\Lambda(1690)$ | 1.16 | 1.09 | −0.08 |
| $\Lambda(2000)$ | 9.55 | 9.84 | +0.30 |
| $\Delta(1232)$ | 28.73 | 28.97 | +0.24 |
| $\Delta(1600)$ | 4.50 | 4.24 | −0.26 |
| $\Delta(1700)$ | 3.89 | 3.99 | +0.10 |
| $K(700)$ | 2.99 | 3.25 | +0.26 |
| $K(892)$ | 21.95 | 21.25 | −0.70 |
| $K(1430)$ | 14.70 | 15.41 | +0.71 |

**Tip:** Compare with the values with uncertainties as reported in *Decay rates* (page 39).

## 7.8 SU(2) → SO(3) homomorphism

The Cornwell theorem from the group theory (see for example Section 3, Chapter 5 of [3]) gives the relation between the rotation of the transition amplitude and the physical vector of polarization sensitivity:

$$R_{ij}(\phi,\theta,\chi) = \frac{1}{2}\mathrm{tr}\left(D^{1/2*}(\phi,\theta,\chi)\sigma_i^P D^{1/2*\dagger}(\phi,\theta,\chi)\sigma_j^P\right)\,, \tag{7.1}$$

where tr represents the trace operation applied to the product of the two-dimensional matrices, $D$ and $\sigma^P$, and $R_{ij}(\phi,\theta,\chi)$ is a three-dimensional rotation matrix implementing the Euler transformation to a physical vector.

$$\begin{bmatrix} -\sin(\chi)\sin(\phi)+\cos(\chi)\cos(\phi)\cos(\theta) & -\sin(\chi)\cos(\phi)\cos(\theta)-\sin(\phi)\cos(\chi) & \sin(\theta)\cos(\phi) \\ \sin(\chi)\cos(\phi)+\sin(\phi)\cos(\chi)\cos(\theta) & -\sin(\chi)\sin(\phi)\cos(\theta)+\cos(\chi)\cos(\phi) & \sin(\phi)\sin(\theta) \\ -\sin(\theta)\cos(\chi) & \sin(\chi)\sin(\theta) & \cos(\theta) \end{bmatrix}$$

$$\begin{bmatrix} -\sin(\chi)\sin(\phi)+\cos(\chi)\cos(\phi)\cos(\theta) & -\sin(\chi)\cos(\phi)\cos(\theta)-\sin(\phi)\cos(\chi) & \sin(\theta)\cos(\phi) \\ \sin(\chi)\cos(\phi)+\sin(\phi)\cos(\chi)\cos(\theta) & -\sin(\chi)\sin(\phi)\cos(\theta)+\cos(\chi)\cos(\phi) & \sin(\phi)\sin(\theta) \\ -\sin(\theta)\cos(\chi) & \sin(\chi)\sin(\theta) & \cos(\theta) \end{bmatrix}$$

## 7.9 Determination of polarization

Given the aligned polarimeter field $\vec{\alpha}$ and the corresponding intensity distribution $I_0$, the intensity distribution $I$ for a polarized decay can be computed as follows:

$$I(\phi, \theta, \chi; \tau) = I_0(\tau)\left(1 + \vec{P}R(\phi, \theta, \chi)\vec{\alpha}(\tau)\right) \tag{7.2}$$

with $R$ the rotation matrix over the decay plane orientation, represented in Euler angles $(\phi, \theta, \chi)$.

In this section, we show that it's possible to determine the polarization $\vec{P}$ from a given intensity distribution $I$ of a $\lambda_c$ decay if we the $\vec{\alpha}$ fields and the corresponding $I_0$ values of that $\Lambda_c$ decay. We get $\vec{\alpha}$ and $I_0$ by interpolating the grid samples provided from *Exported distributions* (page 42) using the method described in *Import and interpolate* (page 59). We perform the same procedure with the averaged aligned polarimeter vector from Section 5.6 in order to quantify the loss in precision when integrating over the Dalitz plane variables $\tau$.

### 7.9.1 Polarized test distribution

For this study, a phase space sample is uniformly generated over the Dalitz plane variables $\tau$. The phase space sample is extended with uniform distributions over the decay plane angles $(\phi, \theta, \chi)$, so that the phase space can be used to generate a hit-and-miss toy sample for a polarized intensity distribution.

We now generate an intensity distribution over the phase space sample given a certain value for $\vec{P}$ [1] using Eq. (7.2) and by interpolating the $\vec{\alpha}$ and $I_0$ fields with the grid samples for the nominal model.

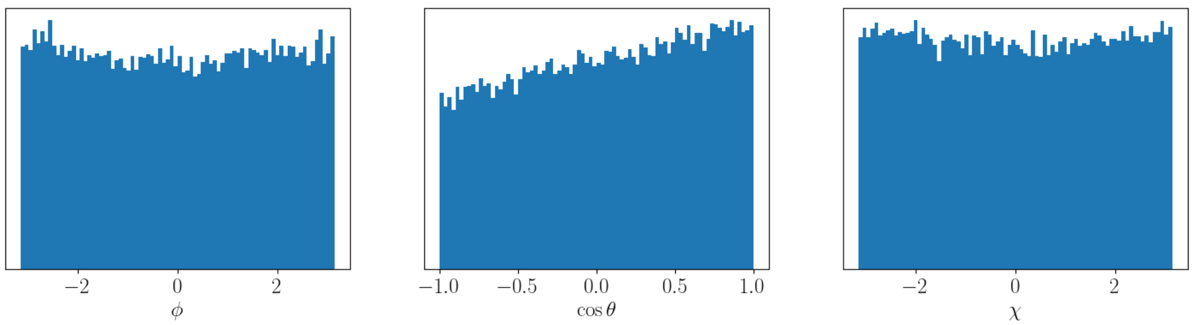

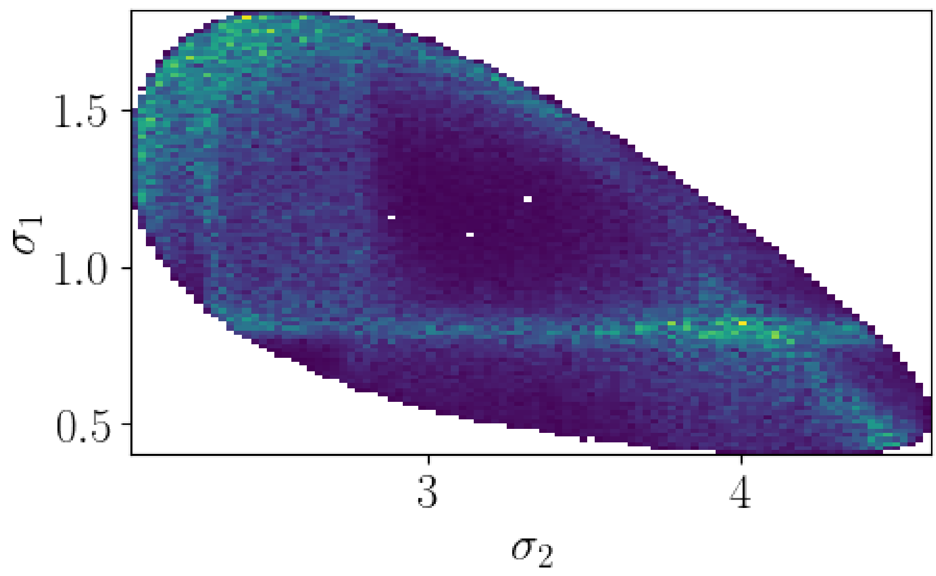


### 7.9.2 Using the exported polarimeter grid

The generated distribution is now assumed to be a *measured distribution* $I$ with unknown polarization $\vec{P}$. It is shown below that the actual $\vec{P}$ with which the distribution was generated can be found by performing a fit on Eq. (7.2). This is done with `iminuit`, starting with a certain 'guessed' value for $\vec{P}$ as initial parameters.

To avoid having to generate a hit-and-miss intensity test distribution, the parameters $\vec{P} = \left(P_x, P_y, P_z\right)$ are optimized with regard to a **weighted negative log likelihood estimator**:

$$\mathrm{NLL} = -\sum_i w_i \log I_{i,\vec{P}}\left(\phi, \theta, \chi; \tau\right) \,. \tag{7.3}$$

with the normalized intensities of the generated distribution taken as weights:

$$w_i = n\, I_i \Big/ \sum_j^n I_j \,, \tag{7.4}$$

such that $\sum w_i = n$. To propagate uncertainties, a fit is performed using the exported grids of each alternative model.

```
┌─────────────────────────────────────────────────────────────────────────┐
│                                Migrad                                   │
├──────────────────────────────────┬──────────────────────────────────────┤
│ FCN = 1.127e+06                  │              Nfcn = 66               │
│ EDM = 2.58e-06 (Goal: 0.0001)    │            time = 4.1 sec            │
├──────────────────────────────────┼──────────────────────────────────────┤
│          Valid Minimum           │        No Parameters at limit        │
├──────────────────────────────────┼──────────────────────────────────────┤
│ Below EDM threshold (goal x 10)  │           Below call limit           │
├───────────────┬──────────────────┼───────────┬─────────────┬────────────┤
│  Covariance   │     Hesse ok     │ Accurate  │  Pos. def.  │ Not forced │
└───────────────┴──────────────────┴───────────┴─────────────┴────────────┘
┌───┬──────┬───────────┬───────────┬────────────┬────────────┬─────────┬─────────┬␣
↪──────┐
│   │ Name │   Value   │ Hesse Err │ Minos Err- │ Minos Err+ │ Limit-  │ Limit+  │␣
↪Fixed │
├───┼──────┼───────────┼───────────┼────────────┼────────────┼─────────┼─────────┼␣
↪──────┤
│ 0 │ Px   │   0.217   │   0.008   │            │            │         │         │␣
↪      │
│ 1 │ Py   │   0.011   │   0.008   │            │            │         │         │␣
↪      │
│ 2 │ Pz   │  -0.665   │   0.007   │            │            │         │         │␣
↪      │
```

(continues on next page)

(continued from previous page)

```
└───┴─────┴────────┴────────┴─────────┴─────────┴───────┴───────┴───────┘

┌────┬─────────────────────────────┐
│    │        Px        Py        Pz │
├────┼─────────────────────────────┤
│ Px │ 6.24e-05 5.25e-08 2.48e-06 │
│ Py │ 5.25e-08 6.27e-05 5.86e-08 │
│ Pz │ 2.48e-06 5.86e-08  5.6e-05 │
└────┴─────────────────────────────┘
```

The polarization $\vec{P}$ is determined to be (in %):

$$
\begin{array}{rcl}
P_x & = & +21.65^{+0.30}_{-0.62} \\
P_y & = & +1.08^{+0.02}_{-0.05} \\
P_z & = & -66.50^{+1.66}_{-0.85}
\end{array}
$$

with the upper and lower sign being the systematic extrema uncertainties as determined by the alternative models.

This is to be compared with the model uncertainties reported by [1]:

$$
\begin{array}{rcl}
P_x & = & +21.65 \pm 0.36 \\
P_y & = & +1.08 \pm 0.09 \\
P_z & = & -66.5 \pm 1.1.
\end{array}
$$

The polarimeter values for each model are (in %):

| Model | $P_x$ | $P_y$ | $P_z$ | ⍰$P_x$ | ⍰$P_y$ | ⍰$P_z$ |
|---|---|---|---|---|---|---|
| **0** | $+21.65$ | $+1.08$ | $-66.5$ | | | |
| **1** | $+21.59$ | $+1.07$ | $-66.4$ | $-0.06$ | $-0.01$ | $+0.13$ |
| **2** | $+21.63$ | $+1.07$ | $-66.5$ | $-0.02$ | $-0.00$ | $+0.04$ |
| **3** | $+21.69$ | $+1.07$ | $-66.6$ | $+0.04$ | $-0.01$ | $-0.10$ |
| **4** | $+21.65$ | $+1.10$ | $-66.5$ | $+0.00$ | $+0.02$ | $-0.04$ |
| **5** | $+21.68$ | $+1.08$ | $-66.5$ | $+0.03$ | $+0.01$ | $-0.04$ |
| **6** | $+21.51$ | $+1.06$ | $-66.0$ | $-0.14$ | $-0.02$ | $+0.48$ |
| **7** | $+21.18$ | $+1.05$ | $-65.3$ | $-0.47$ | $-0.03$ | $+1.18$ |
| **8** | $+21.34$ | $+1.03$ | $-65.6$ | $-0.31$ | $-0.05$ | $+0.87$ |
| **9** | $+21.34$ | $+1.05$ | $-65.6$ | $-0.31$ | $-0.03$ | $+0.90$ |
| **10** | $+21.95$ | $+1.10$ | $-67.4$ | $+0.30$ | $+0.02$ | $-0.85$ |
| **11** | $+21.61$ | $+1.08$ | $-66.4$ | $-0.04$ | $+0.00$ | $+0.12$ |
| **12** | $+21.70$ | $+1.03$ | $-66.6$ | $+0.05$ | $-0.05$ | $-0.10$ |
| **13** | $+21.67$ | $+1.08$ | $-66.6$ | $+0.02$ | $+0.00$ | $-0.05$ |
| **14** | $+21.66$ | $+1.08$ | $-66.5$ | $+0.01$ | $+0.00$ | $-0.02$ |
| **15** | $+21.03$ | $+1.10$ | $-64.8$ | $-0.62$ | $+0.02$ | $+1.66$ |
| **16** | $+21.64$ | $+1.08$ | $-66.5$ | $-0.01$ | $+0.00$ | $+0.03$ |
| **17** | $+21.67$ | $+1.08$ | $-66.6$ | $+0.02$ | $+0.00$ | $-0.09$ |

### 7.9.3 Using the averaged polarimeter vector

Equation (7.2) requires knowledge about the aligned polarimeter field $\vec{\alpha}(\tau)$ and intensity distribution $I_0(\tau)$ over all kinematic variables $\tau$. It is, however, also possible to compute the differential decay rate from the averaged polarimeter vector $\vec{\overline{\alpha}}$ (see *Average polarimetry values* (page 40)). The equivalent formula to Eq. (7.2) is:

$$
\frac{8\pi^2}{\Gamma}\frac{\mathrm{d}^3\Gamma}{\mathrm{d}\phi\,\mathrm{d}\cos\theta\,\mathrm{d}\chi} = 1 + \sum_{i,j} P_i R_{ij}(\phi,\theta,\chi)\overline{\alpha}_j\,, \tag{7.5}
$$

We use this equation along with Eq. (7.3) to determine $\vec{P}$ with `Minuit`.

```
┌─────────────────────────────────────────────────────────────────────────┐
│                                Migrad                                   │
├──────────────────────────────────┬──────────────────────────────────────┤
│ FCN = 1.151e+06                  │              Nfcn = 56               │
│ EDM = 6.08e-08 (Goal: 0.0001)    │            time = 3.4 sec            │
├──────────────────────────────────┼──────────────────────────────────────┤
│          Valid Minimum           │        No Parameters at limit        │
├──────────────────────────────────┼──────────────────────────────────────┤
│ Below EDM threshold (goal x 10)  │           Below call limit           │
├───────────────┬──────────────────┼───────────┬─────────────┬────────────┤
│  Covariance   │     Hesse ok     │ Accurate  │  Pos. def.  │ Not forced │
└───────────────┴──────────────────┴───────────┴─────────────┴────────────┘
┌───┬──────┬───────────┬───────────┬────────────┬────────────┬─────────┬─────────┬␣
↪Fixed │
│   │ Name │   Value   │ Hesse Err │ Minos Err- │ Minos Err+ │ Limit-  │ Limit+  │␣
├───┼──────┼───────────┼───────────┼────────────┼────────────┼─────────┼─────────┼
│ 0 │ Px   │   0.203   │   0.019   │            │            │         │         │␣
↪      │
│ 1 │ Py   │  -0.003   │   0.019   │            │            │         │         │␣
↪      │
│ 2 │ Pz   │  -0.661   │   0.019   │            │            │         │         │␣
↪      │
└───┴──────┴───────────┴───────────┴────────────┴────────────┴─────────┴─────────┴
┌────┬────────────────────────────────┐
│    │        Px         Py         Pz │
├────┼────────────────────────────────┤
│ Px │  0.000364  -1.7e-06  2.29e-06 │
│ Py │  -1.7e-06  0.000367 -4.79e-07 │
│ Pz │  2.29e-06 -4.79e-07  0.000362 │
└────┴────────────────────────────────┘
```

Using the averaged polarimeter vector $\vec{\overline{\alpha}}$, the polarization $\vec{P}$ is determined to be (in %):

$$\begin{array}{rcl} P_x &=& +20.32^{+1.04}_{-2.44} \\ P_y &=& -0.26^{+0.17}_{-0.08} \\ P_z &=& -66.14^{+7.91}_{-3.32} \end{array} .$$

The polarimeter values for each model are (in %):

| Model | $\mathbf{P_x}$ | $\mathbf{P_y}$ | $\mathbf{P_z}$ | ?$\mathbf{P_x}$ | ?$\mathbf{P_y}$ | ?$\mathbf{P_z}$ |
|---|---|---|---|---|---|---|
| **0** | $+20.32$ | $-0.26$ | $-66.1$ | | | |
| **1** | $+20.23$ | $-0.24$ | $-65.9$ | $-0.08$ | $+0.01$ | $+0.26$ |
| **2** | $+20.28$ | $-0.26$ | $-66.0$ | $-0.04$ | $-0.00$ | $+0.12$ |
| **3** | $+20.49$ | $-0.22$ | $-66.8$ | $+0.18$ | $+0.04$ | $-0.63$ |
| **4** | $+20.29$ | $-0.32$ | $-65.9$ | $-0.03$ | $-0.06$ | $+0.21$ |
| **5** | $+20.25$ | $-0.33$ | $-65.8$ | $-0.07$ | $-0.07$ | $+0.36$ |
| **6** | $+19.97$ | $-0.31$ | $-64.9$ | $-0.35$ | $-0.05$ | $+1.24$ |
| **7** | $+18.34$ | $-0.31$ | $-59.7$ | $-1.98$ | $-0.05$ | $+6.43$ |
| **8** | $+19.90$ | $-0.18$ | $-65.0$ | $-0.42$ | $+0.08$ | $+1.17$ |
| **9** | $+19.46$ | $-0.25$ | $-63.2$ | $-0.85$ | $+0.01$ | $+2.90$ |
| **10** | $+21.36$ | $-0.23$ | $-69.5$ | $+1.04$ | $+0.03$ | $-3.32$ |
| **11** | $+20.25$ | $-0.28$ | $-65.9$ | $-0.07$ | $-0.02$ | $+0.26$ |
| **12** | $+19.82$ | $-0.34$ | $-64.2$ | $-0.49$ | $-0.08$ | $+1.97$ |
| **13** | $+20.38$ | $-0.25$ | $-66.3$ | $+0.06$ | $+0.01$ | $-0.20$ |
| **14** | $+20.35$ | $-0.25$ | $-66.3$ | $+0.04$ | $+0.00$ | $-0.12$ |
| **15** | $+17.88$ | $-0.09$ | $-58.2$ | $-2.44$ | $+0.17$ | $+7.91$ |
| **16** | $+20.32$ | $-0.25$ | $-66.1$ | $+0.00$ | $+0.01$ | $-0.00$ |
| **17** | $+20.29$ | $-0.22$ | $-66.2$ | $-0.03$ | $+0.04$ | $-0.08$ |

### Propagating extrema uncertainties

In Section 5.6, the averaged aligned polarimeter vectors with systematic model uncertainties were found to be:

| observable | central | stat + syst |
|---|---|---|
| $\overline{\alpha}_x$ $[10^{-3}]$ | $-62.6$ | 14.8 |
| $\overline{\alpha}_y$ $[10^{-3}]$ | $+8.9$ | 12.7 |
| $\overline{\alpha}_z$ $[10^{-3}]$ | $-278.0$ | 40.4 |
| $\lvert\overline{\alpha}\rvert$ $[10^{-3}]$ | 285.1 | 37.9 |
| $\theta(\overline{\alpha})$ $[\pi]$ | $+0.929$ | 0.017 |
| $\phi(\overline{\alpha})$ $[\pi]$ | $+0.955$ | 0.067 |

This list of uncertainties is determined by the *extreme deviations* of the alternative models, whereas the uncertainties on the polarizations determined in Section 7.9.3 are determined by the averaged polarimeters of *all* alternative models. The tables below shows that there is a loss in systematic uncertainty when we propagate uncertainties by taking computing $\vec{P}$ *only* with combinations of $\alpha_i - \sigma_i, \alpha_i + \sigma_i$ for each $i \in x, y, z$.

```
0%|          | 0/8 [00:00<?, ?it/s]
```

```
0%|          | 0/8 [00:00<?, ?it/s]
```

Polarizations from $\overline{\alpha}$ in cartesian coordinates:

$$
\begin{aligned}
P_x &= +20.32 \pm 3.60 \\
P_y &= -0.26 \pm 0.34 \\
P_z &= -66.14 \pm 11.51
\end{aligned}
$$

Polarizations from $\overline{\alpha}$ in polar coordinates:

$$
\begin{aligned}
P_x &= +20.32 \pm 3.23 \\
P_y &= -0.26 \pm 0.19 \\
P_z &= -66.14 \pm 10.08
\end{aligned}
$$

| $\alpha_x$ | $\alpha_y$ | $\alpha_z$ | $P_x$ | $P_y$ | $P_z$ | $\Delta P_x$ | $\Delta P_y$ | $\Delta P_z$ |
|---|---|---|---|---|---|---|---|---|
| $-62.6$ | 8.9 | $-278.0$ | $+20.32$ | $-0.26$ | $-66.14$ | | | |
| $-77.4$ | $-3.8$ | $-318.4$ | $+17.7$ | $-0.25$ | $-57.4$ | $-2.58$ | $+0.01$ | $+8.7$ |
| $-77.4$ | $-3.8$ | $-237.5$ | $+23.3$ | $-0.55$ | $-74.9$ | $+2.97$ | $-0.30$ | $-8.7$ |
| $-77.4$ | $+21.6$ | $-318.4$ | $+17.6$ | $-0.28$ | $-57.4$ | $-2.72$ | $-0.02$ | $+8.7$ |
| $-77.4$ | $+21.6$ | $-237.5$ | $+23.0$ | $-0.60$ | $-74.7$ | $+2.71$ | $-0.34$ | $-8.6$ |
| $-47.8$ | $-3.8$ | $-318.4$ | $+17.9$ | $-0.04$ | $-58.4$ | $-2.43$ | $+0.21$ | $+7.8$ |
| $-47.8$ | $-3.8$ | $-237.5$ | $+23.9$ | $-0.21$ | $-77.7$ | $+3.60$ | $+0.05$ | $-11.5$ |
| $-47.8$ | $+21.6$ | $-318.4$ | $+17.7$ | $-0.07$ | $-58.3$ | $-2.57$ | $+0.19$ | $+7.8$ |
| $-47.8$ | $+21.6$ | $-237.5$ | $+23.6$ | $-0.26$ | $-77.5$ | $+3.31$ | $+0.00$ | $-11.3$ |

| $\lvert\alpha\rvert$ | $\theta$ $[\pi]$ | $\phi$ $[\pi]$ | $P_x$ | $P_y$ | $P_z$ | $\Delta P_x$ | $\Delta P_y$ | $\Delta P_z$ |
|---|---|---|---|---|---|---|---|---|
| 285.1 | 0.929 | 0.955 | $+20.32$ | $-0.26$ | $-66.14$ | | | |
| 247.1 | $+0.91$ | $+0.89$ | $+23.3$ | $-0.45$ | $-76.1$ | $+3.01$ | $-0.19$ | $-10.0$ |
| 247.1 | $+0.91$ | $+1.02$ | $+23.5$ | $-0.44$ | $-75.9$ | $+3.23$ | $-0.19$ | $-9.8$ |
| 247.1 | $+0.95$ | $+0.89$ | $+23.2$ | $-0.12$ | $-76.2$ | $+2.91$ | $+0.14$ | $-10.1$ |
| 247.1 | $+0.95$ | $+1.02$ | $+23.4$ | $-0.12$ | $-76.1$ | $+3.05$ | $+0.14$ | $-10.0$ |
| 323.0 | $+0.91$ | $+0.89$ | $+17.9$ | $-0.35$ | $-58.2$ | $-2.47$ | $-0.09$ | $+7.9$ |
| 323.0 | $+0.91$ | $+1.02$ | $+18.0$ | $-0.34$ | $-58.1$ | $-2.30$ | $-0.08$ | $+8.0$ |
| 323.0 | $+0.95$ | $+0.89$ | $+17.8$ | $-0.09$ | $-58.3$ | $-2.54$ | $+0.17$ | $+7.8$ |
| 323.0 | $+0.95$ | $+1.02$ | $+17.9$ | $-0.09$ | $-58.2$ | $-2.44$ | $+0.17$ | $+7.9$ |

### 7.9.4 Increase in uncertainties

When the polarization is determined with the averaged aligned polarimeter vector $\vec{\overline{\alpha}}$ instead of the aligned polarimeter vector field $\vec{\alpha}(\tau)$ over all Dalitz variables $\tau$, the uncertainty is expected to increase by a factor $S_0/\overline{S}_0 \approx 3$, with:

$$
\begin{aligned}
S_0^2 &= 3 \int I_0 \left|\vec{\alpha}\right|^2 \mathrm{d}^n\tau \,/ \int I_0 \,\mathrm{d}^n\tau \\
\overline{S}_0^2 &= 3(\overline{\alpha}_x^2 + \overline{\alpha}_y^2 + \overline{\alpha}_z^2)\,.
\end{aligned} \tag{7.6}
$$

The following table shows the maximal deviation (systematic uncertainty) of the determined polarization $\vec{P}$ for each alternative model (determined with the $\overline{\alpha}$-values in cartesian coordinates). The second and third column indicate the systematic uncertainty (in %) as determined with the full vector field and with the averaged vector, respectively.

| $\sigma_\text{model}$ | $\vec{\alpha}(\tau)$ | $\vec{\overline{\alpha}}$ | factor |
|---|---|---|---|
| $P_x$ | 0.62 | 2.44 | 3.9 |
| $P_y$ | 0.05 | 0.17 | 3.5 |
| $P_z$ | 1.66 | 7.91 | 4.8 |

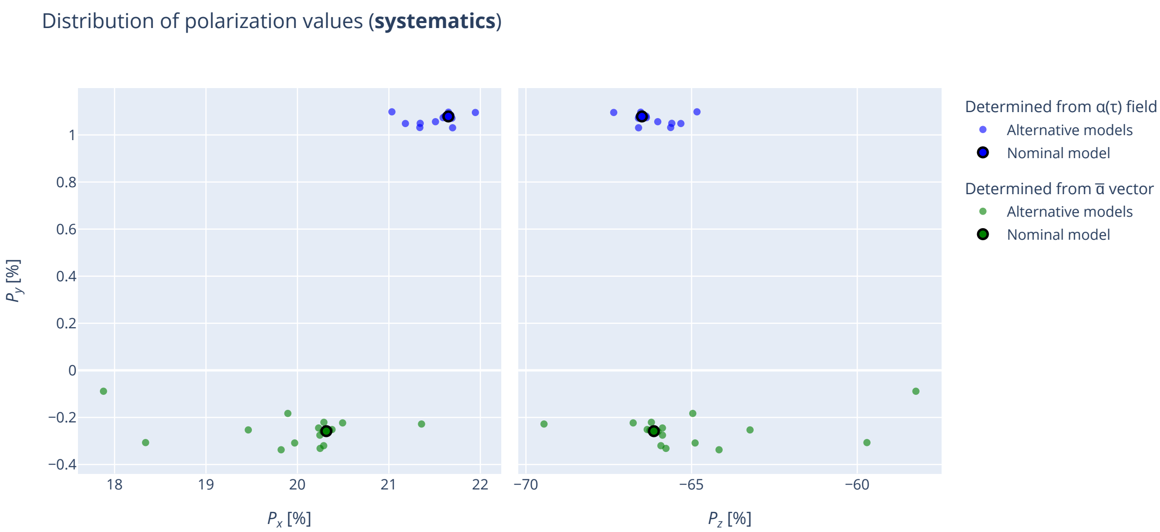

## 7.10 Interactive visualization

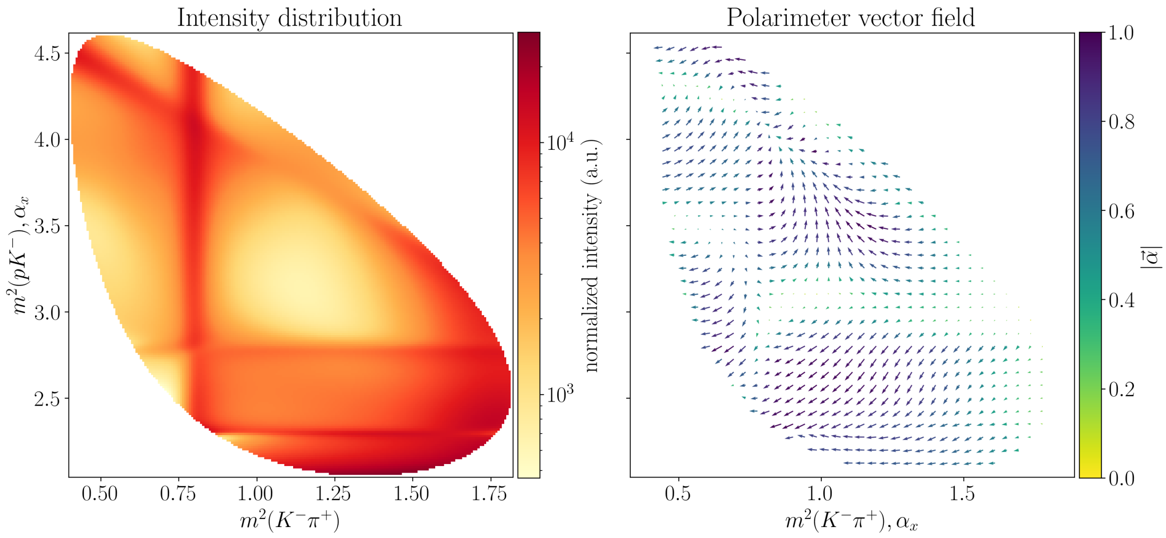


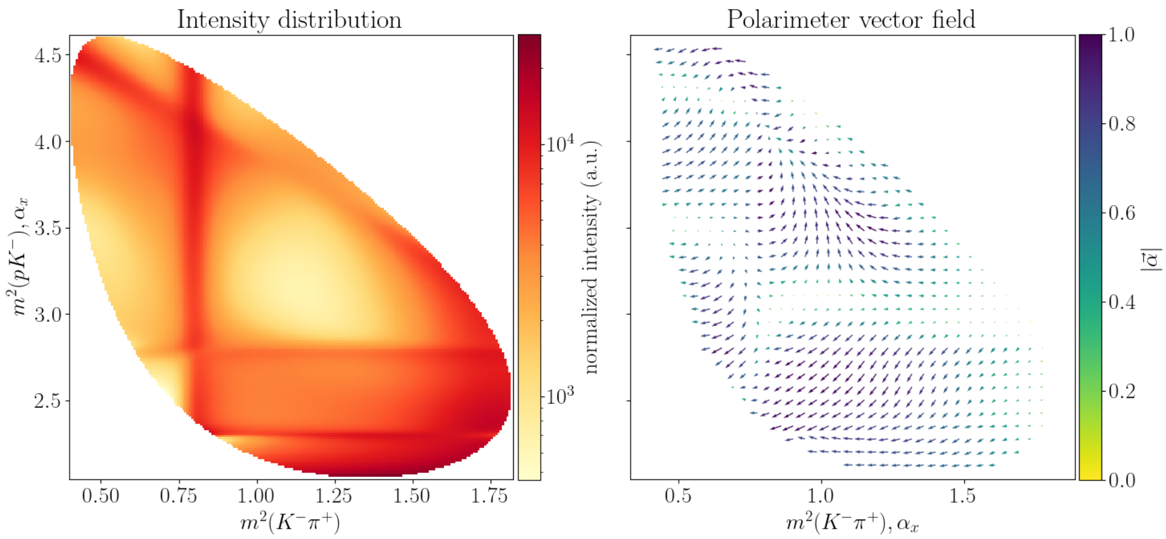


**Tip:** Run this notebook locally in Jupyter or online on Binder to modify parameters interactively!

CHAPTER

EIGHT

# BIBLIOGRAPHY

CHAPTER

# NINE

# POLARIMETRY

```
import polarimetry
```

**formulate_polarimetry**(*builder: DalitzPlotDecompositionBuilder (page 73), reference_subsystem: Literal[1, 2, 3] = 1*) → tuple[PoolSum, PoolSum, PoolSum]

### Submodules and Subpackages

## 9.1 amplitude

```
import polarimetry.amplitude
```

**class AmplitudeModel**(*decay: ThreeBodyDecay (page 77), intensity: Expr = 1, amplitudes: dict[Indexed, Expr] = _Nothing.NOTHING, variables: dict[Symbol, Expr] = _Nothing.NOTHING, parameter_defaults: dict[Symbol, float] = _Nothing.NOTHING*)

Bases: `object`

**decay:** *ThreeBodyDecay* **(page 77)**

**intensity: Expr**

**amplitudes: dict[Indexed, Expr]**

**variables: dict[Symbol, Expr]**

**parameter_defaults: dict[Symbol, float]**

**property full_expression: Expr**

**class DalitzPlotDecompositionBuilder**(*decay: ThreeBodyDecay (page 77), min_ls: bool = True*)

Bases: `object`

**formulate**(*reference_subsystem: Literal[1, 2, 3] = 1, cleanup_summations: bool = False*) → *AmplitudeModel* (page 73)

**formulate_subsystem_amplitude**(*λ0: Rational, λ1: Rational, λ2: Rational, λ3: Rational, subsystem_id: Literal[1, 2, 3]*) → *AmplitudeModel* (page 73)

**formulate_aligned_amplitude**(*λ0: Rational | Symbol, λ1: Rational | Symbol, λ2: Rational | Symbol, λ3: Rational | Symbol, reference_subsystem: Literal[1, 2, 3] = 1*) → tuple[PoolSum, dict[Symbol, Expr]]

**get_indexed_base**(*typ: Literal['production', 'decay'], min_ls: bool = True*) → IndexedBase

Get a basis to generate coupling symbols for the production or decay node.

**class DynamicsConfigurator**(*decay: ThreeBodyDecay (page 77)*)

Bases: `object`

**register_builder**(*identifier, builder: DynamicsBuilder (page 74)*) → None

**get_builder**(*identifier*) → *DynamicsBuilder* (page 74)

**property decay: *ThreeBodyDecay* (page 77)**

**class DynamicsBuilder**(**args, **kwargs*)

Bases: `Protocol`

**simplify_latex_rendering**() → None

Improve LaTeX rendering of an `Indexed` object.

### Submodules and Subpackages

## 9.1.1 angles

```
import polarimetry.amplitude.angles
```

**formulate_scattering_angle**(*state_id: int, sibling_id: int*) → tuple[Symbol, acos]

Formulate the scattering angle in the rest frame of the resonance.

Compute the $\theta_{ij}$ scattering angle as formulated in Eq (A1) in the DPD paper. The angle is that between particle $i$ and spectator particle $k$ in the rest frame of the isobar resonance $(ij)$.

**formulate_theta_hat_angle**(*isobar_id: int, aligned_subsystem: int*) → tuple[Symbol, acos]

Formulate an expression for $\hat{\theta}_{i(j)}$.

**formulate_zeta_angle**(*rotated_state: int, aligned_subsystem: int, reference_subsystem: int*) → tuple[Symbol, acos]

Formulate an expression for the alignment angle $\zeta^i_{j(k)}$.

# 9.2 lhcb

```
import polarimetry.lhcb
```

Import functions that are specifically for this LHCb analysis.

**See also:**

*Cross-check with LHCb data* (page 13)

**load_model**(*model_file: Path | str, particle_definitions: dict[str, Particle (page 77)], model_id: int | str = 0*) → *AmplitudeModel* (page 73)

**load_model_builder**(*model_file: Path | str, particle_definitions: dict[str, Particle (page 77)], model_id: int | str = 0*) → *DalitzPlotDecompositionBuilder* (page 73)

**load_three_body_decay**(*resonance_names: Iterable[str], particle_definitions: dict[str, Particle (page 77)], min_ls: bool = True*) → *ThreeBodyDecay* (page 77)

**class ParameterBootstrap**(*filename: Path | str, decay: ThreeBodyDecay (page 77), model_id: int | str = 0*)

Bases: `object`

A wrapper for loading parameters from `model-definitions.yaml`.

**property values: dict[str, complex | float | int]**

**property uncertainties: dict[str, complex | float | int]**

**create_distribution**(*sample_size: int*, *seed: int | None = None*) → dict[str, complex | float | int]

**load_model_parameters**(*filename: Path | str*, *decay: ThreeBodyDecay (page 77)*, *model_id: int | str = 0*, *particle_definitions: dict[str, Particle (page 77)] | None = None*) → dict[Indexed | Symbol, complex | float]

**load_model_parameters_with_uncertainties**(*filename: Path | str*, *decay: ThreeBodyDecay (page 77)*, *model_id: int | str = 0*, *particle_definitions: dict[str, Particle (page 77)] | None = None*) → dict[Indexed | Symbol, *MeasuredParameter* (page 75)]

**flip_production_coupling_signs**(*obj: _T*, *subsystem_names: Iterable[Pattern]*) → _T

**compute_decay_couplings**(*decay: ThreeBodyDecay (page 77)*) → dict[Indexed, *MeasuredParameter* (page 75)[int]]

**ParameterType**

Template for the parameter type of a for `MeasuredParameter` (page 75).

alias of TypeVar('ParameterType', complex, float)

**class MeasuredParameter**(*value: ParameterType (page 75)*, *hesse: ParameterType (page 75)*, *model: ParameterType (page 75) | None = None*, *systematic: ParameterType (page 75) | None = None*)

Bases: `Generic`[`ParameterType` (page 75)]

Data structure for imported parameter values.

`MeasuredParameter.value` (page 75) and `hesse` (page 75) are taken from the supplemental material, whereas `model` (page 75) and `systematic` (page 75) are taken from Tables 8 and 9 from the original LHCb paper [1].

**value: *ParameterType* (page 75)**

Central value of the parameter as determined by a fit with Minuit.

**hesse: *ParameterType* (page 75)**

Parameter uncertainty as determined by a fit with Minuit.

**model: *ParameterType* (page 75) | None**

Systematic uncertainties from fit bootstrapping.

**systematic: *ParameterType* (page 75) | None**

Systematic uncertainties from detector effects etc..

**property uncertainty: *ParameterType* (page 75)**

**get_conversion_factor**(*resonance: Particle (page 77)*) → Literal[-1, 1]

**get_conversion_factor_ls**(*resonance: Particle (page 77)*, *L: Rational*, *S: Rational*) → Literal[-1, 1]

**parameter_key_to_symbol**(*key: str*, *min_ls: bool = True*, *particle_definitions: dict[str, Particle (page 77)] | None = None*) → Indexed | Symbol

**extract_particle_definitions**(*decay: ThreeBodyDecay (page 77)*) → dict[str, *Particle* (page 77)]

#### Submodules and Subpackages

### 9.2.1 dynamics

```
import polarimetry.lhcb.dynamics
```

**formulate_bugg_breit_wigner**(*decay_chain: ThreeBodyDecayChain (page 78)*) → tuple[*BuggBreitWigner* (page 78), dict[Symbol, float]]

**formulate_exponential_bugg_breit_wigner**(*decay_chain: ThreeBodyDecayChain (page 78)*) → tuple[Mul, dict[Symbol, float]]

See this paper, Eq. (4).

**formulate_flatte_1405**(*decay: ThreeBodyDecayChain (page 78)*) → tuple[*FlattéSWave* (page 78), dict[Symbol, float]]

**formulate_breit_wigner**(*decay_chain: ThreeBodyDecayChain (page 78)*) → tuple[*BreitWignerMinL* (page 78), dict[Symbol, float]]

### 9.2.2 particle

```
import polarimetry.lhcb.particle
```

Hard-coded particle definitions.

**load_particles**(*filename: Path | str*) → dict[str, *Particle* (page 77)]

Load `Particle` (page 77) definitions from a YAML file.

**class ResonanceJSON**(**args, **kwargs*)

Bases: `dict`

**latex: str**

**jp: str**

**mass: float | str**

**width: float | str**

## 9.3 data

```
import polarimetry.data
```

**create_data_transformer**(*model: AmplitudeModel (page 73), backend: str = 'jax'*) → SympyDataTransformer

**create_phase_space_filter**(*decay: ThreeBodyDecay (page 77), x_mandelstam: Literal[1, 2, 3] = 1, y_mandelstam: Literal[1, 2, 3] = 2, outside_value=nan*) → PositionalArgumentFunction

**generate_meshgrid_sample**(*decay: ThreeBodyDecay (page 77), resolution: int, x_mandelstam: Literal[1, 2, 3] = 1, y_mandelstam: Literal[1, 2, 3] = 2*) → Dict[str, ndarray]

Generate a `numpy.meshgrid` sample for plotting with `matplotlib.pyplot`.

**generate_sub_meshgrid_sample**(*decay: ThreeBodyDecay (page 77), resolution: int, x_range: tuple[float, float], y_range: tuple[float, float], x_mandelstam: Literal[1, 2, 3] = 1, y_mandelstam: Literal[1, 2, 3] = 2*) → DataSample

**generate_phasespace_sample**(*decay: ThreeBodyDecay (page 77), n_events: int, seed: int | None = None*) → DataSample

Generate a uniform distribution over Dalitz variables $\sigma_{1,2,3}$.

**compute_dalitz_boundaries**(*decay: ThreeBodyDecay (page 77)*) → tuple[tuple[float, float], tuple[float, float], tuple[float, float]]

**create_mass_symbol_mapping**(*decay: ThreeBodyDecay (page 77)*) → dict[Symbol, float]

## 9.4 decay

```
import polarimetry.decay
```

Data structures that describe a three-body decay.

**class Particle**(*name: str, latex: str, spin: SupportsFloat, parity: Literal[- 1, 1], mass: float, width: float*)

Bases: `object`

**name: str**

**latex: str**

**spin: Rational**

**parity: Literal[-1, 1]**

**mass: float**

**width: float**

**class IsobarNode**(*parent: Particle (page 77), child1: Particle (page 77) | IsobarNode (page 77), child2: Particle (page 77) | IsobarNode (page 77), interaction: LSCoupling (page 78) | tuple[int, SupportsFloat] | None = None*)

Bases: `object`

**parent: *Particle* (page 77)**

**child1: *Particle* (page 77) | *IsobarNode* (page 77)**

**child2: *Particle* (page 77) | *IsobarNode* (page 77)**

**interaction: *LSCoupling* (page 78) | None**

**property children: tuple[*Particle* (page 77), *Particle* (page 77)]**

**class ThreeBodyDecay**(*states: OuterStates (page 78), chains: tuple[ThreeBodyDecayChain (page 78), ...]*)

Bases: `object`

**states: *OuterStates* (page 78)**

**chains: tuple[*ThreeBodyDecayChain* (page 78), ...]**

**property initial_state: *Particle* (page 77)**

**property final_state: dict[Literal[1, 2, 3], *Particle* (page 77)]**

**find_chain**(*resonance_name: str*) → *ThreeBodyDecayChain* (page 78)

**get_subsystem** (*subsystem_id: Literal[1, 2, 3]*) → *ThreeBodyDecay* (page 77)

**get_decay_product_ids** (*spectator_id: Literal[1, 2, 3]*) → tuple[int, int]

**OuterStates**

Mapping of the initial and final state IDs to their *Particle* (page 77) definition.

alias of Dict[Literal[0, 1, 2, 3], *Particle* (page 77)]

**class ThreeBodyDecayChain** (*decay: IsobarNode (page 77)*)

Bases: object

**decay: *IsobarNode* (page 77)**

**property parent: *Particle* (page 77)**

**property resonance: *Particle* (page 77)**

**property decay_products: tuple[*Particle* (page 77), *Particle* (page 77)]**

**property spectator: *Particle* (page 77)**

**property incoming_ls: *LSCoupling* (page 78)**

**property outgoing_ls: *LSCoupling* (page 78)**

**class LSCoupling** (*L: int, S: SupportsFloat*)

Bases: object

**L: int**

**S: Rational**

## 9.5 dynamics

```
import polarimetry.dynamics
```

Functions for dynamics lineshapes and kinematics.

**See also:**

*Dynamics lineshapes* (page 51)

**class P** (*s, mi, mj, **hints*)

Bases: UnevaluatedExpression

**class Q** (*s, m0, mk, **hints*)

Bases: UnevaluatedExpression

**class BreitWignerMinL** (*s, decaying_mass, spectator_mass, resonance_mass, resonance_width, child2_mass, child1_mass, l_dec, l_prod, R_dec, R_prod*)

Bases: UnevaluatedExpression

**class BuggBreitWigner** (*s, m0, Γ0, m1, m2, γ*)

Bases: UnevaluatedExpression

**class FlattéSWave** (*s, m0, widths, masses1, masses2*)

Bases: UnevaluatedExpression

**class EnergyDependentWidth** (*s, m0, Γ0, m1, m2, L, R*)

Bases: UnevaluatedExpression

**class BlattWeisskopf** (*z, L, **hints*)

Bases: UnevaluatedExpression

## 9.6 function

```
import polarimetry.function
```

**compute_sub_function** (*func: ParametrizedFunction*, *input_data: DataSample*, *non_zero_couplings: list[Pattern]*)

**set_parameter_to_zero** (*func: ParametrizedFunction*, *search_term: Pattern*) → None

**interference_intensity** (*func*, *data*, *chain1: list[str]*, *chain2: list[str]*) → float

**sub_intensity** (*func*, *data*, *non_zero_couplings: list[str]*)

**integrate_intensity** (*intensities*) → float

## 9.7 io

```
import polarimetry.io
```

Input-output functions for `ampform` and `sympy` objects.

Functions in this module are registered with `functools.singledispatch()` and can be extended as follows:

```
>>> from polarimetry.io import as_latex
>>> @as_latex.register(int)
... def _(obj: int) -> str:
...     return "my custom rendering"
>>> as_latex(1)
'my custom rendering'
>>> as_latex(3.4 - 2j)
'3.4-2i'
```

This code originates from ComPWA/ampform#280.

**as_latex** (*obj*, ***kwargs*) → str

Render objects as a LaTeX `str`.

The resulting `str` can for instance be given to `IPython.display.Math`.

Optional keywords:

- only_jp: Render a `Particle` (page 77) as $J^P$ value (spin-parity) only.
- with_jp: Render a `Particle` (page 77) with value $J^P$ value.

**as_markdown_table** (*obj: Sequence*) → str

Render objects a `str` suitable for generating a table.

**display_latex** (*obj*) → None

**display_doit** (*expr: UnevaluatedExpression*, *deep=False*, *terms_per_line: int | None = None*) → None

**perform_cached_doit** (*unevaluated_expr: Expr*, *directory: str | None = None*) → Expr

Perform `doit()` on an `Expr` and cache the result to disk.

The cached result is fetched from disk if the hash of the original expression is the same as the hash embedded in the filename.

**Parameters**

- **unevaluated_expr** – A `sympy.Expr` on which to call `doit()`.

- **directory** – The directory in which to cache the result. If `None`, the cache directory will be put under the home directory, or to the path specified by the environment variable `SYMPY_CACHE_DIR`.

**Tip:** For a faster cache, set PYTHONHASHSEED to a fixed value.

**See also:**

*perform_cached_lambdify()* (page 80)

**perform_cached_lambdify**(*expr: Expr, parameters: Mapping[Symbol, ParameterValue] | None = None, backend: str = 'jax', directory: str | None = None*) → ParametrizedFunction | Function

Lambdify a SymPy `Expr` and cache the result to disk.

The cached result is fetched from disk if the hash of the expression is the same as the hash embedded in the filename.

**Parameters**

- **expr** – A `sympy.Expr` on which to call `create_function()` or `create_parametrized_function()`.
- **parameters** – Specify this argument in order to create a `ParametrizedBackendFunction` instead of a `PositionalArgumentFunction`.
- **backend** – The choice of backend for the created numerical function. **WARNING**: this function has only been tested for `backend="jax"`!
- **directory** – The directory in which to cache the result. If `None`, the cache directory will be put under the home directory, or to the path specified by the environment variable `SYMPY_CACHE_DIR`.

**Tip:** For a faster cache, set PYTHONHASHSEED to a fixed value.

**See also:**

*perform_cached_doit()* (page 79)

**get_readable_hash**(*obj*) → str

**mute_jax_warnings**() → None

**export_polarimetry_field**(*sigma1: ndarray, sigma2: ndarray, alpha_x: ndarray, alpha_y: ndarray, alpha_z: ndarray, intensity: ndarray, filename: str, metadata: dict | None = None*) → None

**import_polarimetry_field**(*filename: str, steps: int = 1*) → dict[str, ndarray]

## 9.8 plot

```
import polarimetry.plot
```

Helper functions for `matplotlib`.

**add_watermark**(*ax: Axes, x: float = 0.03, y: float = 0.03, fontsize: int | None = None, **kwargs*) → None

**get_contour_line**(*contour_set: QuadContourSet*) → LineCollection

**use_mpl_latex_fonts**(*reset_mpl: bool = True*) → None

**stylize_contour**(*contour_set: QuadContourSet, *, edgecolor=None, label: str | None = None, linestyle: str | None = None, linewidth: float | None = None*) → None

## 9.9 spin

```
import polarimetry.spin
```

**generate_ls_couplings**(*parent_spin: SupportsFloat, child1_spin: SupportsFloat, child2_spin: SupportsFloat, max_L: int = 3*) → list[tuple[int, Rational]]

```
>>> generate_ls_couplings(1.5, 0.5, 0)
[(1, 1/2), (2, 1/2)]
```

**filter_parity_violating_ls**(*ls_couplings: list[tuple[int, Rational]], parent_parity: SupportsInt, child1_parity: SupportsInt, child2_parity: SupportsInt*) → list[tuple[int, Rational]]

```
>>> LS = generate_ls_couplings(0.5, 1.5, 0)  # Λc → Λ(1520)π
>>> LS
[(1, 3/2), (2, 3/2)]
>>> filter_parity_violating_ls(LS, +1, -1, -1)
[(2, 3/2)]
```

**create_spin_range**(*spin: SupportsFloat*) → list[Rational]

```
>>> create_spin_range(1.5)
[-3/2, -1/2, 1/2, 3/2]
```

**create_rational_range**(*__from: SupportsFloat, __to: SupportsFloat*) → list[Rational]

```
>>> create_rational_range(-0.5, +1.5)
[-1/2, 1/2, 3/2]
```

### Notebook execution times

| Document | Modified | Method | Run Time (s) | Status |
|---|---|---|---|---|
| *amplitude-model* (page 3) | 2023-01-18 12:00 | cache | 21.62 | ✅ |
| *appendix/alignment* (page 54) | 2023-01-18 12:02 | cache | 79.29 | ✅ |
| *appendix/angles* (page 52) | 2023-01-04 14:29 | cache | 3.56 | ✅ |
| *appendix/benchmark* (page 55) | 2023-01-18 12:04 | cache | 149.07 | ✅ |
| *appendix/dynamics* (page 51) | 2023-01-18 12:04 | cache | 4.19 | ✅ |
| *appendix/homomorphism* (page 63) | 2023-01-04 14:35 | cache | 4.66 | ✅ |
| *appendix/ls-model* (page 60) | 2023-01-04 14:40 | cache | 273.6 | ✅ |
| *appendix/phase-space* (page 53) | 2023-01-18 12:05 | cache | 48.6 | ✅ |
| *appendix/serialization* (page 59) | 2023-01-18 15:58 | cache | 123.74 | ✅ |
| *appendix/widget* (page 70) | 2023-01-04 15:02 | cache | 1188.16 | ✅ |
| *cross-check* (page 13) | 2023-01-18 12:06 | cache | 45.81 | ✅ |
| *intensity* (page 21) | 2023-01-18 12:14 | cache | 470.18 | ✅ |
| *polarimetry* (page 27) | 2023-01-04 15:19 | cache | 426.89 | ✅ |
| *resonance-polarimetry* (page 43) | 2023-01-18 13:11 | cache | 3450.05 | ✅ |
| *uncertainties* (page 31) | 2023-01-11 17:15 | cache | 927.81 | ✅ |
| *zz.polarization-fit* (page 64) | 2023-01-04 17:52 | cache | 396.85 | ✅ |

# BIBLIOGRAPHY


[1] LHCb Collaboration *et al*. Amplitude analysis of $\Lambda_c^+ \to pK^-\pi^+$ decays from semileptonic production. *Phys. Rev. D*, 2022. doi:10.48550/arXiv.2208.03262.

[2] M. Mikhasenko *et al*. Dalitz-plot decomposition for three-body decays. *Phys. Rev. D*, 101(3):034033, February 2020. doi:10.1103/PhysRevD.101.034033.

[3] J. F. Cornwell. *Group Theory in Physics: An Introduction*. Academic Press, San Diego, CA, 1997. ISBN:978-0-12-189800-7.

# PYTHON MODULE INDEX

## p

# INDEX

## G



## H



## I



## J



## L



## M



## N



## O



## P

## Q



## R



## S



## T



## U



## V



## W